

Politecnico di Torino

Corso di Laurea Magistrale
Ingegneria Energetica e Nucleare



**Politecnico
di Torino**

Master's Degree Thesis

**ESTIMATING ONSHORE WIND AND SOLAR
PHOTOVOLTAIC TECHNOLOGY TECHNICAL POTENTIAL
APPLYING GIS-BASED METHODOLOGIES:
CASE STUDY LA GUAJIRA**

Relatori:

Prof. Giuseppe Giorgi

Candidate:

Joseph Zuluaga

Co-Relatori:

Dott. Claudio Moscoloni

Ing. Riccardo Novo

Ing. Enrico Giglio

Academic Year 2022/2023

Abstract

As a society, we are currently in an environmental crisis, a moment in which economic decarbonization and a neat energy transition to sustainable sources are urged. Thus, a global and systemic view of the problems that affect us and the possibilities for addressing them is needed. In the context of energy, the utilization of geographic information systems presents an opportunity to conduct macro-level analyses of territories, thereby generating valuable information that can facilitate informed decision-making by private investors, governments, international organizations, and other stakeholders. This, in turn, can promote the aforementioned energy transition. This master's thesis project uses QGIS and WAsP software as the main tools, supported by GRASS GIS and Python, to estimate how much onshore wind (OW) and solar photovoltaic (SPV) potential exists in the northernmost region of South America, La Guajira. This technical potential is calculated following a spatial energy planning strategy in which the maximum theoretical potential for both energy sources is constrained by land availability, environmentally protected spaces, climate factors, safety reasons, and technology efficiencies.

Contents

Abstract	2
Contents	3
1. Introduction	5
1.1. Objective of the study	6
1.2. Current state of case study region	7
1.2.1. Legislation, Barriers, and Opportunities	11
1.3. Wind energy	12
1.4. Onshore wind in Guajira, Colombia	16
1.5. Solar energy	18
1.6. Solar PV in Guajira, Colombia	22
2. Background	25
3. Methodology	28
3.1. Definition of Potential	29
3.2. Geographic Potential for Onshore Wind and Solar PV	30
3.3. Wind energy resource calculation	36
3.3.1. Turbine selection	37
3.3.2. Theoretical-Technical Potential	38
3.3.3. Technical Potential	41
3.4. PV Solar energy resource calculation	43
3.4.1. Technology Selection	43
3.4.2. Theoretical Potential	44
3.4.3. Technical Potential	45
4. Results	49
4.1. Onshore Wind Theoretical-Technical Potential	49
4.2. Onshore Wind Geographic Potential	53
4.3. Onshore Wind Technical Potential	54
4.4. PV solar Theoretical Potential	55
4.5. PV solar Geographic Potential	57
4.6. PV solar Technical Potential	58
5. Discussion	60
6. Conclusion	62

7. Recommendations	64
References	65
Appendix	71
A. Distance-restrictive criteria buffers layers	71
B. Captures from different regions in La Guajira, with all the area-restrictive criteria and their corresponding buffers.	79
C. P&QGIS Scripts	82
D. Other Screenshots:	85

No table of figures entries found.

1. Introduction

The necessity for a quick and thorough energy transition has become critical in an era characterized by accelerated climate change [1][2] and rising concerns over the sustainability of traditional energy sources. In order to mitigate the negative effects on the environment, reduce carbon footprints, and promote sustainable development while incorporating decarbonization, circular economy principles, energy efficiency, and the broader paradigm of sustainability, it is crucial to investigate alternative energy solutions.

The growing carbon footprint due to the burning of fossil fuels has been one of the main causes of global climate change [3]. Extreme weather events, sea level rise, and the emission of greenhouse gases like carbon dioxide (CO₂) and methane (CH₄) into the atmosphere have all occurred at previously unheard-of rates [4][5]. The international community has acknowledged the significance of moving toward renewable energy sources that can significantly cut or eliminate carbon emissions, presenting a workable strategy to battle climate change [6][7].

This project will consider onshore wind and solar photovoltaic energy, employing a methodology [8] to locate available areas to harvest these resources in La Guajira, Colombia. Subsequently, specific wind turbine and photovoltaic panel characteristics will be included in an estimation of energy technical potential, in accordance with the definition in [9]. The project's methodology for assessing these potentials is based on a spatial energy planning approach, using the geographical information system software QGIS, with its built-in Python console and code editor, and the software WAsP, for wind resource calculation.

As stated previously, many environmental reasons validate the importance of renewable energy projects. Additionally, to the climate change mitigation effect, these projects create energy independence and security. For example, approximately 70% is the share of fossil fuels in both Europe's (2020) and Colombia's (2021) *total energy supply* [10][11]. Concerning the installed power generation capacity, Colombia is very fossil-fuel-independent since 68% of total electricity comes from hydroelectric plants [12]. This is positive as it reduces the country's total carbon footprint, but it also makes the nation highly weather-dependent and threatens the availability of water resources.

According to the World Bank, in the past two decades, *water availability* in the country has decreased due to demographic growth and climate change, with one third of the total population under water stress [13]. This only emphasizes the importance of diversifying the national energy mix by increasing participation in renewables such as onshore wind and solar photovoltaic, enhancing energy security, and reducing vulnerability to geopolitical risks and price fluctuations associated with fossil fuel markets [14][15].

1.1. Objective of the study

The main objective of this master's thesis is to estimate, using QGIS and WAsP, the technical potential of Onshore Wind (OW) and Solar Photovoltaic (SPV) energy for the northernmost state of Colombia, La Guajira. The definition of technical potential [9] will be explained in section 3.1, for both onshore wind and solar photovoltaic.

The estimation of the above-mentioned technical potential will be carried out considering the 670 W solar panels found in [16] and the Nordex N149/4.0-4.5 wind turbine found in [17]. Concerning onshore wind, the software WAsP will be used to obtain resource grids for Annual Energy Production, Power Density and Wind Speed. These will, in turn, be employed to obtain an estimation, using QGIS, of how much energy can be generated with the specific technology in the available area found.

As for the solar PV, integrated QGIS and GRASS processing functions will be used to process the input raster and vector layers to obtain daily solar irradiation information, iterating and reaching a yearly average value. In the same manner to onshore wind, this energy potential information must be reduced by only considering the available area and the technical constraint of the selected photovoltaic panel.

This thesis follows a top-down approach for the potential estimation process, described in [9]. The methodology starts with the theoretical potential (the ideal, least constrained maximum resource) and works its way down to the feasible potential (within the boundaries of geography, technology, economics, and sociopolitical constraints). To put it another way, the top-down approach, represented in Figure 1.1, determines how much energy can be generated by considering resource constraints like available space and environmental factors. In contrast, the bottom-up approach employs a design strategy that calls for the system to be able to generate energy equal to the desired load consumption.

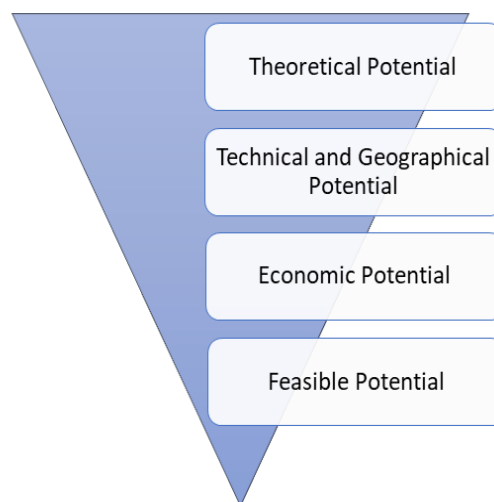


Figure 1.1: Top-Down approach representation.

1.2. Current state of case study region

As previously mentioned, the case study region of the thesis is Colombia. The country has a surface area of 1.109.500 km² and a population of around 50 million, making it the second biggest Spanish speaking country in the world after Mexico [18]. The country is one of the most biodiverse in the world [19], having access to the Atlantic Ocean in the north and to the Pacific on the west coast.

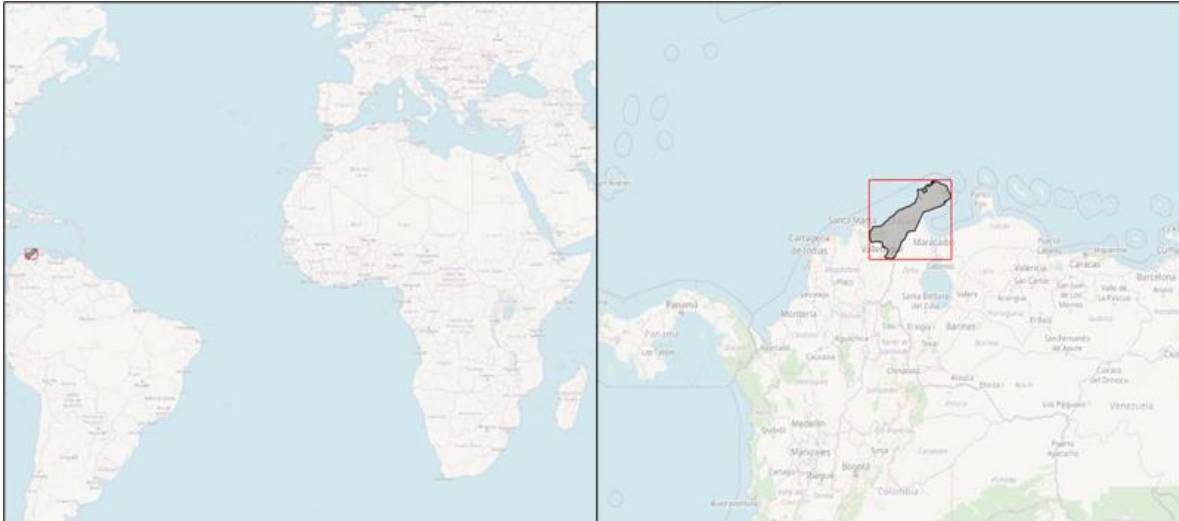


Figure 1.2: Geographical location of La Guajira.

Source: Self-made

In the southern part of the country, the Andes mountains (the longest continental mountain range in the world) divide into three, covering more than one third of the country's area [20]. This geography blesses the country with deserts, jungles, glaciers, abundant water, fertile soil, and biodiversity. The department of La Guajira is the northernmost region in Colombia and South America, and its location in the world can be seen in Figure 1.2. The region lies between the latitudes of 12° 27' 30.6648" North and 10° 24' 0" North, as well as the longitudes of 73° 39' 51.696" West and 71° 6' 48.744" West.

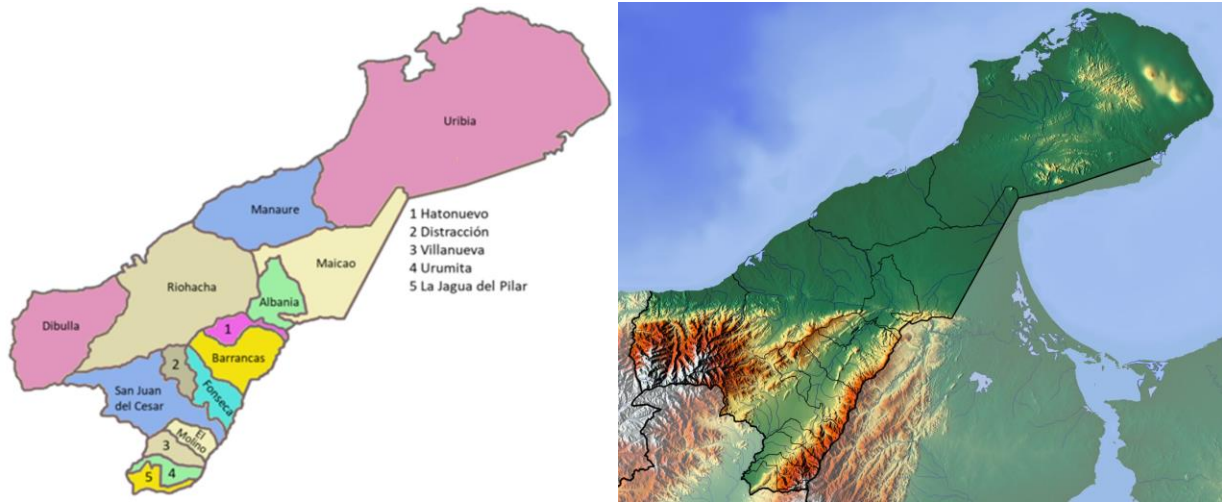
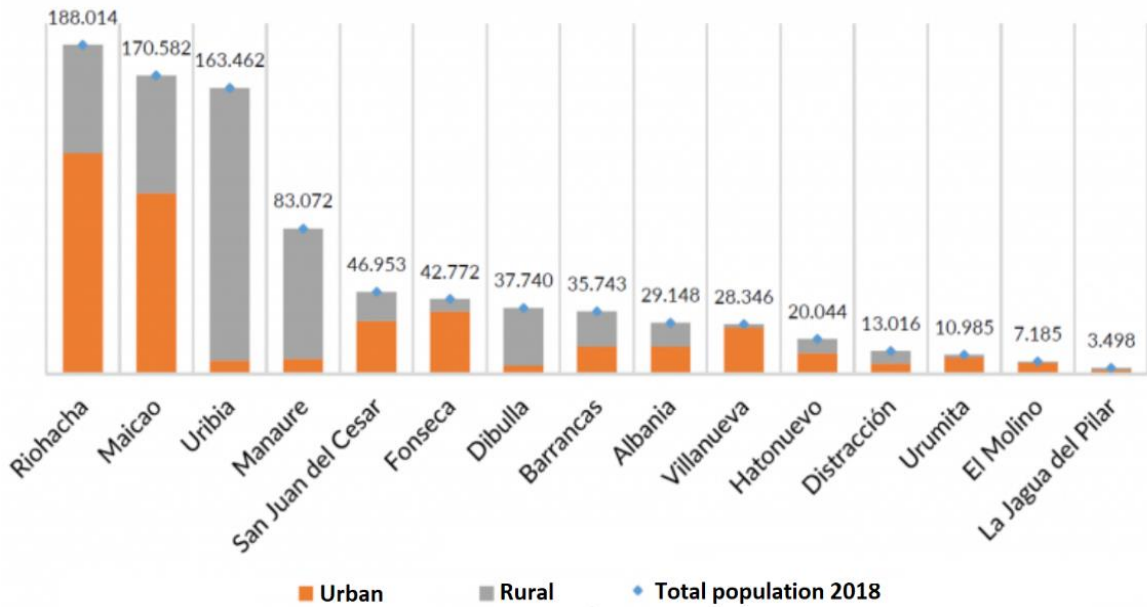


Figure 1.3: Political division and topography of La Guajira.[21][22]

This region is one of the 32 departments of Colombia and, according to the DANE (National Administrative Department of Statistics), has a surface area of 20.848 km² and a population of 880.560, as of 2018. Politically, the department is subdivided into 12 municipalities. This division can be seen in Figure 1.3. In Figure 1.4, the total population (2018) distribution between urban and rural can be observed for each municipality. The municipalities of Riohacha and Maicao each have a homonymous city, with the first being Guajira's capital urban center. Uribia has the highest Rural concentration due to the presence of Colombia's largest indigenous community, the Wayuu [23].



Source: CNPV - DANE. Guajira 360°, 2019

Figure 1.4: Urban and rural population distribution in La Guajira.[24]

In addition, the region has a maximum altitude exceeding 5400 meters above sea level, an average altitude of 300 meters, and a coastline of approximately 480 kilometers [25]. Guajira's residents rely on a wide range of economic activities, from fishing and agriculture to mining and tourism, to briefly define the region's socioeconomic fabric. In 2021, with 66.3% of its inhabitants, La Guajira was the department in Colombia with the highest prevalence of multidimensional poverty [26].

Riohacha, the departmental capital, recorded the highest unemployment rate in the country in April 2021, at 22.7%. The informal sector employs almost two-thirds of the population [27]. This poverty contrasts with the abundant natural resources present in the rest of the country and, especially, with the fact that La Guajira is considered the country's department with the biggest potential for clean energy generation, as stated by the country's Ministry of Environment and Development and the President of Colombia [28][29].

According to the IDEAM (Colombia's Institute of Hydrology, Meteorology, and Environmental Studies), wind speed in La Guajira is twice the world average, reaching 9 m/s at 80 meters above sea level, while solar radiation in that department is 60% higher than the world average [30]. As shown in Figure 1.5, however, the country's total energy supply is dominated by fossil fuels, with only 17% coming from renewable sources. The remaining energy demand is met by oil, gas, and carbon.

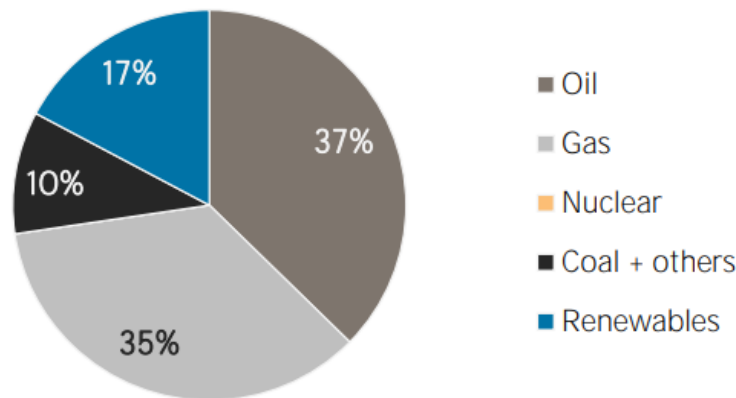


Figure 1.5: Total Energy Supply in Colombia 2019.[32]

In contrast, electricity generation derives approximately 70% of the total installed capacity in 2021 (17.3 GW) [31] from hydropower, generating electricity from a renewable energy source. Approximately 30% of the nation's energy capacity is still derived from fossil fuels, while the remaining 0.2% is comprised of solar, wind, and bioenergy. The previous description is displayed in Figure 1.6.

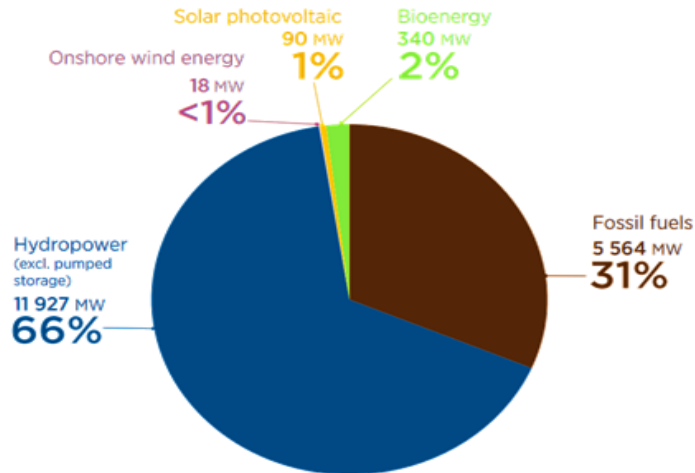


Figure 1.6. Electricity Generation by Source in Colombia 2019 [33]

As a matter of fact, the Colombian government has sought to further exploit other renewable sources, which likewise have considerable potential. A joint estimation was made between IRENA (International Renewable Energy Agency) and UPME (Colombia's mining and energy planning unit), and the results can be seen in Figure 1.7. Estimates were made for onshore wind, solar photovoltaic, small hydroelectric, geothermal, and bioenergy, with wind and solar having the biggest potential. In solar photovoltaic, a distinction is made between rooftop PV and other PV. The first has a potential of about 2 GW, whereas other photovoltaics have a potential of more than 30 GW.

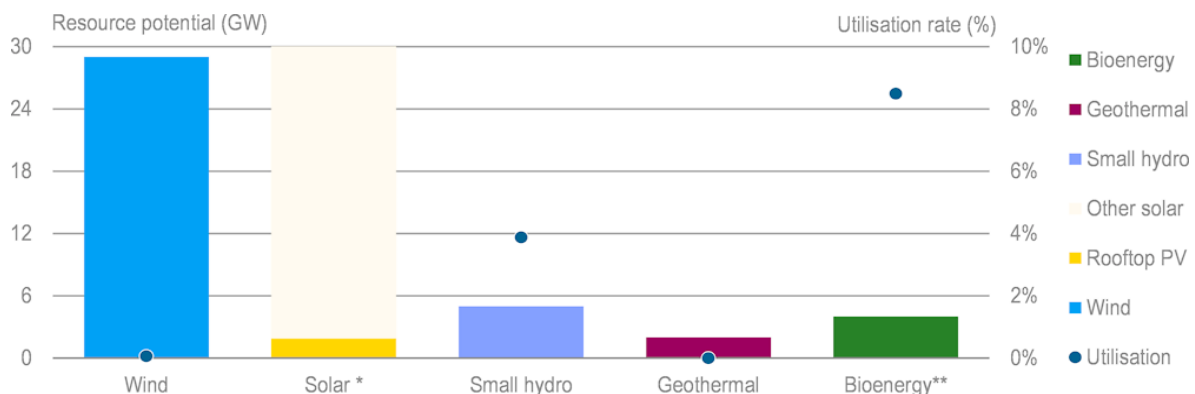


Figure 1.6. Electricity Generation by Source in Colombia 2019 [33]

This estimate, which the authors call "purely illustrative," was calculated by comparing Colombia's average solar radiation to Germany, which has around one-third of the national area as well as lower solar irradiance. Despite this, Germany added around 36 GW of solar PV capacity in 2013 [33][34]. Indeed, utilizing only wind and solar photovoltaic technology would allow Colombia to triple its current installed capacity due to its vast renewable energy potential. It is evident how a society striving for sustainability ought to proceed.

1.2.1. Legislation, Barriers, and Opportunities

Renewable energy development in Guajira, Colombia, is characterized by a complex interplay of barriers and opportunities, with legislative frameworks playing a critical role. The widespread adoption of renewable energy in the region faces several obstacles. Notably, the high initial costs of infrastructure development, particularly for solar and wind power projects, pose a significant financial challenge. Furthermore, renewable energy initiatives in Guajira face additional difficulties due to a lack of financing options. Moreover, insufficient grid infrastructure and transmission capacity constraints impede the efficient integration of renewable energy into existing energy infrastructure.

Despite these limitations, there are opportunities that can help Guajira's renewable energy sector flourish. Colombia's government has proved its commitment to renewable energy production by passing legislation and establishing policies that encourage it. Law 1715 of 2014 [35] promotes the use of non-conventional energy sources by providing incentives, tax breaks, and simplified procedures for renewable energy projects. These legislative measures are intended to create a favorable investment climate and encourage private sector engagement in renewable energy ventures. In other words, this law regulates the incorporation of non-conventional renewable energy sources into the National Energy System.

More recently, the Colombian Congress of the Republic issued Law 2099 of 2021 [36], with the purpose of promoting the use of non-conventional energy sources and encouraging the efficient use of energy resources. Likewise, the new Law introduced amendments and additions to Law 1715 of 2014. The new provisions are issued for the energy transition, the dynamization of the energy market, and the economic reactivation of the country.

The use of GIS-based approaches to estimate the renewable energy potential in La Guajira reveals a complicated interaction of constraints and opportunities, particularly for onshore wind and photovoltaic solar energy. These technologies face social and environmental challenges. Local communities may object to projects out of concern for the potential impact on their way of life and cultural heritage, as evidenced by past efforts to install renewable energy infrastructure. For instance, *Windpeshi*, a wind farm with a planned installed capacity of 205 MW, was forced to halt development indefinitely due to protests and disagreements with surrounding populations [37].

Environmental barriers arise from the need to carefully assess and mitigate any adverse effects on bird species and other local fauna. Implementing comprehensive environmental impact assessments and engaging stakeholders can address these concerns and promote acceptance within local communities.

Nonetheless, La Guajira offers abundant opportunities for renewable energy development. Being the northernmost state of Colombia, it benefits from a geographical advantage, experiencing higher wind speeds compared to other regions. This wind resource is attributed to its distance from the equator and the flat terrain, which facilitate regular and uninterrupted wind flow. These characteristics create an ideal environment for early-stage wind and solar energy development. Capitalizing on this potential necessitates the implementation of appropriate policies and regulations that ensure responsible and sustainable development practices while safeguarding the environment and local communities.

Infrastructure constraints, such as insufficient road networks, may appear to be a barrier, but they also present an opportunity. Because the region's existing infrastructure is limited, strategic planning and investment in transportation networks that may be adapted to assist the renewable energy sector are required. Furthermore, the ongoing construction of La Guajira's power grid provides an advantage. The advancement of grid infrastructure assures that it can support greater power generation from various energy sources, including renewables.

1.3. Wind energy

The air naturally moving above the surface is called wind. There are numerous varieties of wind, each with a unique strength and duration. Atmospheric circulation, which is primarily brought on by the Coriolis effect and uneven global heating, is what creates wind on a global scale. A varying amount of solar energy that reaches the surface at the poles and the equator causes the first effect [38].

Because of the tilt of the Earth's axis, sunlight must travel through a thicker atmosphere at the poles than at the equator, which results in a greater loss of heat. This results in a net loss of heat towards the poles, whereas a net gain is observed near the equator. Due to the imbalance, which suggests that the equatorial region is warmer than the polar regions, an airflow is produced that follows the temperature gradient.

This can be seen in Figure 1.7, where only one convective cell exists that elevates warm, high-pressured air at the equator. The air travels through the atmosphere in the direction of the poles until it cools down, circulating back at a homogeneous flux through the lower part of the convection cells.

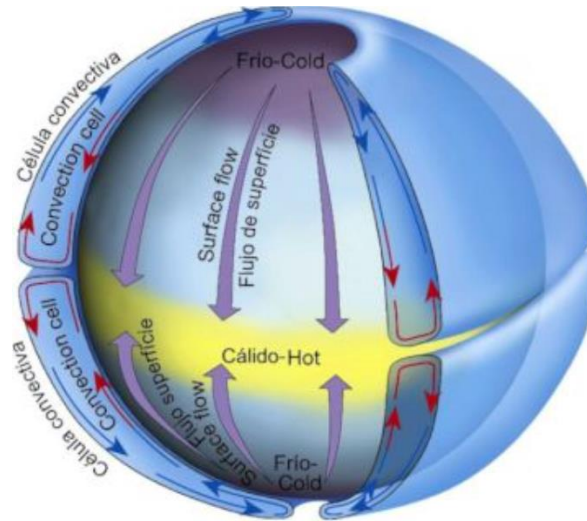


Figure 1.7. Atmospheric circulation without considering Earth's rotation [39]

Nevertheless, given the second contributing factor, the Coriolis effect, the air flow is not straight. The Coriolis force is a hypothetical force that affects a moving object in a rotating frame of reference and deviates the object's course from an inertial frame of reference. Because the Earth rotates more quickly at the Equator than at the Poles, this effect also applies to the planet.

As a result, the air moves in three zones, called *cells*, between the equator and each pole. The cell closest to the equator is called *Hadley Cell*, the closest to the pole receives the name *Polar Cell*. The mid-latitude cell, also known as the Ferrel cell, is a secondary circulation characteristic that is completely dependent on the polar and Hadley cells, which are driven by temperature gradients. The air moves parallel to isobars (geostrophic wind) at an altitude of 1 km above sea level, where friction is low. This can be seen in Figure 1.8. Additionally, in the figure can be seen the polar easterlies, the westerlies, and the NE/SE trade winds, with their respective general sense of flux.

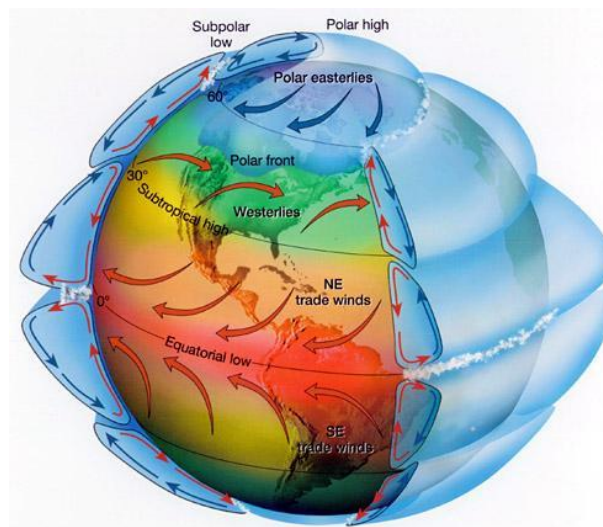


Figure 1.8. Atmospheric circulation considering Earth's rotation [39]

The global winds produced by the aforementioned factors are crucial in determining the primary wind behavior in each place, but additional local elements might impact wind direction. Temperature and pressure gradients always cause local winds, although on a smaller scale. A sea or land breeze, for example, comes from the temperature gradient between the sea and the mainland, which is opposite during the day and night.

Moreover, there is also turbulence, which can be caused by two main groups of sources: modifying factors and local influences. The first group comprises features such as orographic variety and surface roughness changes, which are thus related to landscape shape. The second group includes locally relevant phenomena such as heat convection, barriers (such as trees or buildings), steep terrain, and wind turbines.

The roughness of the terrain, part of the modifying turbulence source group, can cause a phenomenon called “Wind shear”, characterized by a difference in wind speed at different heights above the surface. Lower roughness means faster speeds, such as over water or a remarkably smooth surface (such as ice or mud). This influence is proportional to the height of the barrier. Turbulence is generated both upwind and downwind of the obstacle, and it modifies the air flow rather significantly.

Regarding wind turbine technology, the first thing to understand is that a wind turbine's purpose is to harness the wind's energy. The sole kind of energy in the wind is kinetic energy, and it is dependent on the air mass (density ρ), wind speed U , and the area A that the turbine rotor sweeps. This relation, used to obtain the power P , is represented in Equation 1.

$$P = (\frac{1}{2})\rho AU \quad \text{[Equation 1]}$$

Furthermore, the concept of power coefficient C_p causes the extractable power by a turbine to be less than that determined by Equation 1. The air velocity across the rotor determines the power coefficient, which differs for each turbine. Its highest limit, known as the *Betz limit* (after the scientist who established its formulation), is equal to the proportion 16/27. The wake rotation effect forces the power coefficient to be less than the Betz limit.

In fact, the mechanical energy that can be extracted from wind turbines decreases as air begins to rotate through the rotor. The Tip-speed-ratio, which is the ratio of the wind speed to the tangential velocity at the rotor tip, can be used to correlate the power coefficient. An increased power coefficient, which tends to Betz limit, results from a greater tip speed ratio.

Wind turbines ordinarily are divided into two varieties: horizontal and vertical axis. Horizontal axis wind turbines (HAWTs) are the most widely used and most efficient technology. The rotor is almost always upwind, so it is not shielded by the tower and has

a higher efficiency. For the rotor to face upwind, the yaw control, which allows the nacelle to rotate in the horizontal plane, must be engaged.

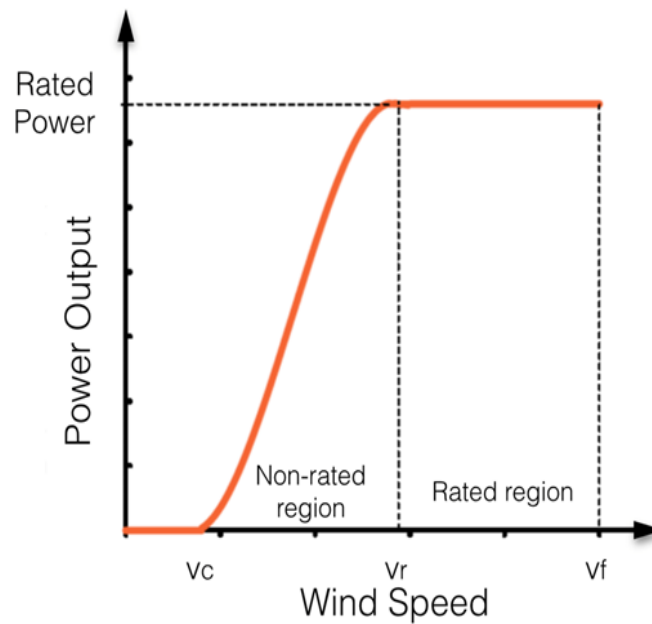
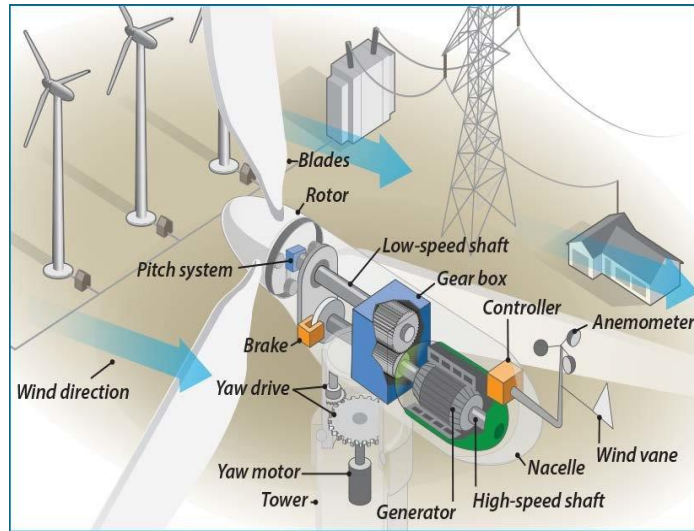


Figure 1.9. HAWT schematic and power curve example.[42][43]

Each HAWT is represented by a power curve graph. This curve relates the wind speed to the turbine's generation of electricity and reveals some crucial technical information about the turbine itself. The wind speed is represented by the horizontal axis, and the curve begins at a particular speed known as the cut-in speed. The power output then increases as the wind speed does, until both are constant and equal to the rated power (at the rated wind speed). After this, the power remains constant even as the speed increases until the velocity hits the cut-out speed, at which time it becomes zero. For

safety purposes, the turbine is inhibited above this speed number. This power curve and a diagram of a HAWT can be observed in Figure 1.9

The International Electrotechnical Commission (IEC) classifies wind turbines into classes, based on average wind speed, 50-year extreme gust, and turbulence [40][41]. The three technical wind speeds are: Class I, stands for high wind speeds, at 10 m/s; class II, for medium wind speeds, at 8.5 m/s; and class III for low wind speeds, at 7.5 m/s. The full classification can be seen in Table 1.1, including types of turbulence and the 50-year extreme gust. Turbulence is the standard deviation of wind speed measured at 15 m/s wind speed.

Wind Turbine Generator Class	I	II	III
Annual average wind speed [m/s]	10	8.5	7.5
Extreme wind speed 50-year gust [m/s]	70	59.5	52.5
Turbulence Class-A	18%		
Turbulence Class-B	16%		

Table 1.1. IEC wind turbine classification.

Source: Selfmade, data from [40]

The vertical-axis wind turbine (VAWT) is the second type of wind generator. They are divided into drag-type and lift-type groups. The drag-type VAWT, also known as the Savonius turbine, operates in a very straightforward manner: as the wind hits the blades, they begin to revolve, powering a generator. Since this process suggests that efficiency is constrained, it is only suggested for low-power applications. It does have the advantage of not requiring a yaw mechanism.

The lift effect drives the lift-type VAWT, commonly known as a Darrieus turbine. The yaw mechanism is not required in this instance either, and the build is straightforward and inexpensive. Low efficiency and high construction costs are the key disadvantages. They also need a starting mechanism. To lessen the cut-in speed, these two types of turbines can also be combined. This project focuses only on horizontal axis wind turbines.

1.4. Onshore wind in Guajira, Colombia

The first wind farm in Colombia was built precisely in La Guajira. Jepirachi was built in 2004 and is powered by 15 Nordex N60/250 generators, each having a capacity of 1.3 MW. This 19.5 MW plant was Colombia's only wind installed capacity until 2023, when development of the country's second wind farm came to an end. Guajira I is the first of numerous onshore projects now under construction in the region [44].

Guajira I has a 20 MW installed capacity with 10 Vestas V100/2000 turbines, each with a rated power of 2 MW and a hub height of 78m. Even though the Guajira I was finished in 2022, it hasn't entered commercial operation, because it is still in the testing phase [45]. The main characteristics of wind farms in Colombia can be seen in Table 1.2.

Wind Farm	Name and year	Jepirachi (2004)	Guajira I (2023)	Windpeshi (?)
	Installed Capacity [MW]	19.5	20	184.5
	Number of Generators	15	10	41
Single Wind Turbine	Single Generator Power [MW]	1.3	2	4.5
	Single Generator Reference	Nordex N60/250	Vestas V100/2000	Nordex N149/4.0-4.5
	Wind turbine diameter [m]	60	98	149.1
	Hub height [m]	60	78	150
	Cut-in speed [m/s]	2.5	3.5	3
	Nominal speed [m/s]	15	12	12
	Cut-out speed [m/s]	25	22	26
	Survival speed or revolutions	60 [m/s]	13.4 [rev/minute]	12.3 [rev/minute]

Table 1.2. Main characteristics of current onshore wind installed capacity in Colombia.

In Colombia, sixteen onshore wind farm projects have been approved and are either under construction or in the pre-construction phase over the past few years. The whole list of projects is illustrated in Figure 1.10. Within this list, the previously mentioned project Guajira I was the first wind farm to be finished and is expected to soon also be connected to the national grid. Among the rest of the projects, some wind farms are worth mentioning. For example, *Windpeshi*, with around 200 MW of installed capacity, 20 times the size of the biggest wind farm in the country.

All these projects are creating a significant electric input to the national electric system. Equally important is the creation of infrastructure for distributing the produced power, which is estimated to be over 2.5 GW when all 16 wind farms are finished. Moreover, the total investment in all projects exceeds US\$2.500 million. The investment in the project is directly related to the installed capacity. For instance, the biggest planned wind farm is called Guajira II, with an expected installed capacity of ~370 MW; likewise, this project has the highest investment cost of all.

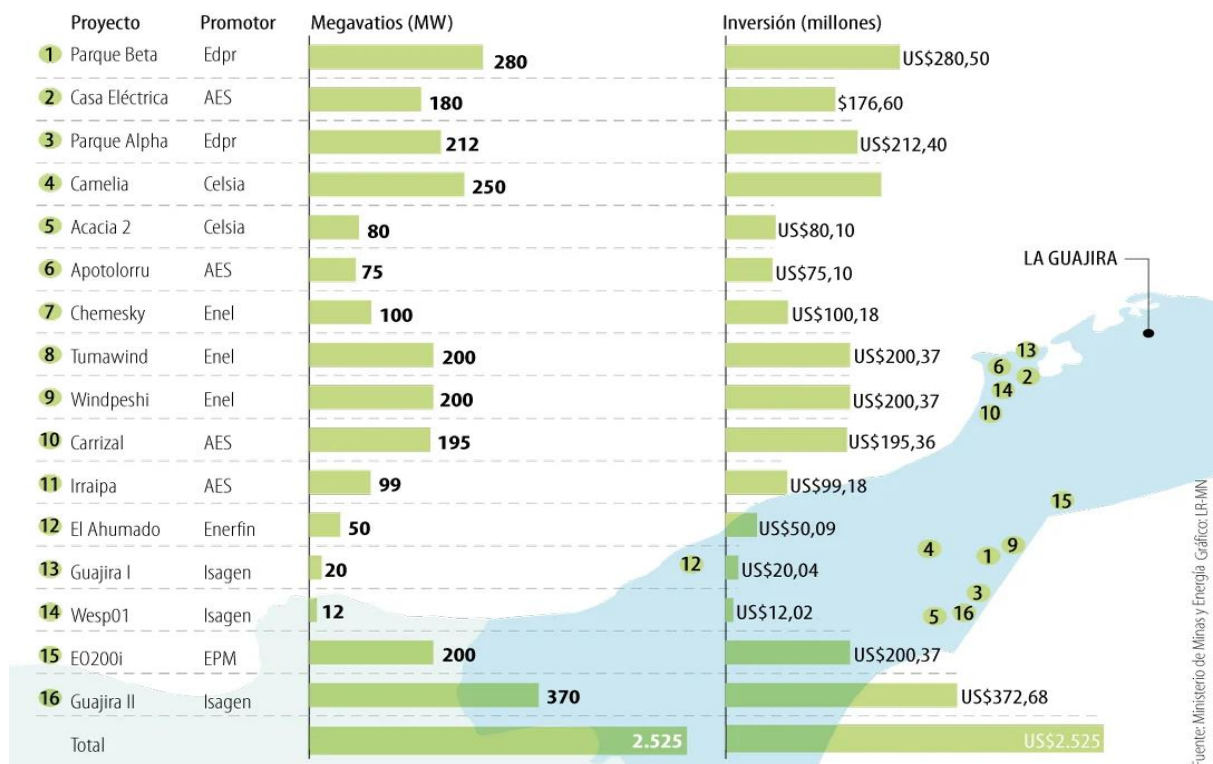


Figure 1.10. Onshore wind farm projects under construction with respective capacity [MW] and investment (millions of US) [44]

A very interesting comparison is that when all these projects are finished, the eolic share in the national installed capacity for electricity, calculated at 17.3 GW (2021) [31], would be around 12.7%. This is a very important step in the energy transition of the country because Colombia pledged to reduce its GreenHouse gas emissions by 51% by 2030 [46].

1.5. Solar energy

The sun's massive body emits radiation in the form of photons, which travel through space and reach the Earth. Some of this radiation is temporarily absorbed by

the Earth's atmosphere before being reradiated, some is reflected into space, and the remaining portion reaches the Earth's surface, as seen in Figure 1.11.

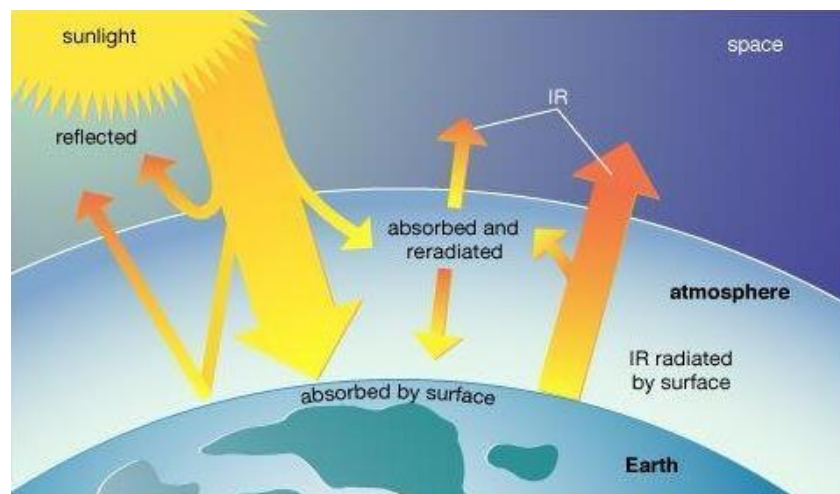


Figure 1.11. Solar radiation dynamics with Earth. [50]

This radiation travels in the form of waves, and depending on wavelength and frequency, the energy can be harvested with a specific technology, for a range of wavelengths or frequencies. The complete range of frequencies is called the electromagnetic spectrum. The energy from the sun is currently harvested by two main types of technology: solar thermal and solar photovoltaic (SPV), with the main difference that the first one converts sunlight into heat (which can then be further transformed into electricity through a thermal cycle), and the latter converts irradiation directly into electricity.

In Figure 1.12, starting from the left, is displayed the solar PV general description. Monocrystalline and polycrystalline silicon cells, thin film cells, and organic/polymer cells are the commercial products for this technology, the first two are the most widespread. Efficiency is normally lower than 20%, even if the theoretical efficiency for pure silicon panels with no defects is calculated to be ~30% [49].

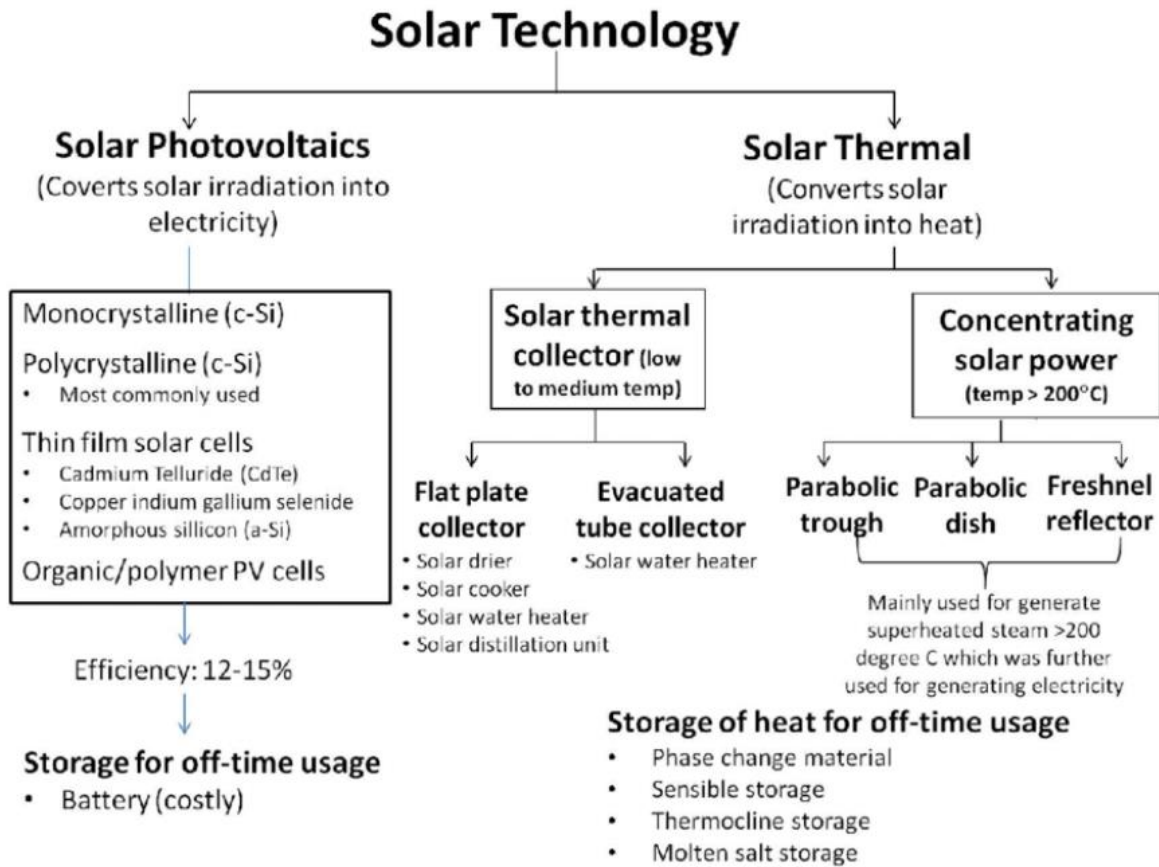


Figure 1.12. General view of solar technologies [48]

On the other hand, solar thermal technologies depend on the dimensions of the working temperature and the scale of the project. For residential and medium-scale projects, flat plate collectors or vacuum tube collectors are used for heating spaces and water, and even as input for solar cooling cycles. Meanwhile, for higher temperatures and larger-scale projects, concentrated solar power plants reflect a vast area of radiation into a single point, multiplying the heating effect and using this heat as an input for electricity-producing thermal cycles.

Solar thermal energy harvests radiation with a low frequency and a high amplitude; this type of solar energy normally raises the temperature of matter it encounters. This property is leveraged to heat a “transfer fluid”, which subsequently transfers heat to a “receiver fluid”, utilized to generate steam. A turbine converts steam into mechanical energy, which powers a generator to generate electricity. This principle can be applied to small or medium appliances, like residential homes and buildings. This can be observed in Figure 1.13.

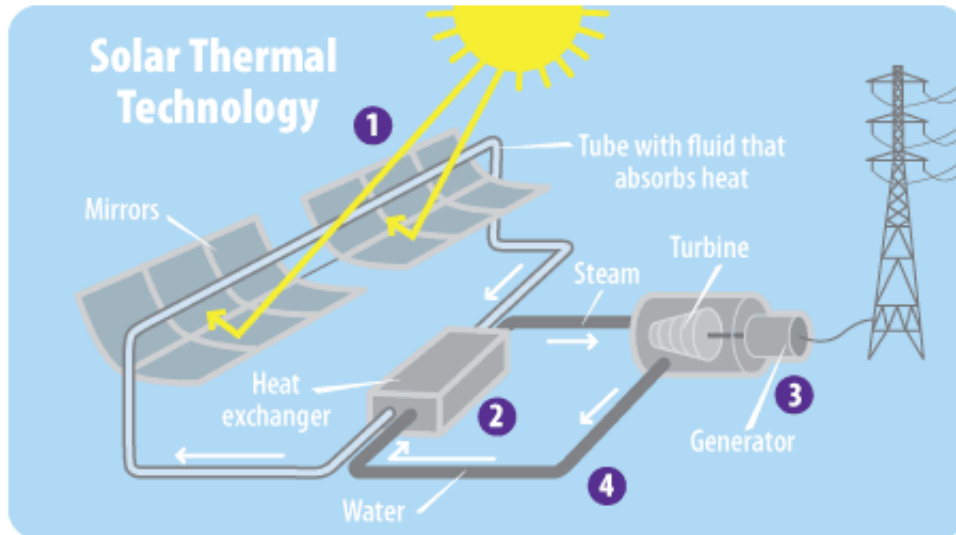


Figure 1.13. Schematic of solar thermal technology [47]

Another example of solar energy transformation is solar PV technology. This technology utilizes panels made with semiconductor materials to transform sun beams into electric current; all this is possible because of the properties of semiconductor materials like silicon. When a photon traveling in sunlight hits a photovoltaic panel, the architecture of the panel itself directs, in a specified sense of flow, the energy generated due to this impact.

Millions of photons arriving at the solar panel generate in turn millions of infinitesimal electric charges (electrons), which, when directed in a single direction, are converted into an electric current. This is also a very simplified description of the photovoltaic effect used to generate electric power. The amount of energy produced by the panels is determined by both the angle at which sunlight strikes and the number of hours of sunlight. This phenomenon is represented in Figure 1.14.

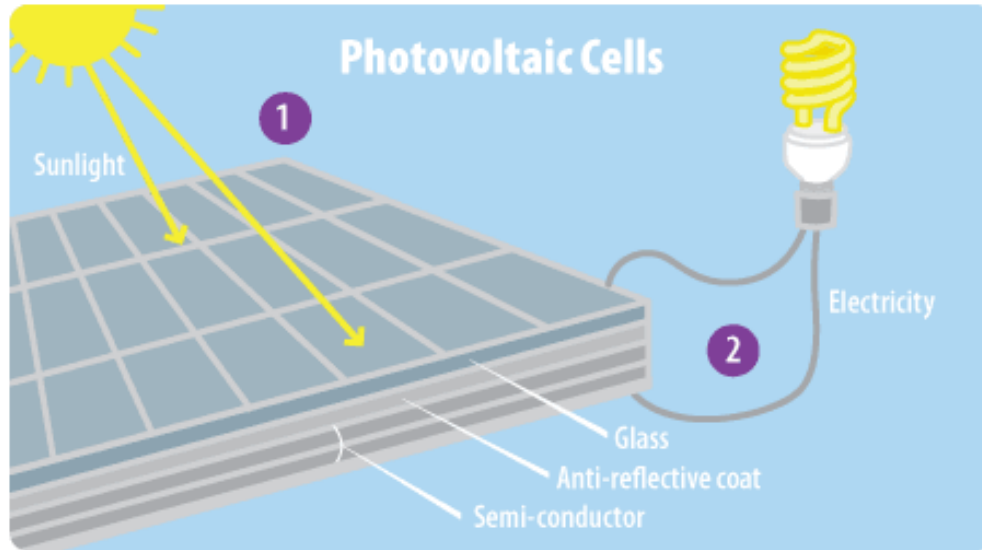


Figure 1.14. Schematic of solar photovoltaic technology [47]

Aside from the angle and duration of the sun, a range of additional factors can influence how efficiently PV solar generation works. The presence of clouds and other airborne particles, for example, can absorb and scatter sunlight, reducing the quantity of solar energy reaching the solar panels. This is why solar energy generation is most advantageous on sunny, clear days.

1.6. Solar PV in Guajira, Colombia

The country has a positive photovoltaic solar energy potential compared to the rest of the world. Being located close to the equator, no big changes happen throughout the year with respect to solar radiation. Most of the national territory has a resource of solar brightness (hours of sunshine) of around 4, 8, and even 10 hours of sunshine per day on the annual daily average, which are high values compared to countries such as Germany, which has 3 hours of sunshine on the annual average. This translates into an average daily solar radiation of 4.5 kWh/m², higher than the world average of 3.9 kWh/m² [51].

There are currently ~290 MW of photovoltaic installed capacity in Colombia, roughly 1.5% of the nation's total electric capacity [52]. It's worth noting that none of these solar farms are in La Guajira, considering that the department has the highest average solar radiation value in the country, with 6.0 kWh/m² [53]. However, Colombia is pursuing a renewable energy transition, with plans to increase that 1.5% photovoltaic share to an ambitious 30% by 2027 [53].

Proyecto	Promotor	Capacidad	Departamentos	Proyecto	Promotor	Capacidad	Departamentos
• Autog Celsia Solar Yumbo	Celsia	9,8 MW	Valle del Cauca	• La Loma Solar	Enel	170 MW	César
• Bayunca 1	Egal	3 MW	Bolívar	• La Medina	Grenergy	9,9 MW	Tolima
• Bosques Solares de los Llanos 1	Trina	19,9 MW	Meta	• La Paila	Celsia	9,9 MW	Valle del Cauca
• Bosques Solares de los Llanos 2		19,9 MW		• La Sierpe Solar	Aages	19,9 MW	Sucre
• Bosques Solares de los Llanos 3		19,9 MW		• Llanos 34	Geopark	9,9 MW	Casanare
• Bosques Solares de los Llanos 4		19,9 MW		• Los Caballeros	Grenergy	9,9 MW	Tolima
• Bosques Solares de los Llanos 5		17,9 MW		• Melgar	Celsia	9,9 MW	
• Buga 1	Celsia	9,9 MW	Valle del Cauca	• Palmira 3		9,9 MW	Valle del Cauca
• Cabrestero	Parex	3 MW	Casanare	• Parque Fotovoltaico Montelibano Solar	Grenergy	9,9 MW	Córdoba
• Carmelo	Celsia	9,9 MW	Valle del Cauca	• Pétalo de Córdoba	GreenYellow	9,9 MW	
• Celsia Solar Bolívar		8 MW	Bolívar	• Puerto de Cartagena	Puerto de Cartagena	2,2 MW	Bolívar
• Celsia Solar Espinal		9,9 MW	Tolima	• San Felipe	Celsia	9,9 MW	Tolima
• Cerritos	Grenergy	9,9 MW		• San Fernando	ECP	61 MW	Meta
• Delphi Helios	Ebsa	16 MW	Meta	• Sincé	Termotasajero Dos	19,9 MW	Sucre
• Dulima	Celsia	19,9 MW	Tolima	• Sol de Inirida	Celsia	2,2 MW	Guainía
• El Paso Solar	Enel	67 MW	César	• Solar Castilla ECP	ECP	20 MW	Meta
• Flandes	Celsia	19,9 MW	Tolima	• Termotasajero Dos Solar	Termotasajero Dos	4 MW	Norte de Santander
• GR Parque Solar Tucanes	Grenergy	9,9 MW	Bolívar	• Tuluá	Celsia	13,3 MW	Valle del Cauca
• Granja Solar Energía de Pereira	Empresa de Energía de Pereira S.A. ESP	5 MW	Risaralda	• Yuma		9,9 MW	Tolima

Fuente: Ministerio de Minas y Energía

Gráfico: LR-GR-ER

Figure 1.15. Balance of photovoltaic farms in Colombia (2023)

“It is projected, for example, that by 2027 the country will have a capacity of close to 32GW, of which more than 11GW will come from non-conventional renewable sources...” was the communication given by XM, the government-designated operator of the National Interconnected System (SIN) and manager of the Wholesale Energy Market (MEM) [54][55]. In Figure 1.15 are listed all the photovoltaic farms that are currently functioning or under construction in Colombia, according to the Ministry of Mines and Energy [51][56].

The total installed capacity of these 30 farms, when finished, adds up to 710MW, 4.1% of the previously mentioned national installed capacity in 2021, 17.3 GW. For instance, one of the most relevant projects seen in Figure 1.15 is La Loma, in the department of Cesar, which is 70% complete and has a potential of 187 megawatts using 400,000 solar panels distributed over 437 hectares (4.37 km²). This solar park anticipates supplying 370,000 people with electricity per year.

Parque	Power [MW]	Municipio
Chivo Mono I	750.0	Albania
Guardintera	181.3	El Molino
Leo Solar II	80.0	San Juan del Cesar
Wimke	76.0	San Juan del Cesar
Leo Solar I	19.9	San Juan del Cesar

Figure 1.16. Photovoltaic farms in La Guajira (March 2023)

Now, in terms of La Guajira's photovoltaic future, there are 5 PV plants that are up to date with their registrations as of May 2023, and another 13 that are reported because they haven't provided any reports or have ceased construction. With a combined installed capacity of around 1,107 MW, these could be the region's first solar installations. It is unknown how many of the remaining 13 projects, with a total potential capacity of 1,991 MW, will resume construction or withdraw.

2. Background

This section examines various projects that have used Geographic Information Systems, also known as GIS, in the process of estimating renewable potential, such as onshore wind and solar photovoltaic. Every academic paper or thesis is unique, because different case study regions introduce new variables that influence the estimation process. The definition of potential differs slightly, as do the methods for obtaining it.

The site selection problem for renewables is frequently addressed using a multi-criteria decision-making (MCDM) approach in conjunction with geographic information system (GIS) software to determine the most suitable area or alternative. Such is the case in [58], where the authors evaluate criteria for site selection of solar photovoltaic projects using a fuzzy additive estimation approach for the weight coefficients. In other words, they are determining the degree of importance of the most important criteria that affect site selection. The list of criteria can be seen in Figure 2.1

Their methodology can be understood in four consecutive stages: First, identifying the criteria; second, applying a questionnaire to both academia and industry to avoid and analyze possible bias; third, statistical analysis of the survey; and fourth, determining the degree of importance of each criterion. This project was particularly important because the authors created their criterion list based on more than 50 different GIS related projects that were assessing solar PV [Appendix A], wind, and concentrated solar power energy, starting in 2008 until 2021, and including more than 20 countries, across the world.

Their project concluded that the resulting criteria weights would have a strong bias depending on the type of experts that answered the questionnaire: experts from academia would prioritize economic matters, then technical, environmental matters, and ultimately social/political matters. However, experts from industry understand that a whole project can be jeopardized by a social/political reason and that it cannot move forward if there is any environmental violation. Hence, for Industry experts, the most important elements to consider are the same as Academia, the economical part, followed by environmental, social/political, and lastly, technical.

In addition, several other studies have provided insights to the methodology and investigated the estimation of renewable energy potential and the use of GIS systems. The second relevant study is [9], titled "*The feasible onshore wind energy potential in Baden-Württemberg: A bottom-up methodology considering socioeconomic constraints*" and can be found in [9].

Studies using combined GIS and decision making for solar PV site selection.

Authors	Year	RE source	Main-criteria	Sub-criteria	Alternatives	Case study	Fuzzy sets	Proposed methodologies
Carrión et al.	2008	Solar PV	4	18	–	Spain		GIS
Aragonés-Beltrán et al.	2010	Solar PV	12	50	4	Spain		AHP and ANP
Janke	2010	Solar PV-Wind	–	8	–	USA		Multi-criteria GIS modelling
Charabi and Gastli	2011	Solar PV-CSP	3	9	–	Oman	x	GIS-based spatial fuzzy multi-criteria evaluation
Uyan	2013	Solar	2	5	–	Turkey		GIS and AHP
Sánchez-Lozano et al.	2013	Solar PV	4	10	–	Spain		GIS, AHP, and TOPSIS
Effat	2013	Solar PV	–	5	8	Egypt		GIS and AHP
Sun et al.	2013	Solar PV	–	5	–	China		GIS
Sánchez-Lozano et al.	2014	Solar PV	4	10	–	Spain		GIS and ELECTRE
Asakereh et al.	2014	Solar PV	–	–	–	Iran	x	Fuzzy AHP and GIS
Jun et al.	2014	Solar PV-Wind	5	13	7	China		ELECTRE-II
Wu and Gang	2014	Solar PV-Wind	5	23	5	China		AHP
Vafaeipour et al.	2014	Solar	4	14	25	Iran		SWARA, WASPAS, and Delphi
Watson and Hudson	2015	Solar PV-Wind	4	7	–	UK		GIS and AHP
Borgogno Mondino et al.	2015	Solar PV	–	8	20	Italy		GIS and Artificial Neural Network (ANN)
Tahri et al.	2015	Solar PV	4	7	–	Morocco		AHP and GIS
Lee et al.	2015	Solar PV	3	12	15	Taiwan	x	Fuzzy AHP and DEA
Fernandez-Jimenez et al.	2015	PV	–	–	–	Spain		GIS
Sánchez-Lozano et al.	2016	Solar PV	–	10	–	Spain		GIS, AHP, TOPSIS, and ELECTRE TRI
Merrouni et al.	2016	Solar PV-CSP	–	13	–	Morocco		GIS
Noorollahi et al.	2016	Solar PV	4	11	31	Iran	x	Fuzzy AHP and GIS
Sabo et al.	2016	Solar PV	5	8	–	Malaysia		GIS
Suh and Brownson	2016	Solar PV	6	8	3	Korea	x	Fuzzy AHP and GIS
Kareemuddin and Rusthum	2016	Solar PV	–	–	–	India		GIS and Image Processing
Georgiou and Skarlatos	2016	Solar PV	4	10	–	Cyprus		GIS and AHP
Al Garni and Awasthi	2017	Solar PV	2	7	–	Saudi Arabia		GIS and AHP
Aly et al.	2017	Solar PV-CSP	4	7	–	Tanzania		GIS and AHP
Anwarzai and Nagasaka	2017	Solar PV-Wind	–	9	–	Afghanistan		GIS
Liu et al.	2017	Solar PV	3	8	4	China		Grey cumulative prospect theory
Sindhu et al.	2017	Solar PV	5	18	5	India	x	AHP and Fuzzy TOPSIS
Doljak and Stanojević	2017	Solar PV	3	7	–	Serbia		GIS and AHP
Zoghi et al.	2017	Solar	4	15	–	Iran	x	GIS and AHP
Lee et al.	2017	Solar PV	4	10	5	Taiwan	x	Fuzzy ANP and VIKOR
Suuronen et al.	2017	Solar PV	3	12	–	Chile		GIS and AHP
Yushchenko et al.	2018	Solar PV-CSP	–	19	–	West Africa		GIS and AHP
Wu et al.	2018	Rooftop PV	5	16	5	China		ANP and VIKOR
Wang et al.	2018	Solar	5	15	7	Vietnam	x	Fuzzy AHP, DEA, and TOPSIS
Merrouni et al.	2018	PV	4	8	–	Morocco		GIS and AHP
Ozdemir and Sahin	2018	Solar PV	–	5	3	Turkey		GIS and AHP
Fang et al.	2018	PV	4	10	4	China		Rough PT-based TOPSIS
Yousefi et al.	2018	Solar PV	3	9	–	Iran	x	GIS and Boolean-Fuzzy Logic Model
Majumdar and Pasqualetti	2019	Solar PV	4	9	–	USA		GIS and Multi-Criteria Analysis
Solangi et al.	2019	Solar PV	6	20	14	Pakistan	x	AHP and Fuzzy VIKOR
Wu et al.	2019	CSP	5	13	5	China	x	PROMETHEE
Giamalaki and Tsoutsos	2019	Solar PV-CSP	–	10	–	Greece		GIS and AHP
Doorga et al.	2019	Solar PV	3	9	–	Mauritius		GIS and AHP
Colak et al.	2020	Solar PV	–	10	–	Turkey		GIS and AHP
Sreenath et al.	2020	Solar PV	–	6	11	Malaysia		ForgeSolar software
Haddad et al.	2021	CSP	4	7	–	Algeria		GIS and AHP
Lindberg et al.	2021	PV	–	–	–	Sweden		GIS
Soydan	2021	Solar PV	–	11	–	Turkey		GIS and AHP

Figure 2.1. List of relevant projects involving GIS, decision making and potential estimation of renewable energy projects in the past 15 years [58].

Their methodology can be summarized in 3 steps: the first is to find the available area for onshore wind of their case study region in Germany; the second, to site select wind turbines following a LCOE¹ minimization criterion to obtain a techno-economical potential; and the third, locate wind farms and obtain a cost-potential curve on a wind farm level, including all the costs and feasibility constraints of their case study region. This project was the base definition of potential for this master's thesis. This definition will be explained in Section 3.1.

Another very important reference for the current project was the work done in [60], titled "*Wind Turbines and Rooftop Photovoltaic Technical Potential Assessment - Application to Sicilian Minor Islands*". This project follows a very similar methodology, employing the same software, QGIS and WASP, with a few exceptions, such as the case study region's latitude in the Mediterranean Sea, which results in different work conditions for onshore wind and solar PV.

The Methodology followed uses the wind software WasP, where it is possible to integrate the Generalized Wind Climate (GWC) downloaded from *The Global Wind Atlas* database together with a terrain analysis applying the IBZ model (includes terrain roughness and orography), and the generator's power and thrust curve.

The authors use this to create specific turbine sites, and thus the technical potential after micro-siting. Regarding solar rooftop PV, the solar radiation models were done by SEBE (Solar Energy on Building Envelopes), included in QGIS's UMEP (Urban Multi-scale Environment Predictor) plug-in. This plug-in uses a shadow casting algorithm [62] to calculate pixel-wise potential solar energy.

The last project that is worth detailing in this section is [8], with the translated title from Spanish: "Wind energy and territory: geographic information systems and multi-criteria decision methods in La Guajira (Colombia)". Within all the projects read and revised, this one was particularly important because it was the only one that applied GIS methodology in the same study region, La Guajira.

This project starts with spatial planning by using GIS software and finding the geographic potential in La Guajira. The authors then included in their methodology a *multi-criteria decision-making* approach with AHP, to qualify the available area and see where the best turbine-siting spots are. They conducted expert interviews to assign weight to the AHP criteria.

These studies demonstrate the range of methodologies used to estimate the technical potential of onshore wind and solar photovoltaic resources. Incorporating findings and insights from such studies will enrich the current master's thesis, considering GIS methodologies, decisions, and important considerations, as well as socioeconomic, environmental, and regulatory issues unique to the region.

¹ Levelized Cost of Electricity

3. Methodology

This chapter provides an overview of all the choices, calculations, and strategies used to achieve the goal of the thesis. The next section details the process used to estimate renewable potential in detail and provides justification for the methods chosen. The following schemes, Figure 3.1, and Figure 3.2, display the algorithms followed to assess the onshore wind and solar photovoltaic technical potential, respectively. The complete definition of potential is given in Section 3.1.

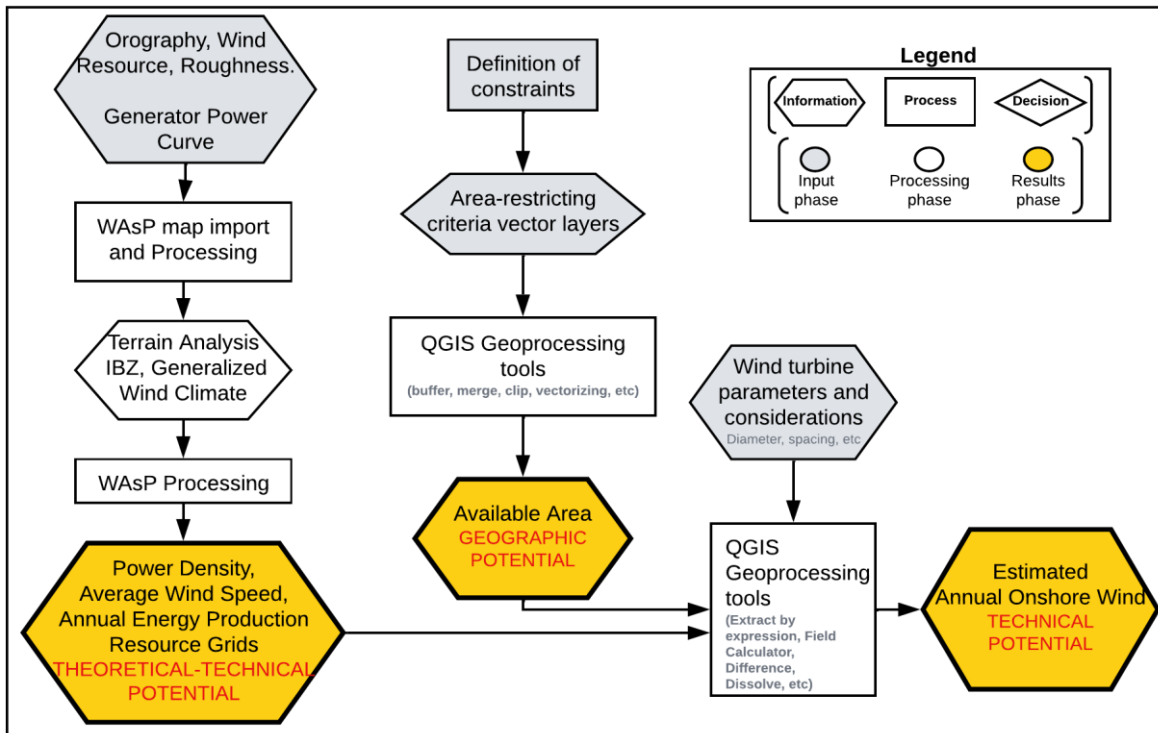


Figure 3.1. Algorithm flowchart for onshore wind technical potential calculation

Source: Self-made

In Figure 3.1, and according to the legend in it, the hexagons stand for information and the rectangles represent processes. Both types of figures can be of the colors gray, white, or yellow; a gray symbol means the process or information is an input to the whole process. Some examples are the wind turbine generator’s power curve, or the action of defining which criteria will determine the available area in the case study region.

Additionally, a white symbol implies that the information or process is a result or a transformation of the initial inputs. For example, the QGIS Geoprocessing tools use information in the form of layers to operate, modify it, and generate new information. The last is the yellow-colored symbol, which can only be information and denotes that this symbol is part of the results phase, the estimated potentials.

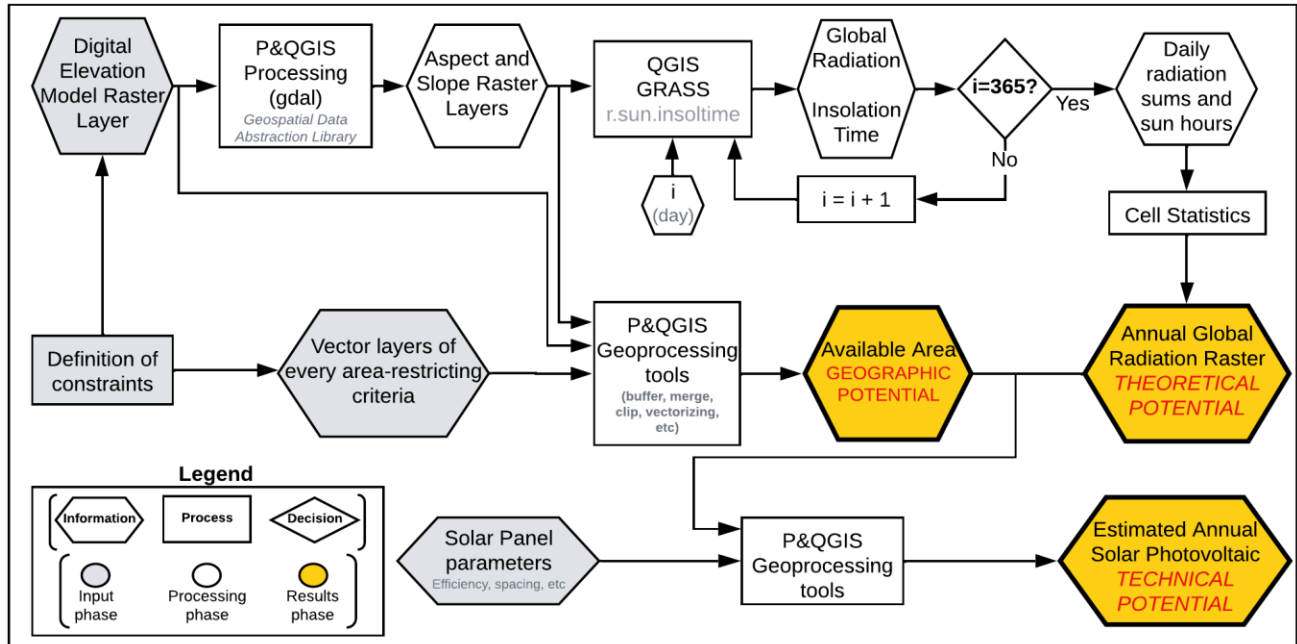


Figure 3.2. Algorithm flowchart for solar photovoltaic technical potential calculation
Source: Selfmade

The same legend is shared between Figure 3.2 and Figure 3.1. The only new symbol appearing in Figure 3.2 is the decision, always in the processing phase. The decision represents an iteration in a process. In this case, using a Python script, QGIS is verifying which day of the year (an integer from 1 to 365) the insolation time processing algorithm will calculate the daily sums raster.

In the following sections of this methodology chapter, the concept of the different potentials will be addressed and clarified for the specific region chosen. Thus, the geographic potential will be the first to be calculated for both wind and solar. Then, in Section 3.3, the methodology to calculate the theoretical-technical and technical potential is displayed. In the subsequent Section 3.4, the procedure for assessing the theoretical and technical potential of solar photovoltaics is presented.

3.1. Definition of Potential

The definition of theoretical, geographic, and technical potential in [9] is the foundation of this project. According to the author, theoretical potential refers to "the physically usable amount of energy within a given region and time." Geographical potential is further defined as "the area available for energy production, taking into account constraints such as natural protected areas and other land uses such as urban structures and transport routes." Lastly, the author defines technical potential as "the amount of installable capacity under technical constraints within a given region and time."

Based on these definitions and applying them to the case study of La Guajira, Colombia, the first potential to be calculated will be the geographic, because all area-restrictive constraints are shared, except for two that will be mentioned further. The complete step-by-step is shown in Section 3.2. Further potentials will be calculated individually for onshore wind (OW) and solar photovoltaic (SPV). Regarding OW, and as mentioned previously, the first step is to obtain a partial theoretical-technical potential using the software WAsP. Aspects such as efficiency and significant coefficients are already accounted for, but this cannot yet be considered the final technical potential.

There exists a difference worth mentioning between both algorithms shown in Figure 3.1 and Figure 3.2: for onshore wind, instead of only theoretical potential, technical aspects are included in the WAsP Processing rectangle. The power and thrust curves are used to generate the resource grids, embedding aspects such as efficiency and technical limits in them. This is an incomplete technical potential and will be referred to as theoretical-technical potential.

3.2. Geographic Potential for Onshore Wind and Solar PV

The purpose of the subsequent section is to demonstrate step-by-step how to determine the geographic potential, first for onshore wind and then for solar PV. Since the definition in Section 3.1 stated that the geographic potential is an area, by the end of this section, two vector maps (.shp files) representing the available area for each technology will be displayed. The starting point is the total area of La Guajira. This whole potential will be realized in QGIS.

Criteria Restriction by Distance		Criteria Restriction by value	
Airports	<3000 [m]	Altitude for Onshore Wind	>1500 m a.g.l
Archeological sites	<500 [m]	Altitude for Solar PV	>2000 m a.g.l
Coastline	<200 [m]	Slope for Onshore Wind	>20%
Electric Network	<100 [m]	Slope for Solar PV	>15%
Hospital	<3000 [m]		
Mangroves	<1500 [m]		
Military Zone	<3000 [m]		
Minery	<200 [m]		
Natural Protected Zones	<2000 [m]		
Political borders	<200 [m]		
Railroad	<100 [m]		
Rivers	<1500 [m]		
Streams	<500 [m]		
Roads	<100 [m]		
Rural Areas	<500 [m]		
Urban Areas	<2000 [m]		
Water Bodies	<1500 [m]		

Table 3.1. Criteria to find restricted areas.

The list of area-restricting criteria to find the available area is provided in Table 3.1 [8]. These criteria contemplate all the important environmental aspects dictated by Colombian law, and the equally important social, economic, and techno-economic factors. Next to the criteria's name is a distance or a value parameter, together with a "greater than" or a "less than" sign. This information determines the restricted range for those specific criteria.

For instance, the list of area-restricting criteria came from [8], contemplating all the important environmental aspects dictated by Colombian law, as well as important economic and techno-economic criteria. The airport criteria has a restricted distance of <3000m, this means that the area of 3 km around the whole airport will be unavailable, and further removed from the total available area.

A pre-processing phase of downloading all the vector layers of criteria was made. To make the process more organized, each layer was given a clear and concise name, clipped to the extent of La Guajira because most of the vector files covered the entire country (or even larger areas), and then saved in its own folder. Most of the layers were obtained from Colombia's official governmental geographic institutes and from QGIS's integrated plug-in *QuickOSM* (Open Street Maps).

The main government-related website to download GIS files is the Geographic Institute Agustin Codazzi, or IGAC, for its name in Spanish. Other important sites are INVIAS, the national roads institute, mainly for the distance to roads and railroads; the ICANH, the Colombian institute of anthropology and history, for the distance to archeological sites; the UPME, especially for the distance to the electricity network; and the SINAP, the Colombian's national system of protected areas, which establishes safe distances to water bodies, mangroves, national protected parks, and all the environmental criteria.

Subsequently, having all the vector files loaded into QGIS, a *Buffer* was created for all the criteria with restrictions by distance. The output is a new vector file, that was saved in the same individual folder with the respective criteria. Every input layer and created buffer were styled to be easier to distinguish from each other. A capture of all the criteria and the respective buffers can be seen in Figure 3.3.

For example, as a reference and only for visualization motives, protected areas were displayed as light green polygons with a darker green squared mesh inside; rivers and streams were styled as light blue lines with a darker blue buffer around them; coastlines and department borders are just a solid red line and can be seen above all the rest of the layers. The remaining criteria follow the same styling procedure.

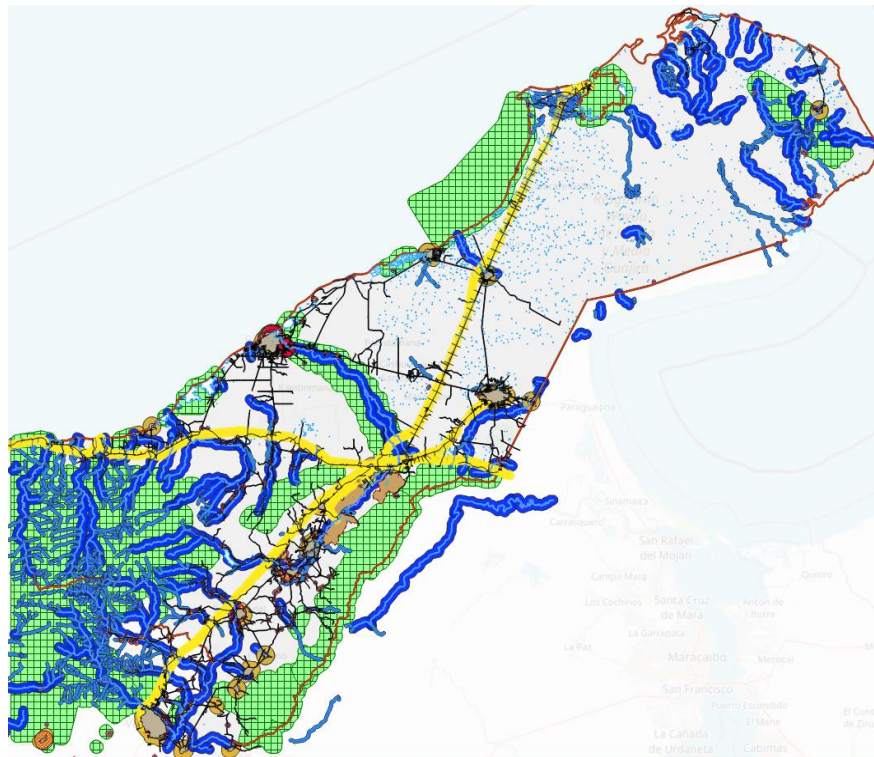


Figure 3.3. Set of Buffers of all area restriction criteria.

Once all the buffers were created, all the resulting files were put together with an integrated QGIS geoprocessing tool called “Dissolve”. This tool takes all the vector layers and combines them into a single file, where all the features are joined. This is useful because all the distance-restricted areas are now a single vector file, easy to manipulate and without risk of damaging the original data. This file can be seen in Figure 3.4.

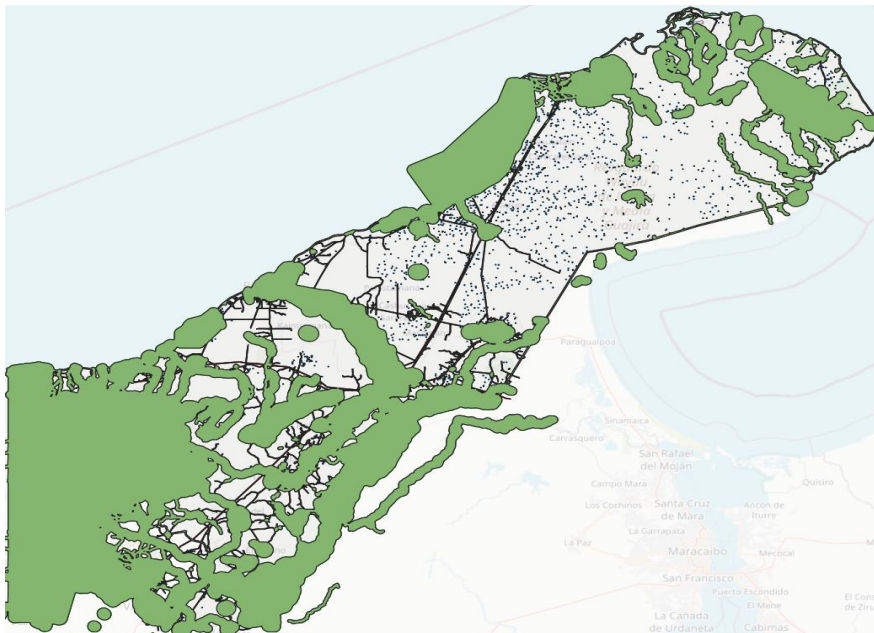


Figure 3.4. Vector file: area of criteria restricted by distance

Furthermore, it is important to know that the area of criteria restricted by distance is shared between onshore wind and solar PV, but the same cannot be said about the value restricted criteria. For onshore winds, the restricted range for slope is greater than 20%, and for altitude it is greater than 1500 meters above sea level. For solar PV, the restricted slope values are greater than 15%, and the restricted altitude values are greater than 2000 meters above sea level.

All the slope and altitude outputs are areas in a vector layer file. They were created starting from a DEM (Digital Elevation Model) raster file that was previously downloaded from the online platform of Global Wind Atlas for the case study region. The DEM Raster can be seen in Figure 3.5. This is a crucial input for further analysis of potential wind and solar resources.

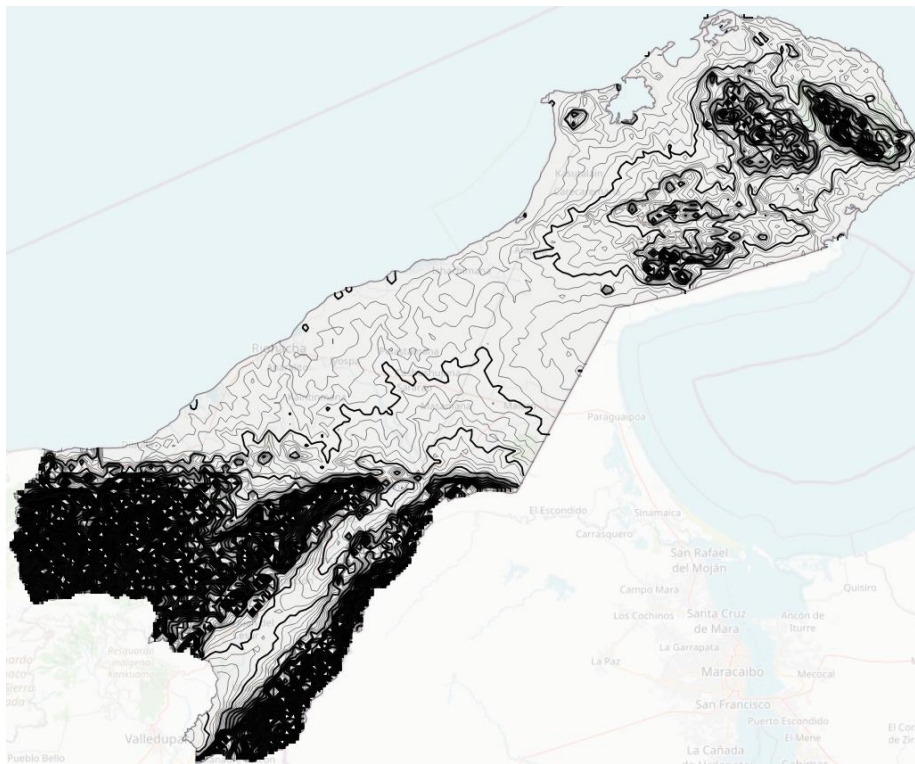


Figure 3.5. Digital Elevation Model for La Guajira contour lines.

In Figure 3.5, the DEM for La Guajira has been clipped to the extent of land, with bathymetry omitted given that it is irrelevant to the current project, thereby reducing the computational load. The DEM has also been styled using thin contour lines every 10 meters, and bold lines every 50 meters of height increase. In the south-west part of the department, dense and steep mountains are visualized as almost completely black, the reason being that the orography changes from sea-level to more than 5,600 m a.s.l. in less than 50 km. The rest of the department is relatively flat and at low altitudes.

From here on, it's necessary to distinguish between onshore wind and solar PV, since the value-restricted criteria are not shared. These criteria are shown for onshore wind in Figure 3.6, and for solar PV in Figure 3.7.

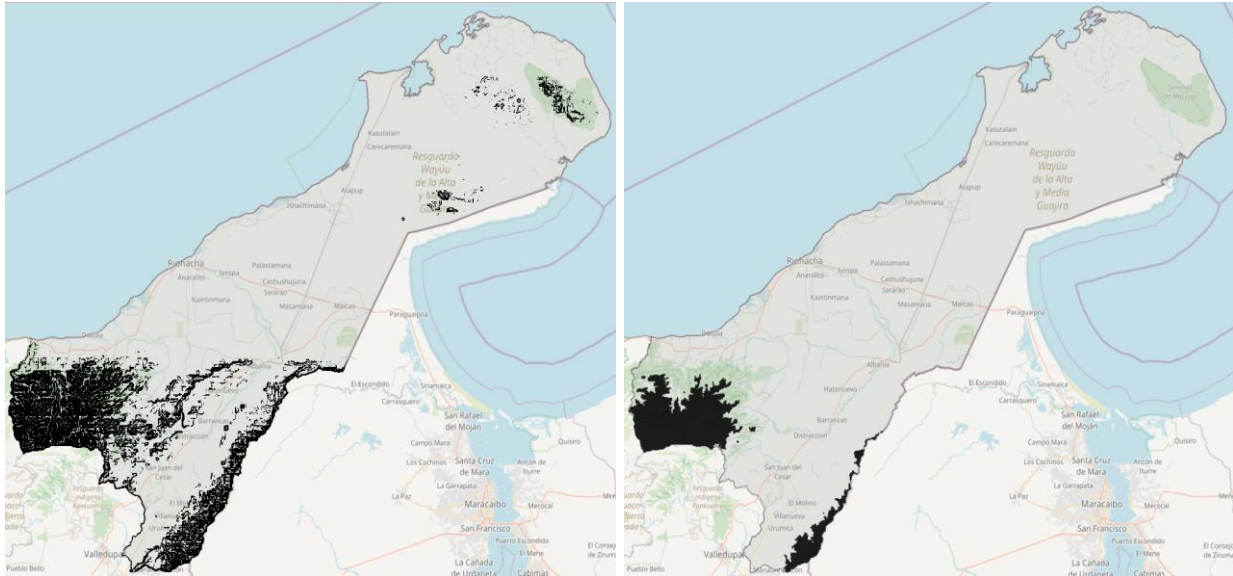


Figure 3.6. Slope greater than 20% and altitude greater than 1500m a.g.l for onshore wind.

This data was obtained from [8] and it shows common values for slope. The region of the case study contains few urban areas, and all rural areas are small in size and lack sufficient infrastructure (such as roads or an electric network) to withstand newly installed power plants. Providing power to non-interconnected areas using renewable energy is possible, but it is beyond the scope of this project.

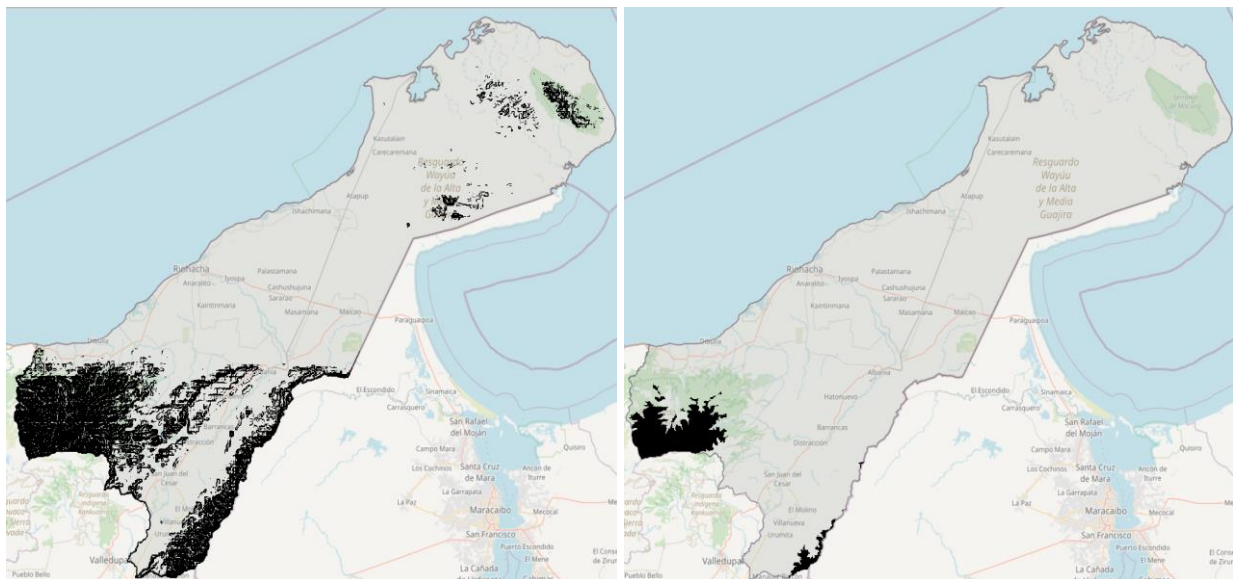


Figure 3.7. Slope greater than 15% and altitude greater than 2000m a.g.l for solar PV.

The next step is to merge the distance-restricted and the value-restricted criteria for both energy sources, starting with offshore wind. The unique dissolved layer is dissolved again with the slope and elevation vector layers from the onshore wind. This creates the “Total restricted area for onshore wind” vector layer. This area can be seen in Figure 3.8 in blue color.

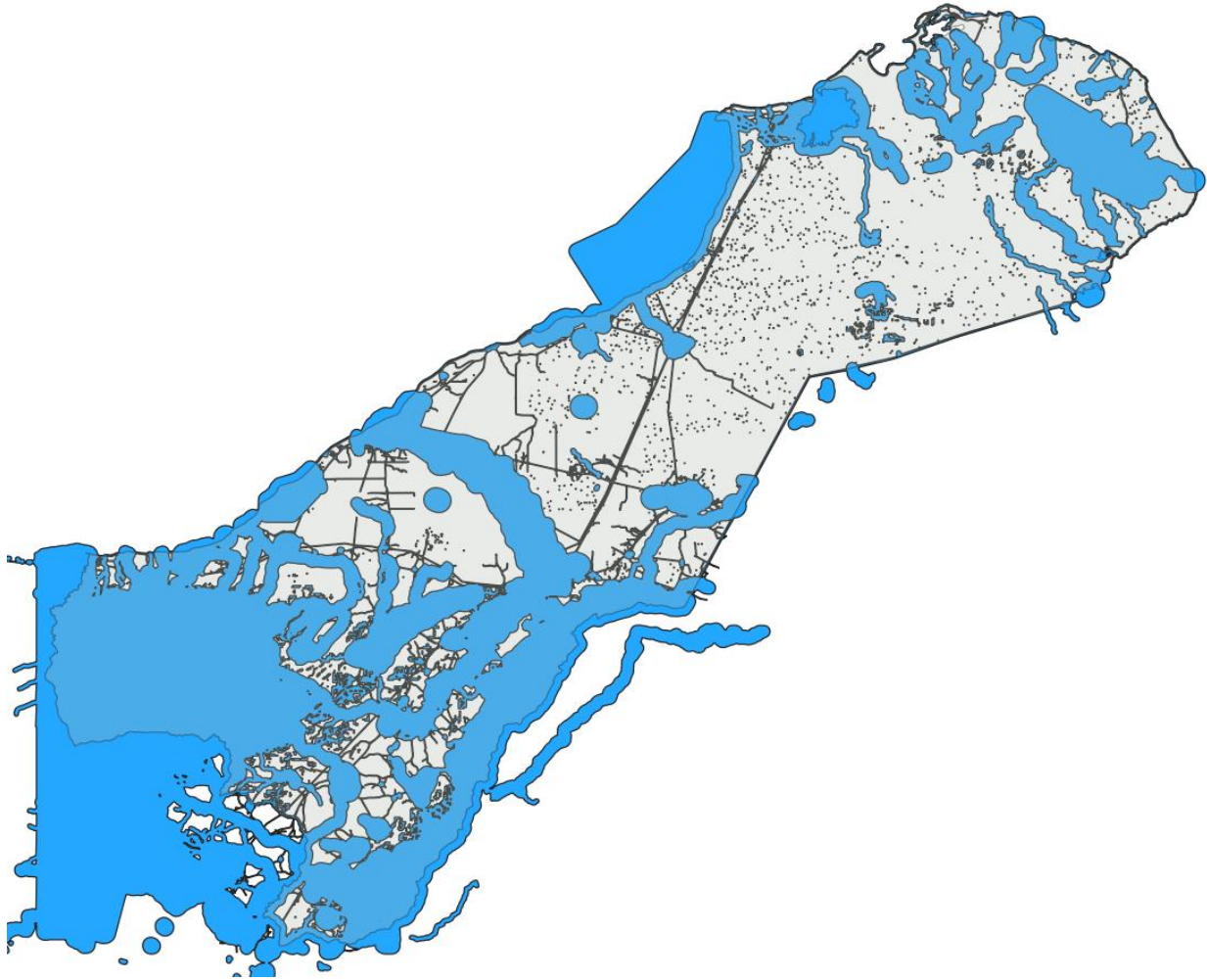


Figure 3.8 Total restricted area for onshore wind energy in La Guajira.

The same process is done to obtain the “Total restricted area for solar PV” vector layer, which can be seen in Figure 3.9 in orange color. These layers are part of the last calculation to obtain the available area. Graphically speaking, the available area is only the result of subtracting the restricted areas from the total area; this is precisely one of the strengths of QGIS. To obtain the total area of the department, the *Coastline and borders* layer, a simple vector layer with geometry *multi-linestring*, was converted to *polygon* geometry, using the “Line to Polygon” processing function.

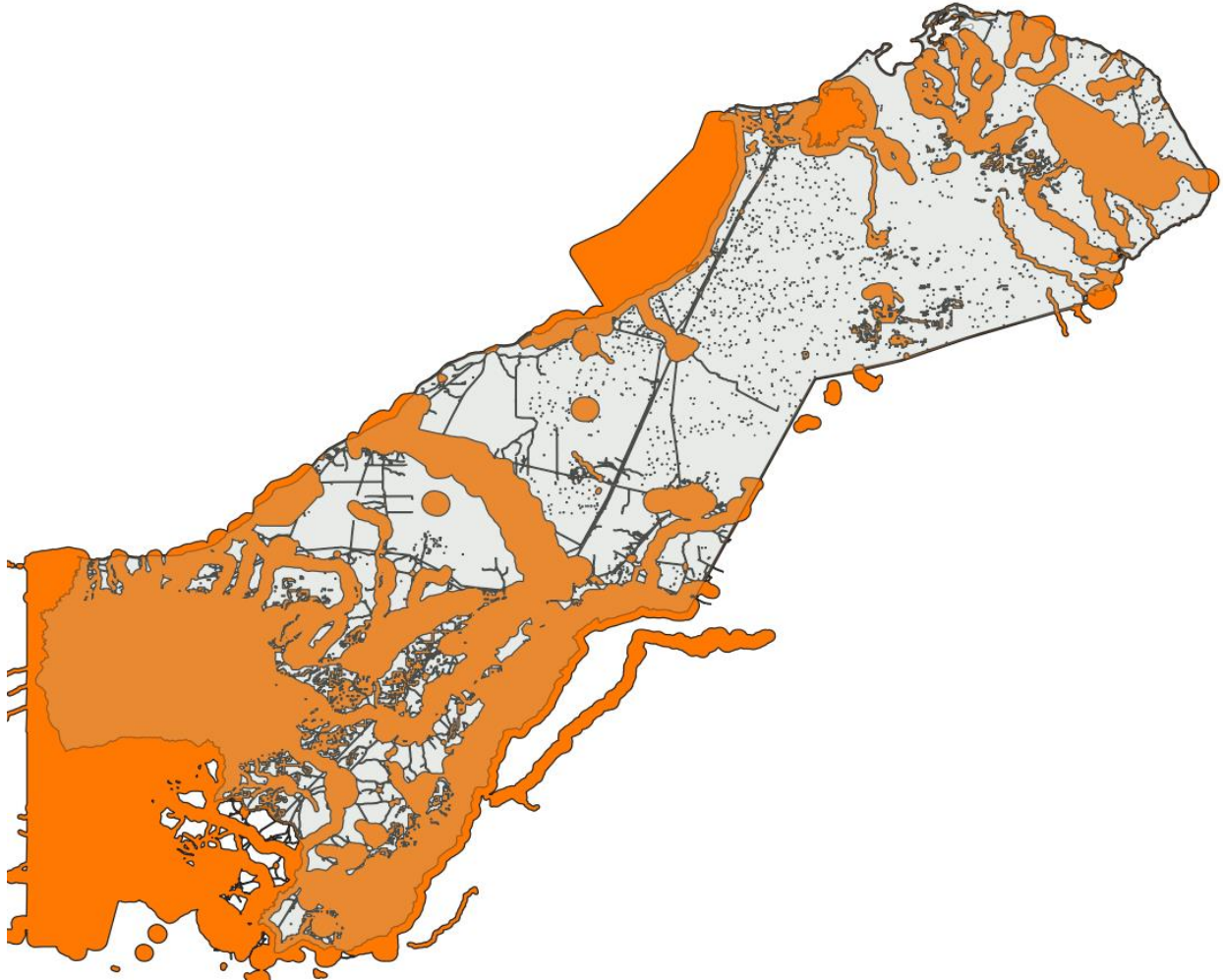


Figure 3.9 Total restricted area for solar PV energy in La Guajira.

The ultimate step is to repeat twice the processing function “Difference”, total area, called “Input layer”, and total restricted area, called “Overlay layer” in the software. The result will be the two geographic potentials (.shp vector layers) mentioned in the beginning of the current section. In Section 4.1.2. the result of the onshore wind will be displayed. Conversely, for solar PV, the result will be in Section 4.22.

3.3. Wind energy resource calculation

This part covers the Theoretical-Technical Potential and the complete Technical Potential for Onshore Wind. In addition to using QGIS, the implementation of another software, WAsP (Wind Atlas Analysis and Application Program) was necessary in this phase. This software suit was developed by the Danish technical university DTU, and enables wind resource assessment, turbine siting, and energy yield computation for single wind turbines and wind farms in locations throughout the world with varying terrain.

3.3.1. Turbine selection

The selected wind turbine is the N149/4.0–4.5 from the company Nordex. This wind turbine was chosen for two reasons: the first is the fact that nearby onshore wind projects, like “Windpeshi” (184.5MW), that are still under construction, chose this technology, which implies it had already been approved by the Colombian government and all the involved parties.

The latter reason is that the mentioned wind farm under construction invested in buying 41 of these generators, a considerably big installed capacity when compared to the only wind farm in the country, Jepirachi (2004), which has only 20 MW with 15 generators. The wind potential will be carried out in the following sections, but prior to the estimation, choosing this generator, one that’s already chosen by this big project, gives realism to the calculation.

The wind turbine’s power and thrust curve were obtained from [17], manually introduced into WasP to create the model of the generator. The specifications of this turbine and its respective power curve can be seen in Figure 3.10.

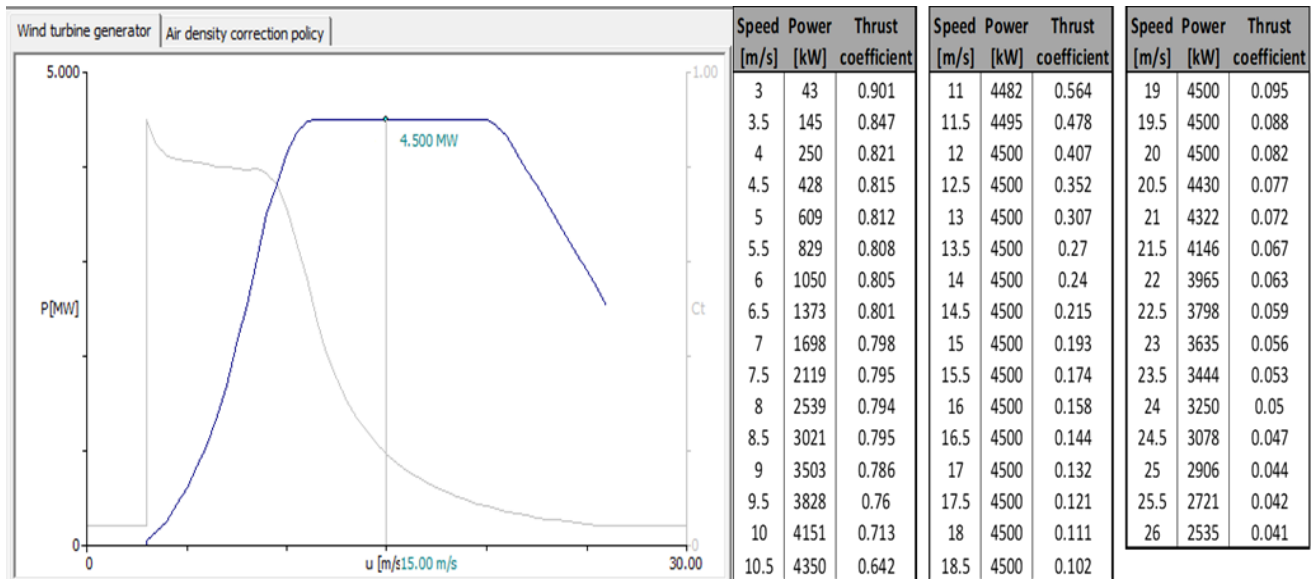


Figure 3.10. Power - thrust curves and table for generator Nordex N149/4.0-4.5

The study of turbine productivity is a fundamental aspect of the construction of a wind park. The market offers different types of wind turbines that are divided into classes, according to parameters defined by the International Standard IEC 61400. This standard determines if a turbine is suitable for the normal wind conditions of a particular site. Turbine classes are determined by three parameters, as explained in Section 1.3.

In the power graph in Figure 3.10, the rated power is located between the speeds of 12 and 20 m/s. The cut-in speed for this generator, the minimum speed at which it will start producing power, is 3m/s. Between the cut-in and the lower rated power speed, the turbine is working in a non-rated region. Something similar happens between the upper-rated power speed and the cut-out speed.

3.3.2. Theoretical-Technical Potential

The objective of using the software WASP is to obtain quality raster layers for Annual Energy Production, Power Density and Wind Speed. Firstly, a file containing the “Generalized Wind Climate”, or GWC, is downloaded from the Global Wind Atlas platform and added to the WASP workspace. The GWC displays important information, such as climate data. This tab exhibits a table filled with wind speeds, divided into different wind classes and different heights above ground level.

The information in the table can be selected in whole rows (constant height), in whole columns (same R-class) or by individual cells. In either case, a wind rose divided into 12 sections (30° each) shows the direction and frequency in which wind flows. In this wind, north would be 0°, east 90°, south 180°, and west 270°; section 1 is aligned with the 0° north direction, having its leftmost and rightmost limits of 15° in the counterclockwise and clockwise directions, respectively. For example, in Figure 3.11, the selection of R-class 1 indicates a clear and predominant wind direction coming from section 4, with a shape parameter of 11.2 m/s and a mean wind speed of 9.98 m/s.

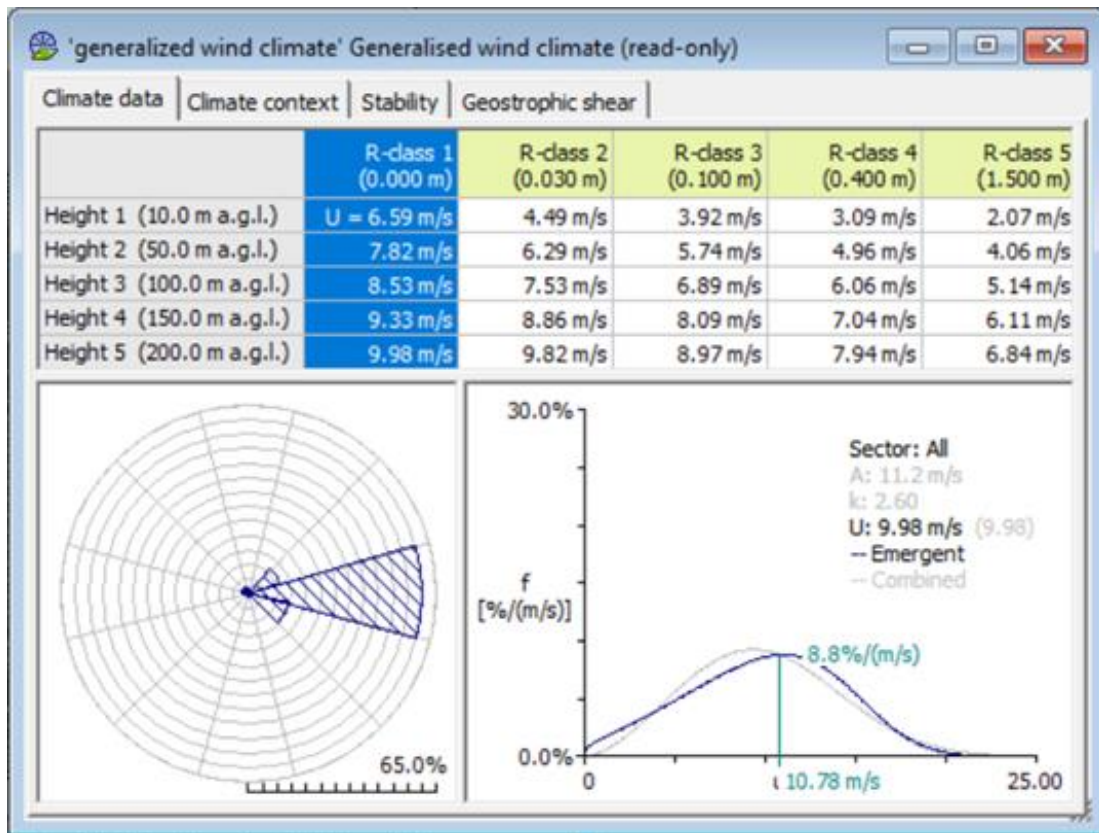


Figure 3.11. Climate Data of Generalized Wind Climate parameters.

Orography and roughness information were obtained from the *Global Wind Atlas*. This information was then imported into the WASP Map Editor to geo-reference with the

chosen target map projection: UTM-WGS 1984, zone 19N, the same used in the QGIS project, with CRS 3857. In this step, the degrees format was given as DDDMM (where D stands for Degrees and M for Minutes). The metric unit was chosen as km; the output would be created by a given center in latitude-longitude coordinates, and a 500 km map extension. This is a very vast area with a big computational load that took a couple hours of processing.

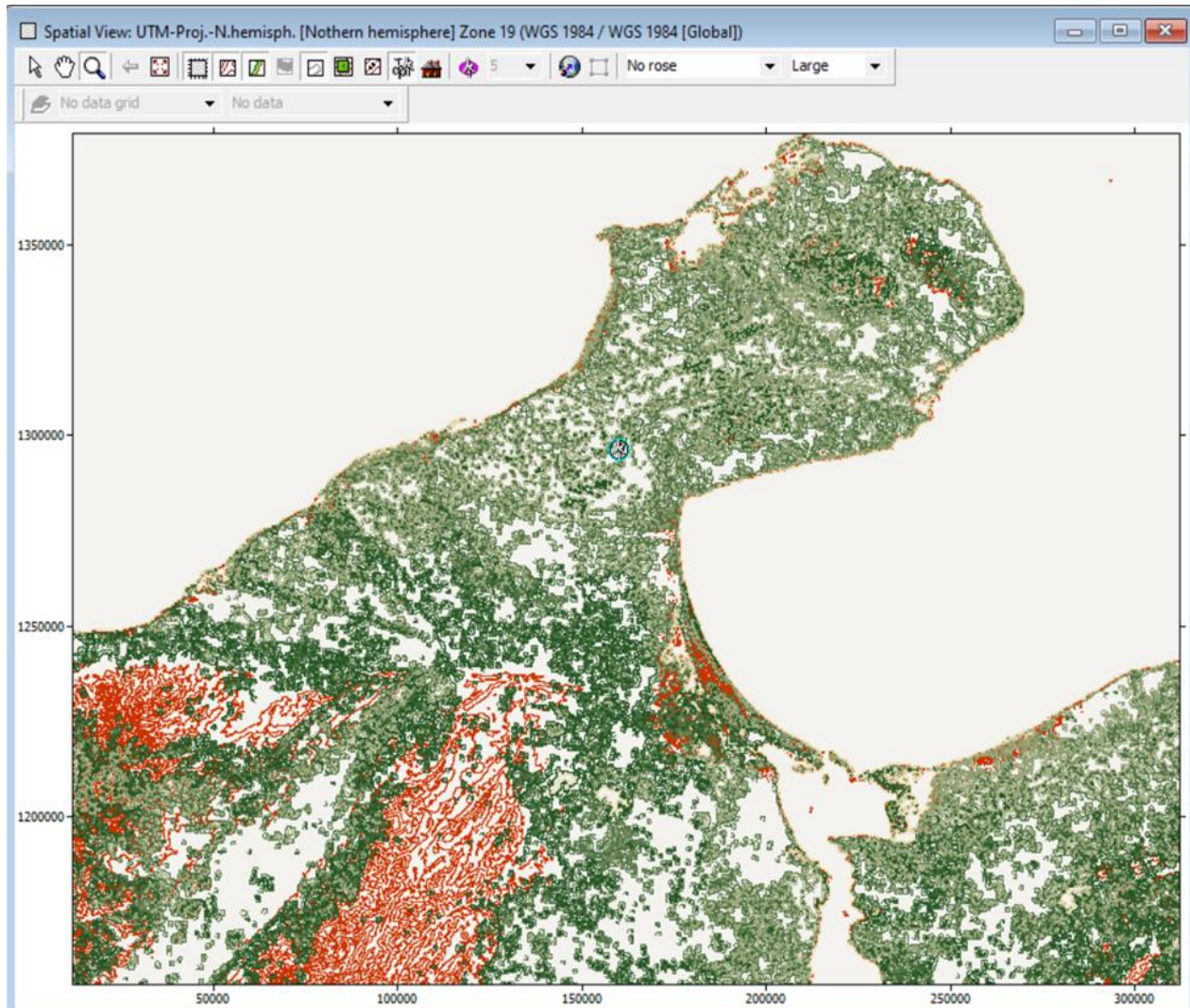


Figure 3.11. Terrain Analysis (IBZ) for La Guajira including roughness and orography.

After doing this process for both terrain roughness and elevation, the result will be a vector file called Terrain Analysis (IBZ), done with the standard linearized model included in all WAsP distributions. This vector file can be seen in Figure 3.12. Next up, the turbine model is uploaded either to a random turbine site or to a resource grid. In this case, since the intention is not to microsite any turbines, it will be uploaded to a resource grid, to rather understand how these turbines would perform in the whole territory.

Then, a Resource Grid is created. The resolution was set to 750m (square grid) because this is the 5-diameter security distance to ensure turbines are not affected between them. The number of grid cells for the calculation is 97,393. Each one of these cells will have a value for Annual Energy Production (AEP), Mean Wind Speed, and Power Density. These were the most important variables for the technical potential estimation. The resource grid's spatial view can be seen in Figure 3.12. Here, all the necessary parameters were input.

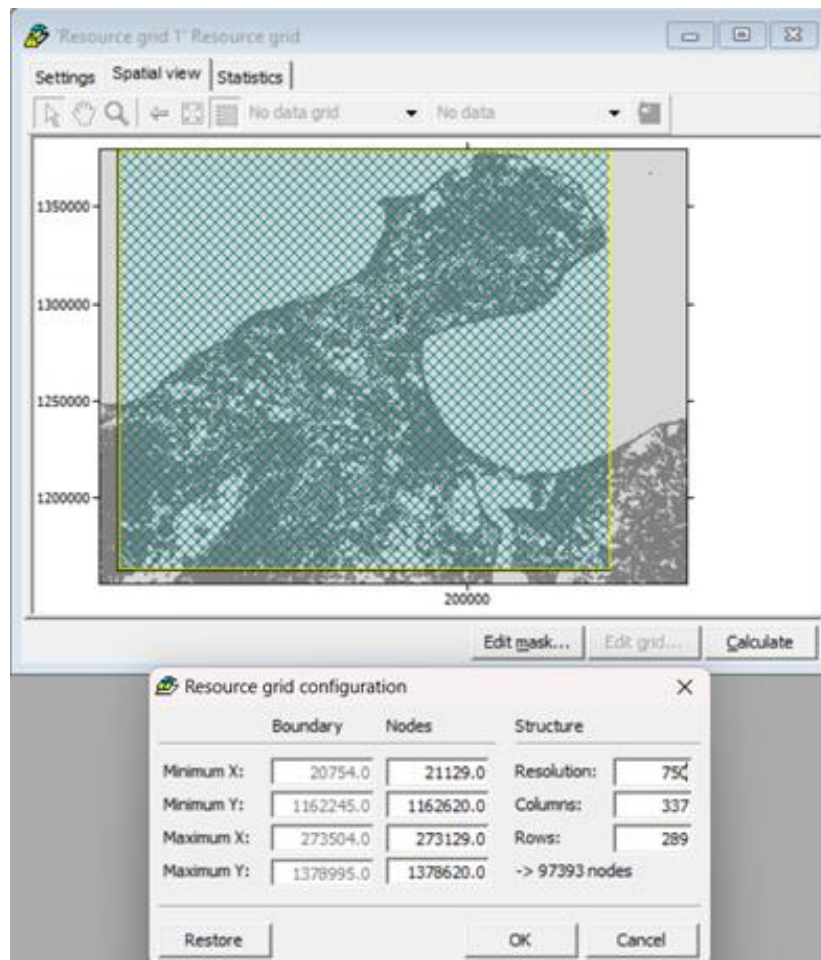


Figure 3.12. Resource Grid spatial view and configuration parameters.

The following step is to calculate the AEP, performance tables, Predicted Wind Climate (PWC) and site effects. This same option can be used for single turbine sites, already modeled wind farms, or resource grids, which is the best option to obtain geographic information in the form of raster layers. The output format is ASCII and can be easily imported into QGIS when the simulation is over. The resulting resource grids for AEP, Mean Wind Speed and Power Density can be found in Section 4.1.

3.3.3. Technical Potential

The technical potential will be realized using only the vector grids created in Section 4.1. Additionally, only the Annual Energy Production is of interest for the estimation of the potential. Firstly, the vector grid will be clipped only to the geographic potential, using QGIS geoprocessing tools. This result can be seen in Figure 3.13.

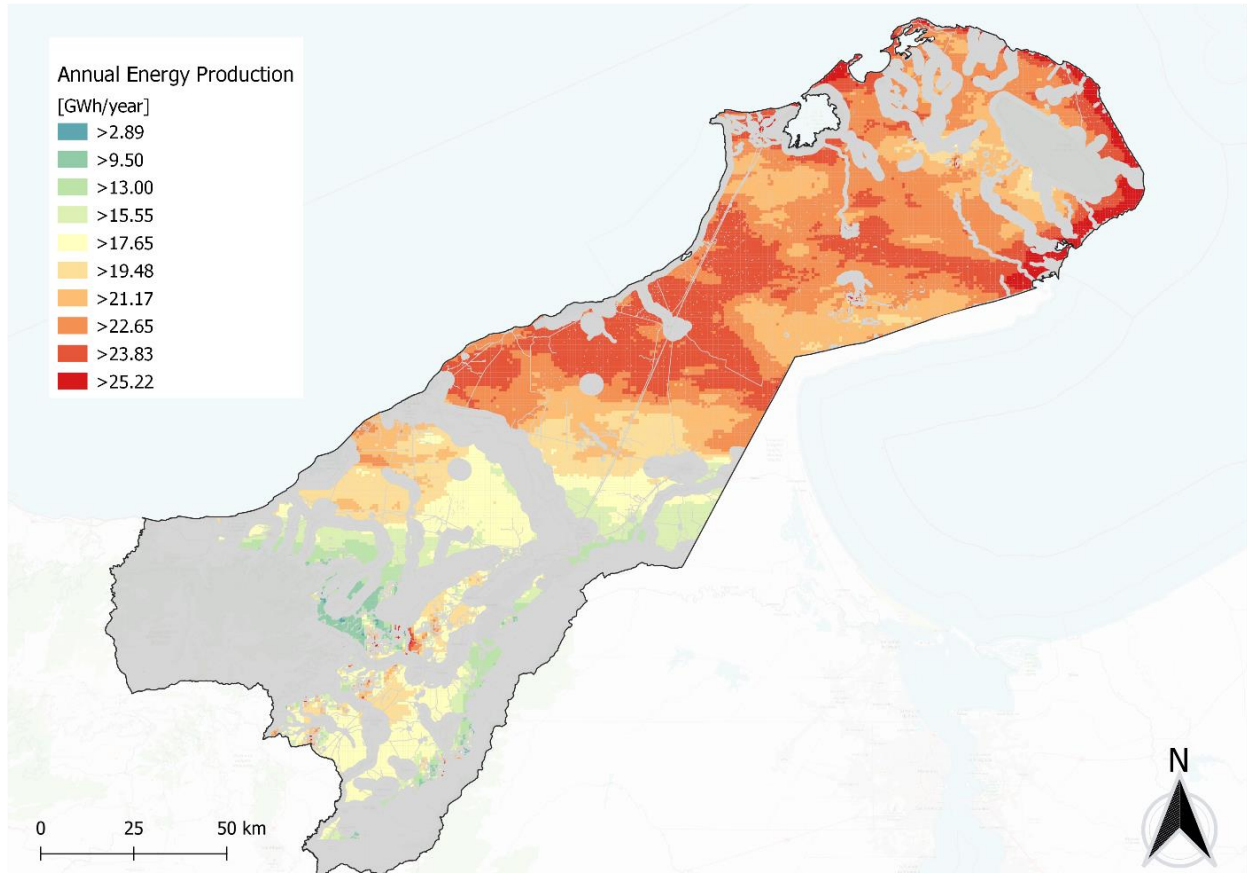


Figure 3.13. Annual Energy Production in Available Area for Onshore Wind.

There exists a situation with the current AEP vector grid, and it happens that by removing areas, some of the resolution cells are no longer capable of being considered as a possible turbine installation site. Further filtering will be done to all the resolution cells that, for any number of reasons, don't have at least 60% of the area of a full resolution cell.

To understand this filter better, it's crucial to remember that between each resolution cell center, five wind-turbine diameters exist. Knowing that 4D is still a safe distance for wind turbines, the proportion of the areas of a 5D sided square versus a 4D sided square is around 60%. The amount of space in the grid had an impact on many cells, and as a result, thousands of these had their areas reduced or split into numerous sub-cells, none of which could be potential locations for the installation of wind turbines.

The filtered AEP map is shown on the left side of Figure 3.14. If compared to the non-filtered version, some darker zones can be seen. On the right side of the figure, a zoomed zone shows in gray all the cells that were removed. The resulting grid cells are not divided and have enough area for a wind turbine to be placed in them.

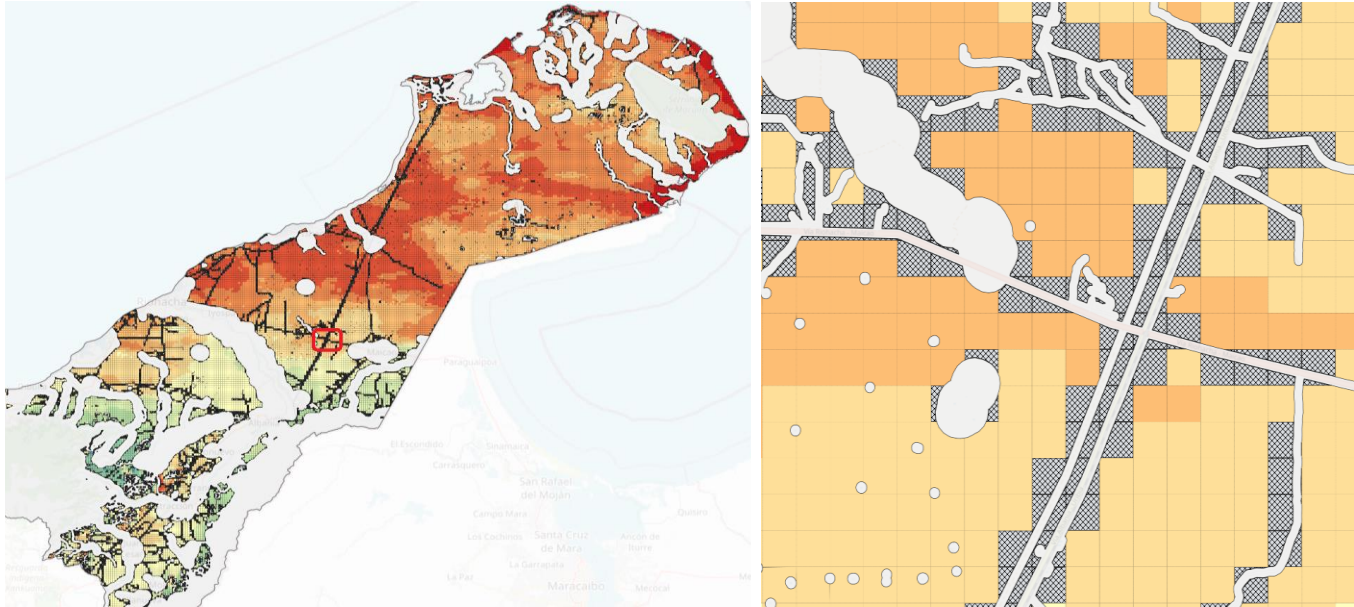


Figure 3.14 Filtered AEP for onshore wind on available area.

This graphic technical potential is hard to understand and dimension, reason why, to really have a grasp of how much energy can be generated up to the technical constraints in the region of Guajira, the Total Annual Energy production for the whole region will be found. A python script capable of interacting with the user was done, to visualize all the fields in a selected active layer and let him or her choose what column to add. The script is in Appendix C and can be freely modified, used, or improved according to the need.

The resulting filtered AEP vector layer was obtained by applying two specific conditions in the *expression* box of the processing function: the first condition was using the “num_geometry()” function to count the number of parts into which every cell was divided. This number n should be less than 2, which leaves only whole resolution cells to work with. The second condition was for that whole cell to have an area ($\$area$) greater than 0.36 km², the area of a 4D instead of 5D square.

The last step is to create a table summarizing all the important information. Among the aspects to include are total available area, maximum installed capacity, total AEP, and number of available cells. Total Area and Total AEP were calculated with a Python script created from own source and can be found in Appendix C. This information can also be checked with the “Statistics tab that is in the ”

3.4. PV Solar energy resource calculation

This section covers the solar panel chosen, the theoretical and technical potential for Solar Photovoltaic. As a complement to using QGIS, python scripts and console, and GRASS's processing tools are very important and powerful.

3.4.1. Technology Selection

The technology selected is the solar panel in [16], a monocrystalline module from the company Vertex, with a maximum power output of 670 W and a maximum efficiency of 21.6%. This panel was chosen because it's distributed by a renown company, has a high energy yield, and is one of the highest installed powers per panel in the market. Additionally, a panel with all these characteristics is practically designed for utility-scale systems, very much in line with the current project.



Figure 3.15. Schematic of Vertex panels in a desert-like zone that resembles the Guajira region

The panels model is the Vertex TSM-DE21, a 2.4 x 1.3 meter panel, with only 33 kg of weight. For the maximum output, 670W, the open circuit voltage is 46.1 V, short circuit current of 18.62 A. The panel has a NOCT (Nominal Operating Cell Temperature) of 43°C, but a working range of up to ~85°C. A representation of the exact Vertex panel being used in a flat, desertic zone like Guajira can be seen in Figure 3.15, only with visualization purposes. The complete datasheet can be found in [16], including electrical schematics, I-V curves, and P-V curves.

The guajira region has a potential estimated way over the 32GW of installed capacity, as was mentioned in Section 1.6. Hence the importance to have high output panels for such a high irradiance region.

3.4.2. Theoretical Potential

The theoretical potential for solar PV comes from the use of the integrated GDAL processing section. Everything starts from a DEM raster file, the same used in Section 3.2 for the geographic potential calculation. With this file, and with P&QGIS, further Aspect and Slope raster files were obtained, using a python script that can be found in Appendix C section.

Some of the important considerations for the Aspect and Slope calculation are to define well the folder in which all the files will be saved, ideally in the same folder. The code has a variable storing the address of a main folder, and inputs and outputs are referenced using this variable.

After finding these files, *Aspect* and *Slope* have been found, you can work with them directly if the region is not too big, or you can clip them to a smaller extent, which is this project's case, so the computational load is kept at minimum. The extent of the layer used in this project is like 290km². Resolution normally is just some hundreds of meters, so any information that is just useless, is not worth calculated.

The next step is to use the *r.sun* processing tools from GRASS, another integrated processing library in QGIS. The exact function that will be used is *r.sun.insoltime*. This function creates a model of solar irradiance and irradiation; the output of a single simulation is a set of raster files, obtained all by daily sums of hours of sun, Global Radiation, Beam Radiation, Reflected Radiation, and Diffuse Radiation.

The processing is done for a single day of the year, input as a number between 1 and 365. The inputs for this process are the DEM, Slope and Aspect raster layers, with or without clipping. Single values for Slope and Aspect can be input, but the whole raster file makes it a better simulation. Some other not-necessary parameters such as input raster files for longitudes, latitudes, radiation coefficients (for real-sky beam and diffuse), *Linke* coefficient and horizon information were left at their default configuration.

The Albedo coefficient in the ground was set to be between 35% to 40% for the dry sand and arid ground in La Guajira [63]. Regarding the Advanced Parameters section in the configuration of the process, the time step when computing all-day radiation sums was defined, in decimal hours, to be 0.5; every 30 minutes. The sampling distance step coefficient was left at default in 1.0, and the input file was to be read in one single chunk, not partitioned. The GRASS GIS 7 region was set manually by dragging in the canvas a rectangle that would cover all the land, without leaving too much free space.

Now, as for the simulation day, only having a precise day simulation was not enough. Even if Colombia doesn't have strongly marked seasons like countries with higher latitudes, not every day offers the same exact radiation. For this reason, a python script

was created to run 365 simulations, iterating the day number, and then saving them into a previously specified folder, each with a distinctive number in their name. Specifically, this process took a lot of computational load, and here is when clipped inputs are an advantage in processing. Additionally, for this same reason, already having the Global Radiation for every day, was enough information to do the technical potential estimation planned. The Python script for this can be found in Appendix C.

Furthermore, when all the 365 Global Radiation raster files were obtained, another processing tool called *Cell Statistics* was used. Here, and by selecting all the 365 .tif raster files, the mean value for each pixel in every raster throughout the year was averaged. This single raster file was called Yearly Mean Global Radiation. The resolution was increased for this raster, going from square pixel size of ~280m to exactly 200m. The resulting raster file can be observed in Section 4.4, together with the vectorized version.

3.4.3. Technical Potential

The first step to finding the PV technical potential is to obtain the Yearly Mean Global Radiation vectorized grid on the available area for solar PV found in Section 3.2. A minimum area threshold of 30m² (less than 0.1% of initial cell) is set, to eliminate very reduced pixels. This vector layer can be seen in Section 4.6.

The next step is to calculate the important photovoltaic parameters that characterize the chosen technology. This is the only aspect missing to include in the potentials estimated so far, the efficiency of the specific Vertex PV panel, the rule of thumb spacing methods to properly account the available area, and the performance ratio to obtain the Annual Electricity production.

In the case study specific context, panels will be situated in flat terrain. The mutual-shading phenomenon is important because it has a large influence on the electrical yield due to the space that must be left between the modules. According to what was done in [60], the worst scenario was taken for the calculation of the spacing between the modules, the day of winter solstice.

Because Colombia lies in the northern hemisphere, on the winter solstice the row spacing required to avoid mutual shading is maximal [65]. This distance, as shown graphically in Figure 3.16, can be determined according to [66] using the following formula:

$$d = d1 + d2 = L * \left(\frac{\sin(\beta)}{\tan(h_0)} + \frac{\sin(\beta)}{\tan(\beta)} \right) \quad (2)$$

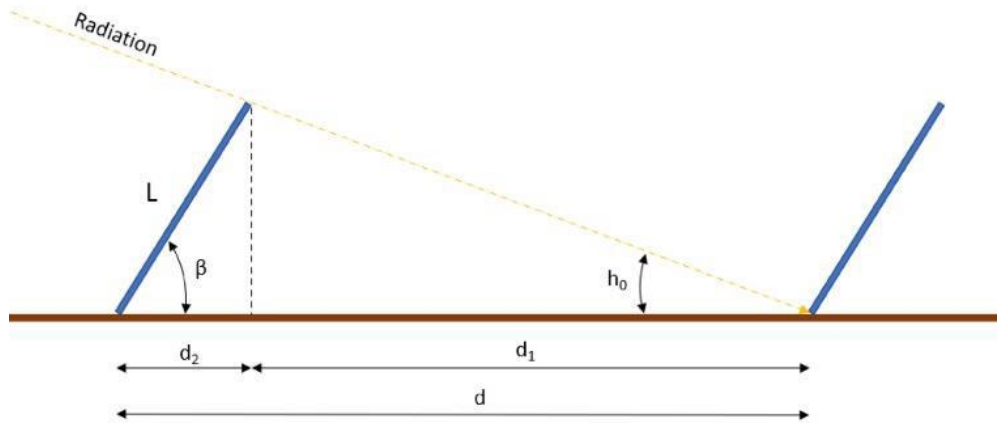


Figure 3.16. Interrow spacing diagram

It can be observed that the distance between the rows depends on the variation of the sun's altitude during the day and the year. In turn, the solar elevation angle depends on the declination angle δ , the latitude φ , the hour angle ω . According to [68], it can be calculated for a given latitude and a given day and hour as follows:

$$\sin(\alpha_s) = \sin(\varphi) * \sin(\delta) + \cos(\varphi) * \cos(\delta) * \cos(\omega) \quad (3)$$

By combining the two formulas, (2) and (3), and knowing the physical dimensions of the panel, it is possible to calculate the distance between the rows at the winter solstice.

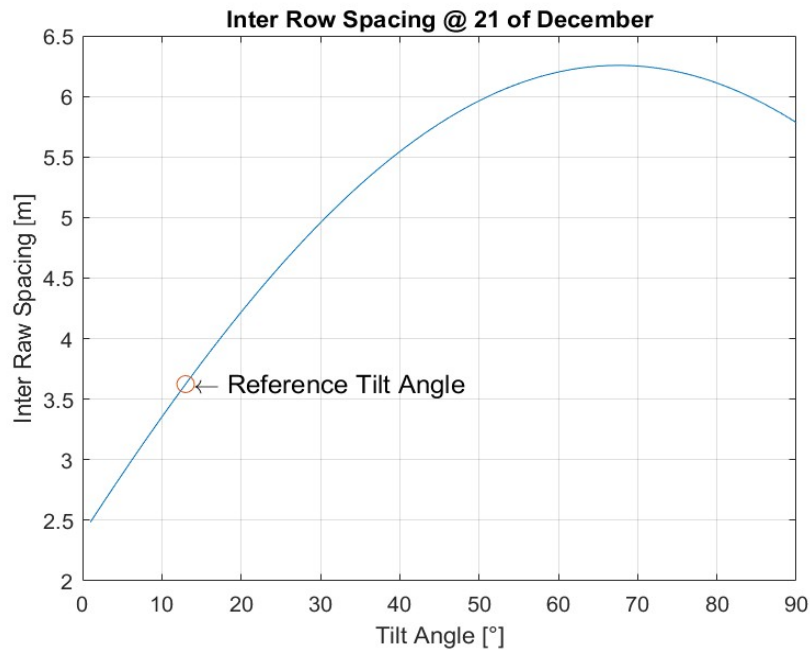


Figure 3.17. Values of interrow spacing and tilt angle for panels located in longitudes of la guajira.

Figure 3.17 shows the value of the interrow spacing [m] to be assumed as a function of the tilt angle [°]. In this case, the reference tilt angle is 13.3°, according to [67] and the inter row spacing is 3.62 m. This interrow spacing is the same d found in equation (2) and Figure 3.16. At this point, knowing the row spacing d and the physical dimension L of the panel (1.3 m), it is possible to obtain the reduction coefficient for flat surfaces (originally roofs), named Coverage Index Coefficient, $CCOV$, calculated as:

$$C_{COV} = L / d \quad (4)$$

The resulting coverage index coefficient is $CCOV = 0.3591$. The following parameter is the C_{APV} , defined as an overall corrective coefficient. Since the fraction intended for general services is set at 15%, the overall coefficient is equal to $C_{APV}=0.85$. Now it's possible to calculate the Annual Electricity Production (PV AEP), which can be estimated as follows [69]:

$$AEP = H_G * S_{PV} * \eta_{STC} * PR \quad (5)$$

In (5), the H_G stands for the Global Radiation, measured in [kWh/m²]. The factor S_{PV} stands for the total available area, measured in [m²]. Finally, the expression η_{STC} is the efficiency of the PV module at standard test conditions, and PR represents the ratio of the final system yield to the reference yield, comparing the energy that is generated with the amount of energy produced under the same irradiation but under ideal no-loss conditions.

The only parameter missing to calculate PV AEP is the Performance Ratio. The Performance Ratio, in this study, considers both Physical (shading or differences with STC) and electrical (cable losses, AC-DC conversion) phenomena and it can be calculated considering different loss factors, described as follows [69]:

$$PR = \eta_{mis} * \eta_{d-r} * \eta_{wir} * \eta_{temp} * \eta_{shad} * \eta_{CPU} \quad (6)$$

- η_{mis} : tolerance with respect to STC data and mismatch of module current-voltage characteristics; Value of 0.97 [69]
- η_{d-r} : dirt and reflection of the front glass. Value of 0.976 [70][71];
- η_{wir} : cable losses. Value of 0.994 [72];
- η_{temp} : over temperature compared to STC. Value of 0.89 [16];
- η_{shad} : shading losses. Value of 0.98 [73];
- η_{CPU} : MPP tracker and DC-AC conversion losses. Value of 0.98 [74];

Considering the efficiency of the module and the value of the performance ratio PR , the overall efficiency of the system for converting solar energy into electricity is obtained as follows:

$$\eta_{SYST} = \eta_{STC} * PR = 16.8\% \quad (7)$$

The AEP is now calculated using the field calculator from QGIS, following (5). Every pixel from the yearly mean global radiation vector grid was multiplied to the respective area of the resolution cell containing this radiation value. Then, C_{COV} , the area coefficient considering the interrow spacing was included, together with the overall system efficiency. The resulting PV AEP vector grid can be seen in Section 4.6, together with all the results from this section.

4. Results

In this section, all the results from geographic, theoretical, and technical potential will be organized, with onshore wind first and solar PV second.

4.1. Onshore Wind Theoretical-Technical Potential

Upon completion of the procedure in Section 3.3.2, the results are the resource grids for Annual Energy Production. This is a file that can only be accessed on WAsP, which is a great disadvantage because it is licensed software. Hence, the output raster was submitted to a vectorization process.

The ASCII file was imported into QGIS as a raster file, and as a first step, a grid vector layer was created from the processing options. This grid has the same 750m dimension as the WAsP raster file. The second step is to create centroids on every square of the recently created vector grid. Thirdly, another processing function will sample the value of every raster pixel for the recently created centroids.

Every single centroid now has copied within itself the value of the raster pixel that was in a layer beneath it. The last step is to open the initial vector grid's properties to join the sampled value in the centroids. The reason for this long process is that QGIS doesn't allow geometries like squares to be sampled from raster's, only from point geometries like centroids.

Lastly, it is recommended to export as a new vector file the recently joined grid to make the process permanent. The same process was done for all three outputs from WAsP. Since only onshore projects are carried out, an extra clipping step was made so that the resource only fits in the land area.

The raster resource grid from WAsP and the Vector grid from QGIS for Annual Energy Production can be seen in Figures 4.1 and 4.2, respectively. The raster and vector resource grids for Power Density can be seen in Figures 4.3 and 4.4, respectively. Likewise, the raster and vector resource grids for Mean Wind Speed can be seen in Figures 4.5 and 4.6, respectively.

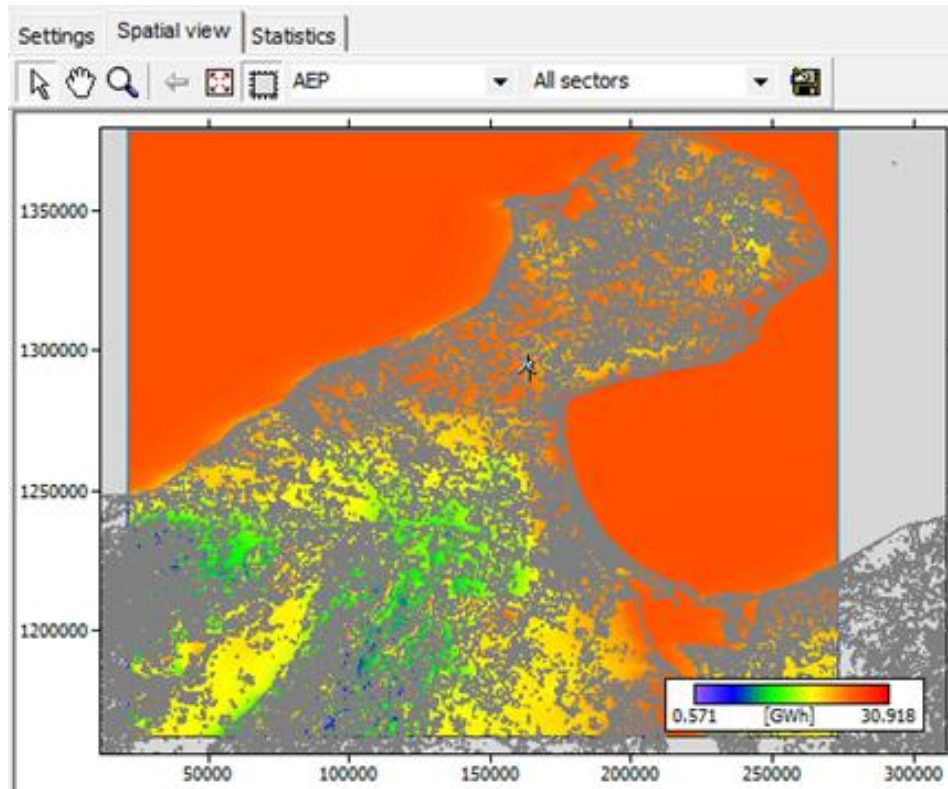


Figure 4.1. WASP spatial view of the resource grid for Annual Energy Production

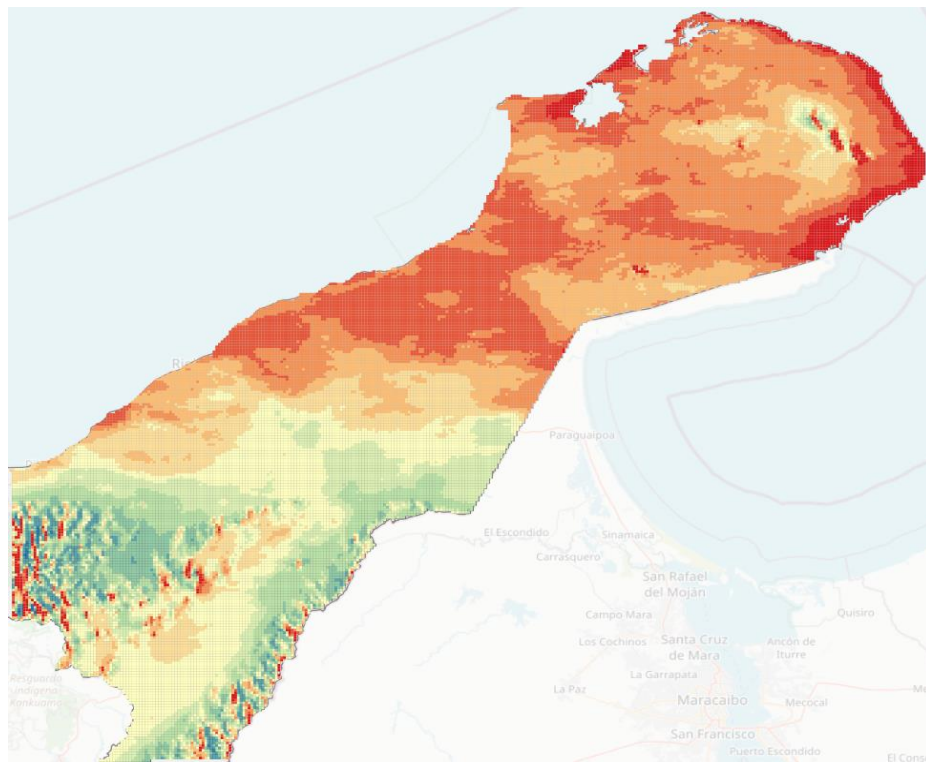


Figure 4.2. QGIS Vectorized resource grid for Annual Energy Production

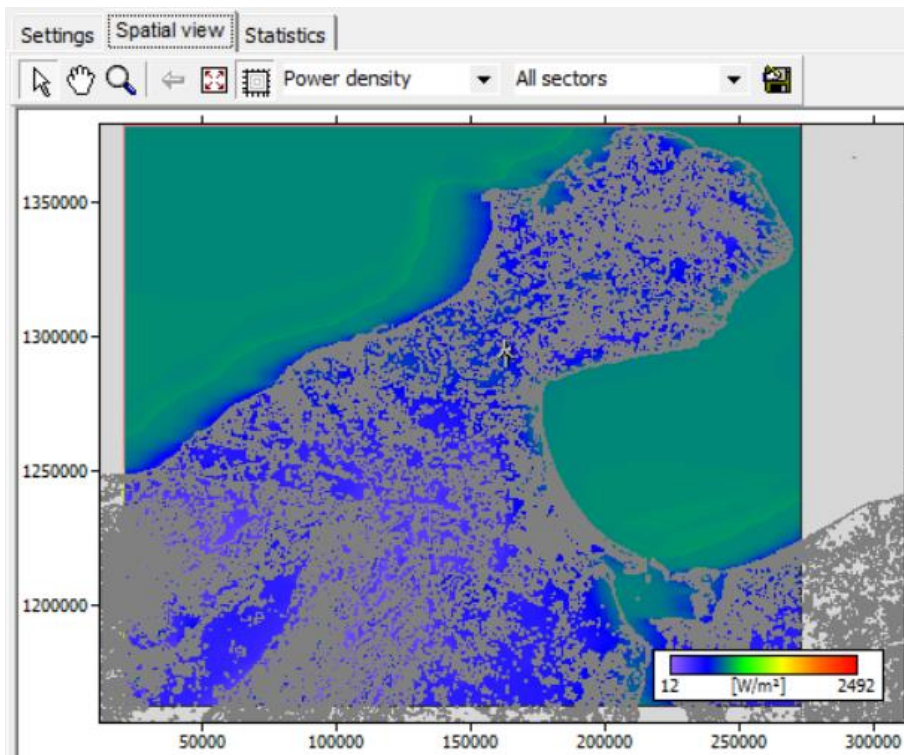


Figure 4.3. WASP spatial view of the resource grid for Power Density.

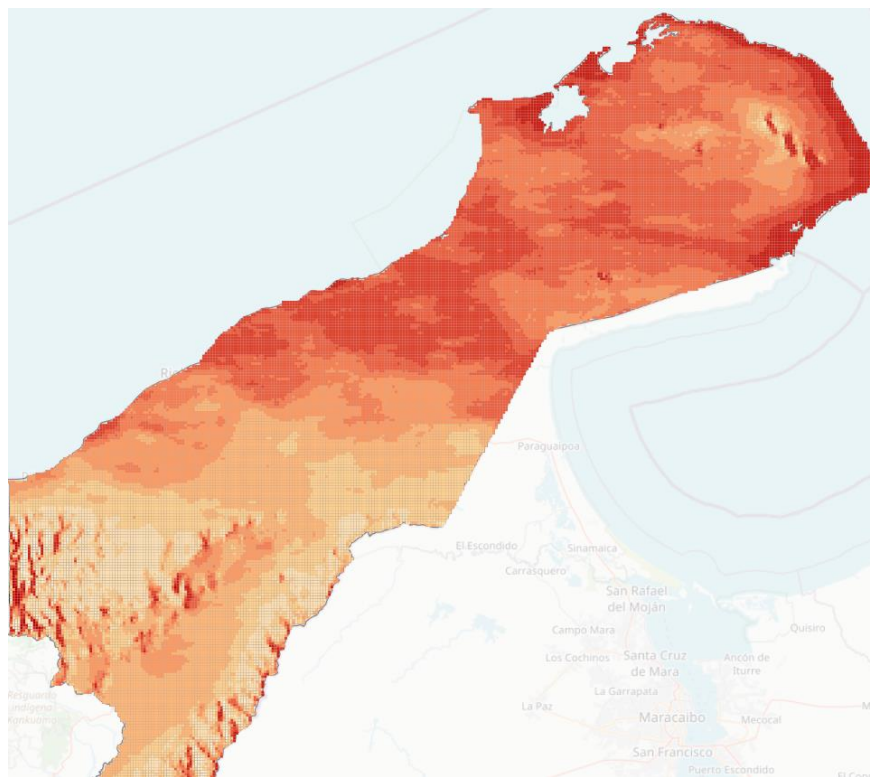


Figure 4.4. QGIS Vectorized resource grid for Power Density.

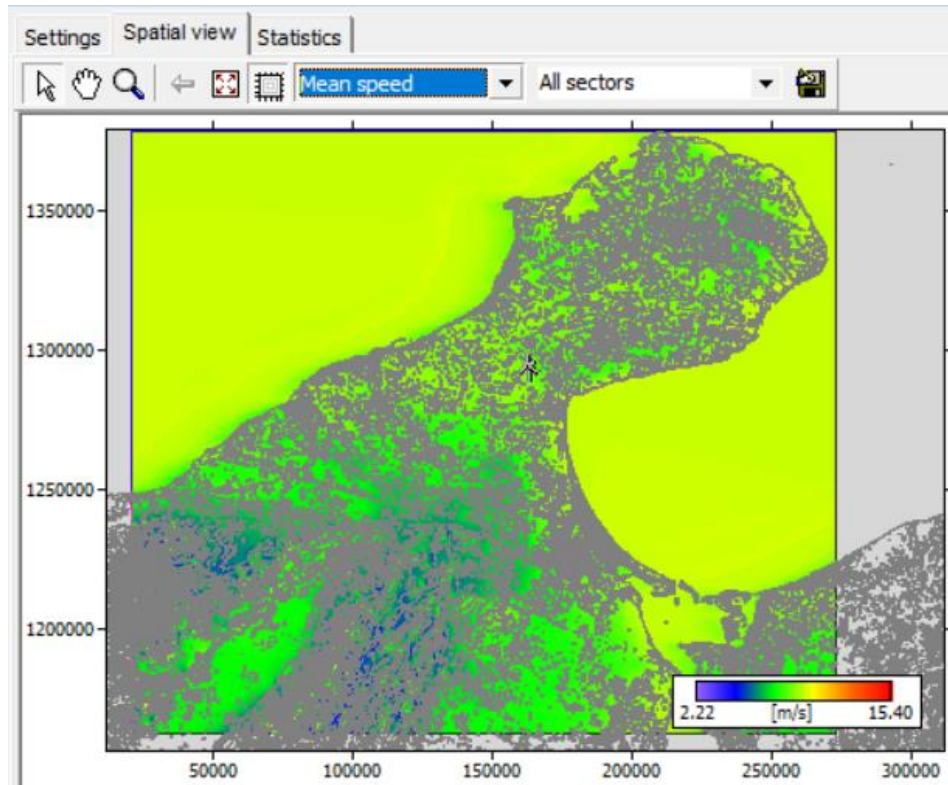


Figure 4.5. WASP spatial view of the resource grid for Mean Wind Speed.

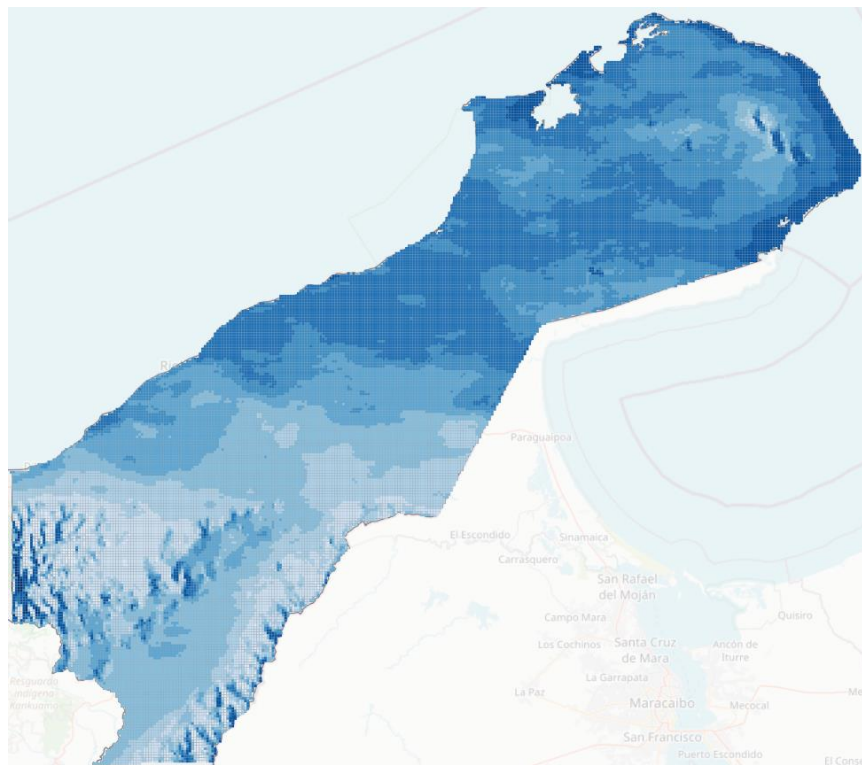


Figure 4.6. QGIS Vectorized resource grid for Mean Wind Speed.

4.2. Onshore Wind Geographic Potential

After following all procedures in Section 3.2, the available area for onshore wind technology is obtained. In Figure 4.7, La Guajira is represented as a gray polygon to help visualize better the areas that were restricted and removed from the total area while following the methodology. In light blue, and full of missing sections, is the available area, or geographic potential, for La Guajira.

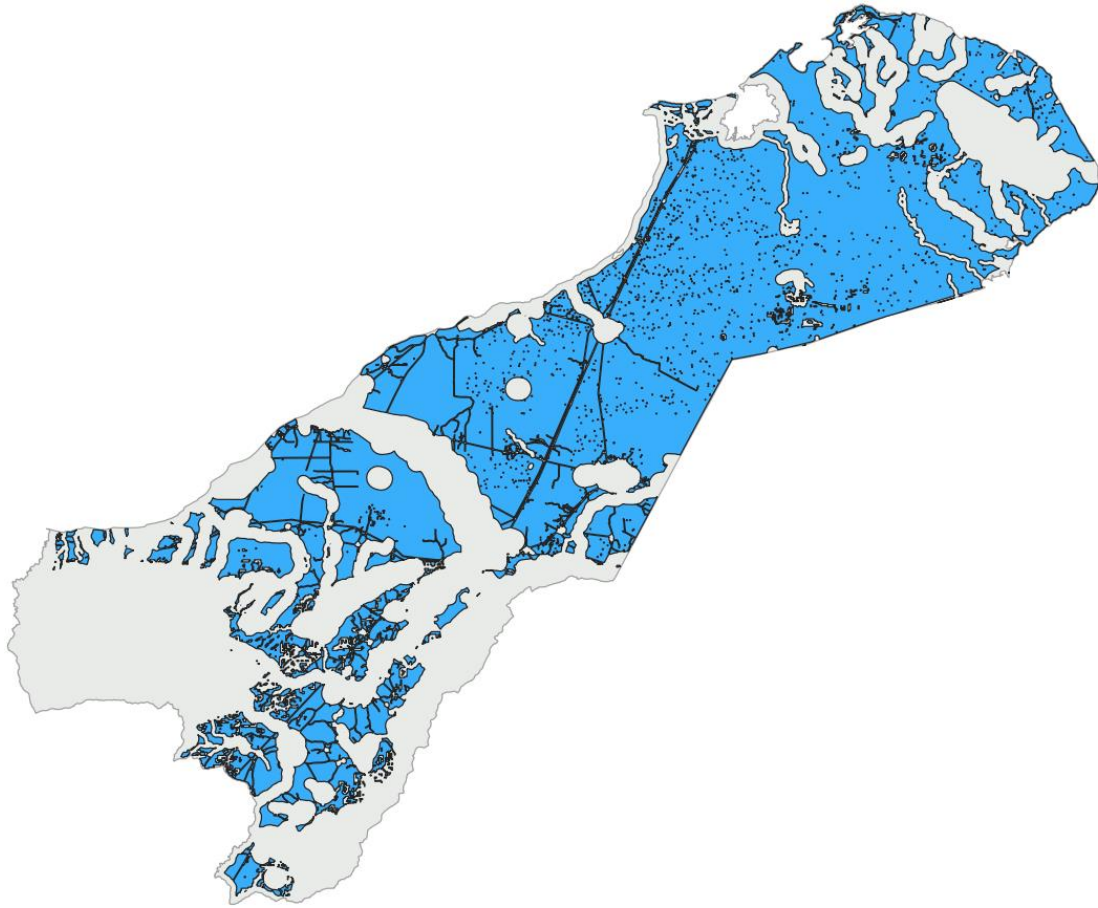


Figure 4.7. Available Area for Onshore Wind Technology

The total area calculated by QGIS, the plugin Area Ratio, and the value of the blue multipolygon geometry for available area, are all shown in Table 4.1. In the end, 52.1% of the department's land will be considered for the following technical potential estimation.

Guajira Total Area [km ²]	Available Area for Onshore Wind [km ²]	Ratio [%]
21'583.7	11'252.9	52.1%

Table 4.1. Guajira Total Area and Available Area for Onshore Wind

4.3. Onshore Wind Technical Potential

The first result of onshore wind technical potential is the vector resource grid on the available area for wind projects and filtered only to cells that have a minimum 4 diameters of wind turbine safety distance. These assumptions can be understood better with Section 3.3.3 and with Figure 4.8.

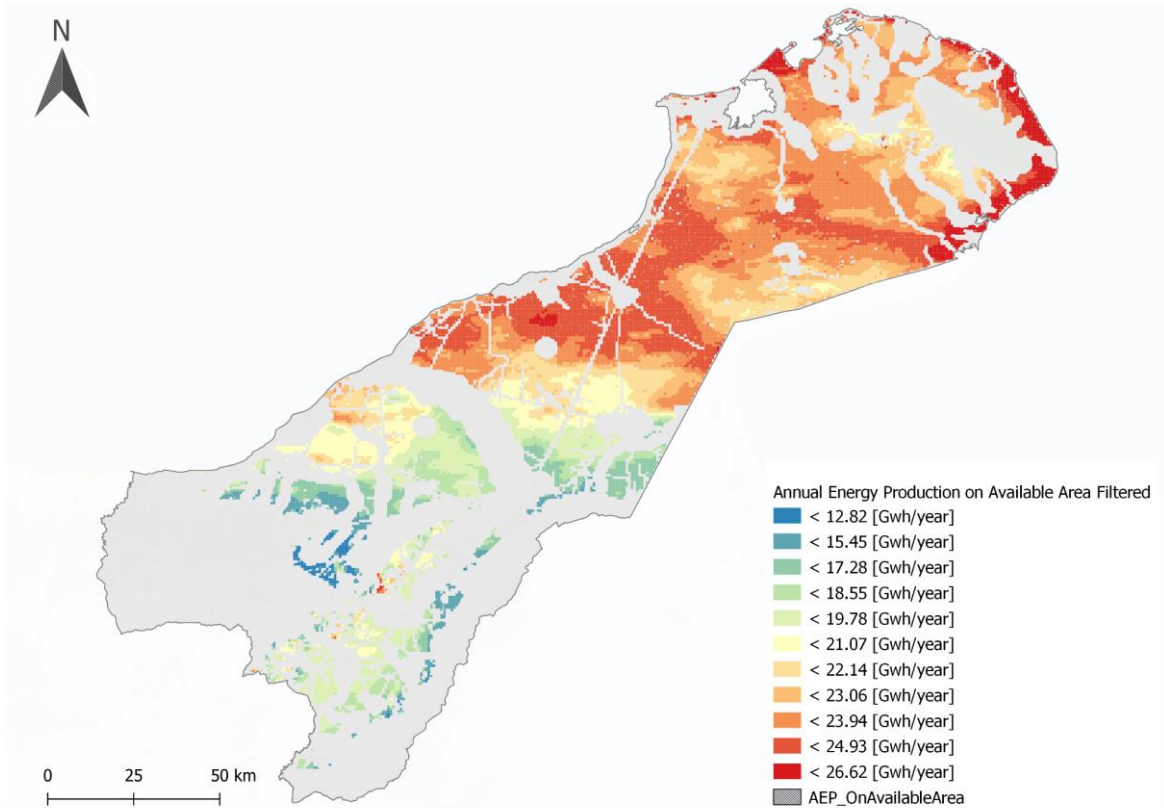


Figure 4.8. Filtered Annual Energy Production in Available Area for Onshore Wind

Moreover, a summarizing table for onshore wind was made. Here is displayed the most important information to better understand the results. This can be seen in Table 4.2.

Total Available Area [km2]	Installed Capacity [GW]	Total Annual Energy Production [GWh/year]	Number of available cells (Generators)
9'460	81.79	399'820	18'176

Table 4.2. Summarizing table for results of technical estimation for onshore wind

4.4. PV solar Theoretical Potential

The solar PV theoretical result was obtained after running the GRASS and P&QGIS processing function “*r.sun.insoltime*” 365 times, changing the day parameter (and thus sun position). Subsequently, another processing function for raster layers called *Cell Statistics* was applied to all the “Global radiation” raster layers, carrying pixel wise operations, like the average. The resulting averaged global radiation raster file can be seen in Figure 4.9.

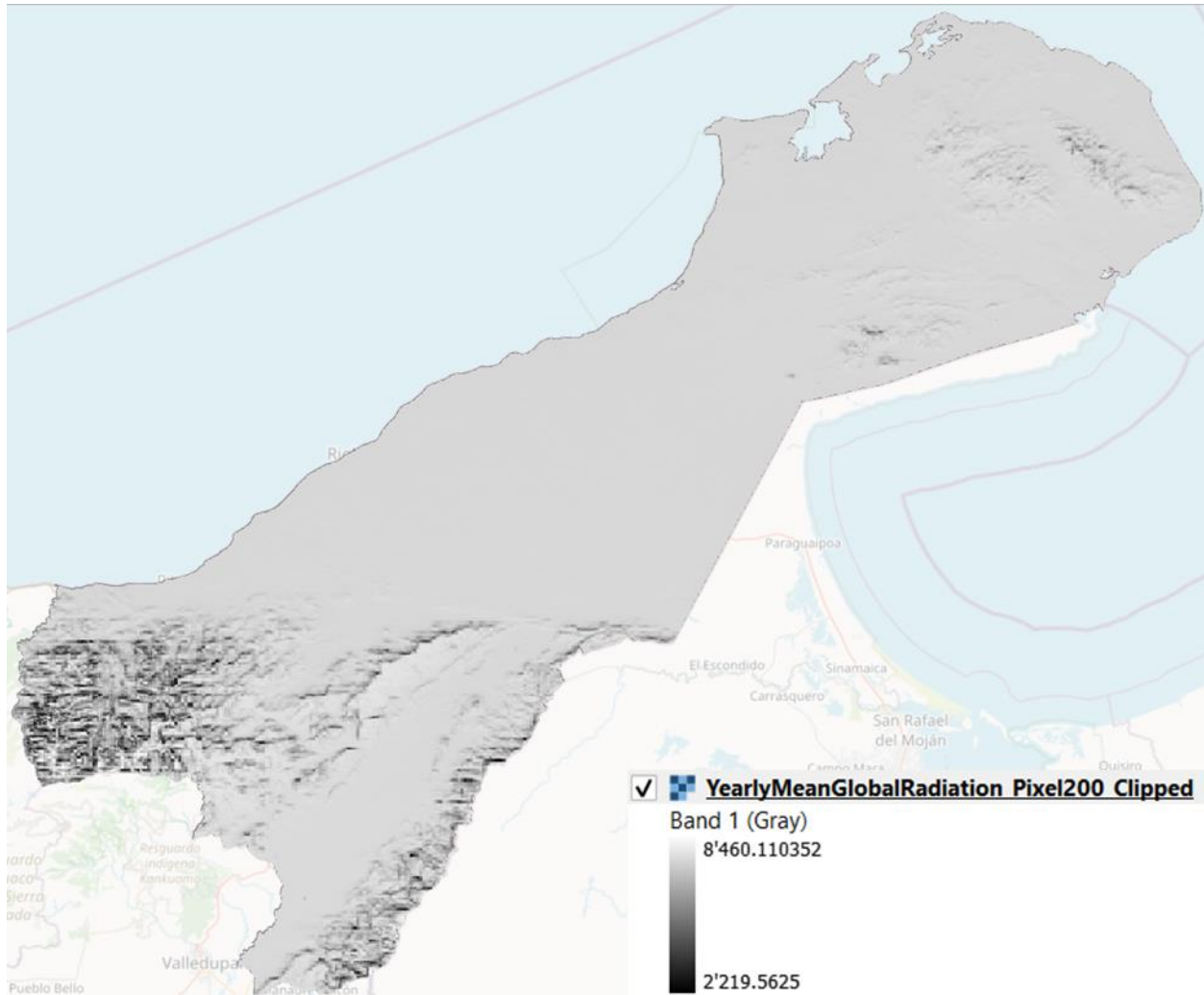


Figure 4.9. Yearly Mean Global Radiation raster file

This raster file layer, with pixel size 200mx200m, underwent the same vectorization process as the one described in Section 4.1, for the onshore wind resource grids. The resulting vector grid for global radiation can be seen in Figure 4.10.

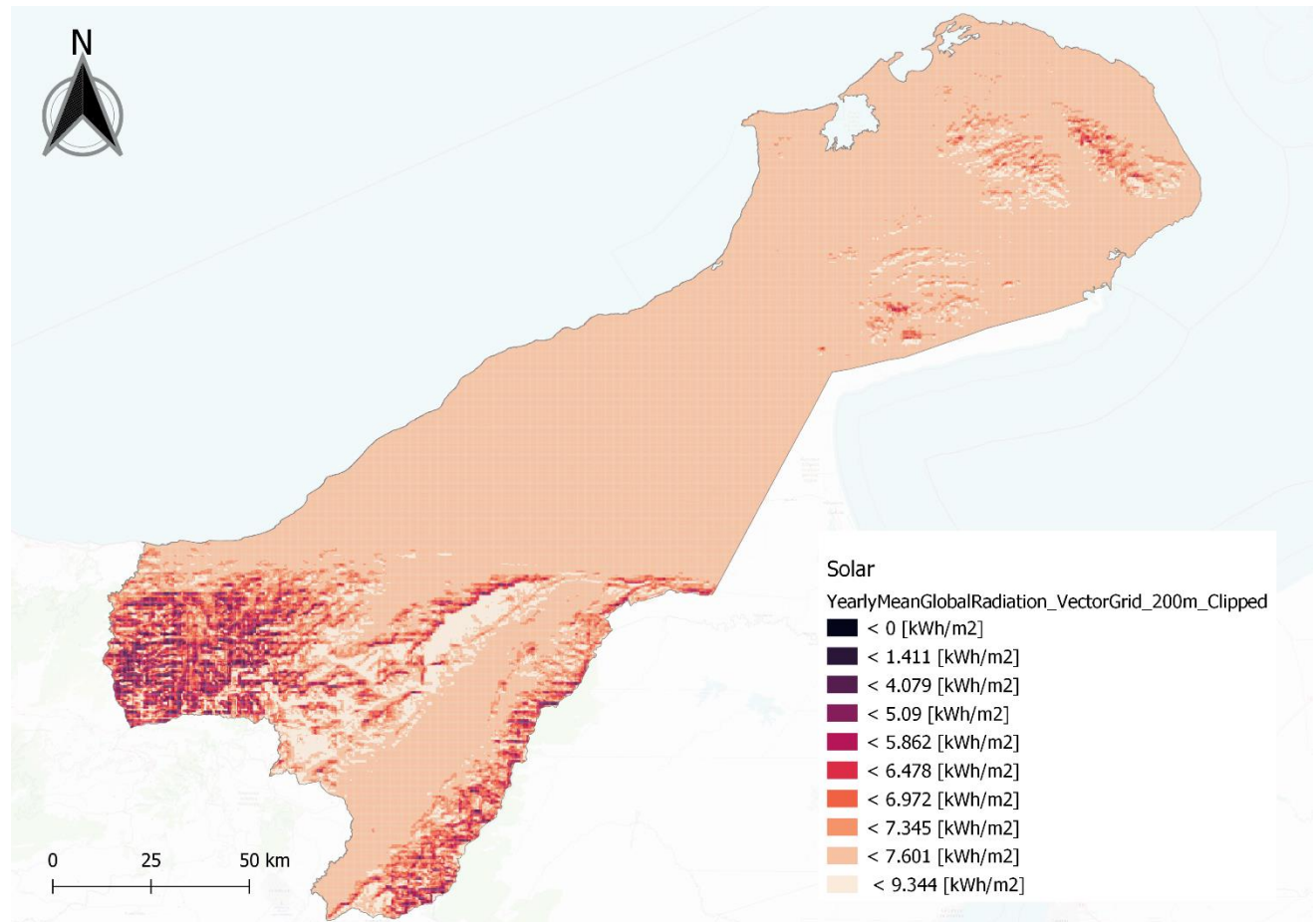


Figure 4.10. Yearly mean global radiation vector grid for La Guajira (scale)

There is an important change in resolution when comparing the theoretical potential vector resource grids from onshore wind and solar PV. The main reason for this difference is that solar panels don't need such safety distances between them, as the energy flux flows mostly vertically, directly to the panel. Instead of 750x750m resolution cells for wind, in this case cells have a smaller size of 200x200m. This almost quadrupled the number of cells, increasing the computational load for the estimation process.

4.5. PV solar Geographic Potential

After following all procedures in Section 3.2, the available area for Solar PV technology is obtained. In Figure 4.11, La Guajira is represented as a gray polygon to help visualize better the areas that were restricted and removed from the total area while following the methodology. In bright orange, and with many holes and missing sections, is the available area, or geographic potential, for La Guajira.



Figure 4.11. Available Area for Solar Photovoltaic Technology

In Table 4.3, can be seen the total area calculated by QGIS, plugin *Area Ratio*, as well as the value of the orange multipolygon geometry for available area. In the end, 51% of the department's land will be considered for the following technical potential estimation.

Guajira Total Area [km ²]	Available Area for Solar Photovoltaic [km ²]	Ratio [%]
21'583.7	11'014.6	51.0%

Table 4.3. Guajira Total Area and Available Area for solar PV

4.6. PV solar Technical Potential

The first result of solar photovoltaic's technical potential is the vectorized Yearly Mean Global Radiation, constrained by the geographical potential, and filtered by a condition of minimum cell area, like in Section 4.1. This vector layer can be seen in Figure 4.12.

Figure 4.12. Yearly Mean Global Radiation vector grid with cell areas at least 30 m².

Furthermore, an annual Electricity Production vector layer was made by using the Field Calculator. Every 200x200 m cell carried global radiation per unit area data. At our disposal is also the total available area of each resolution cell, the coefficient C_{COV} to define the real area occupied by solar panel, respecting interrow spacing, and the system efficiency (STC efficiency times the performance ratio). This is all that's needed to obtain pixel-wise Annual Electricity Production. The resulting vector grid for solar PV AEP can be seen in Figure 4.13.

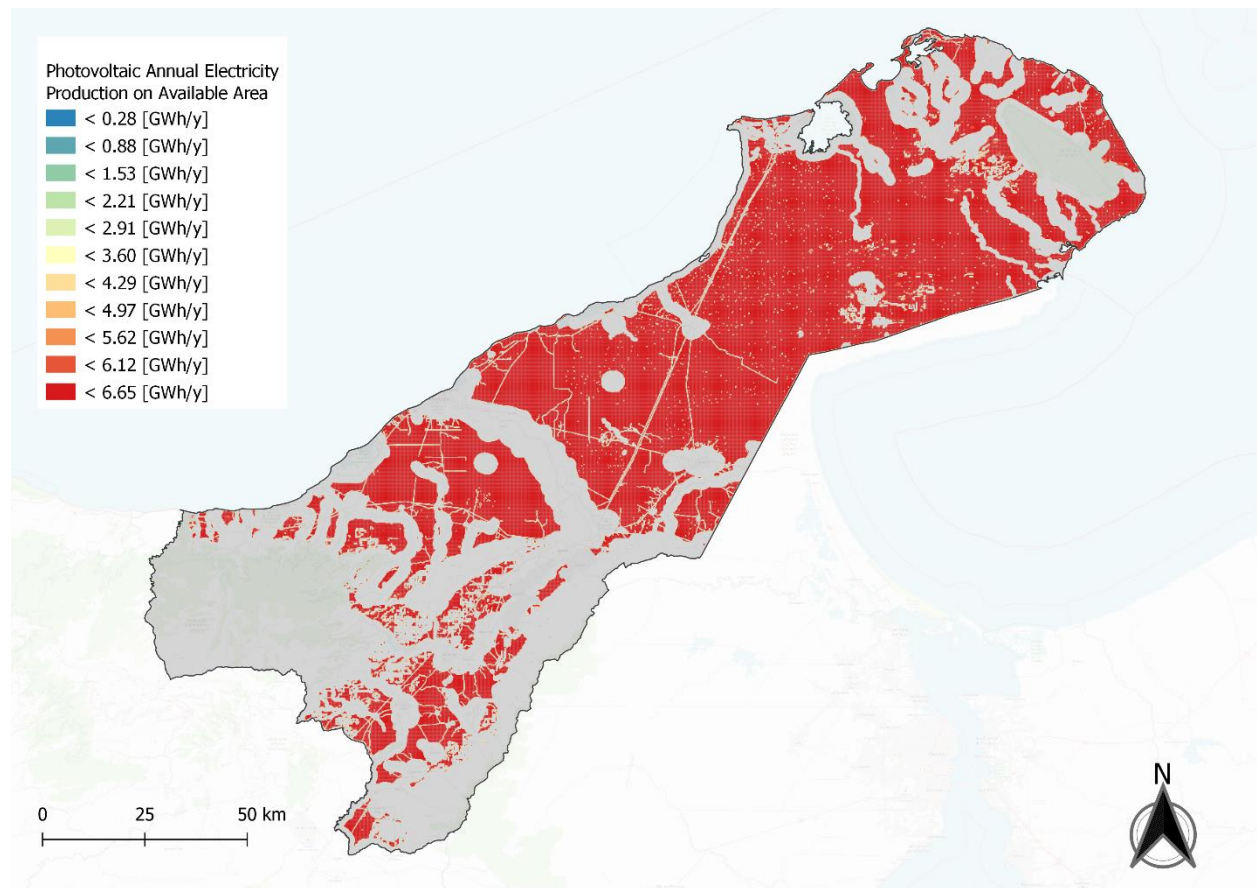


Figure 4.13. Annual Electricity Production for solar PV

Even if the whole selected area looks green, the lower AEP values are only in smaller cells. The magnitude of AEP depends on the area multiplying the global radiation per unit area. This is a normal behaviour that happens because of the resolution chosen. A pixel level close-up was made for visualizing the other colors in the legend. This can be seen in Figure 4.14.

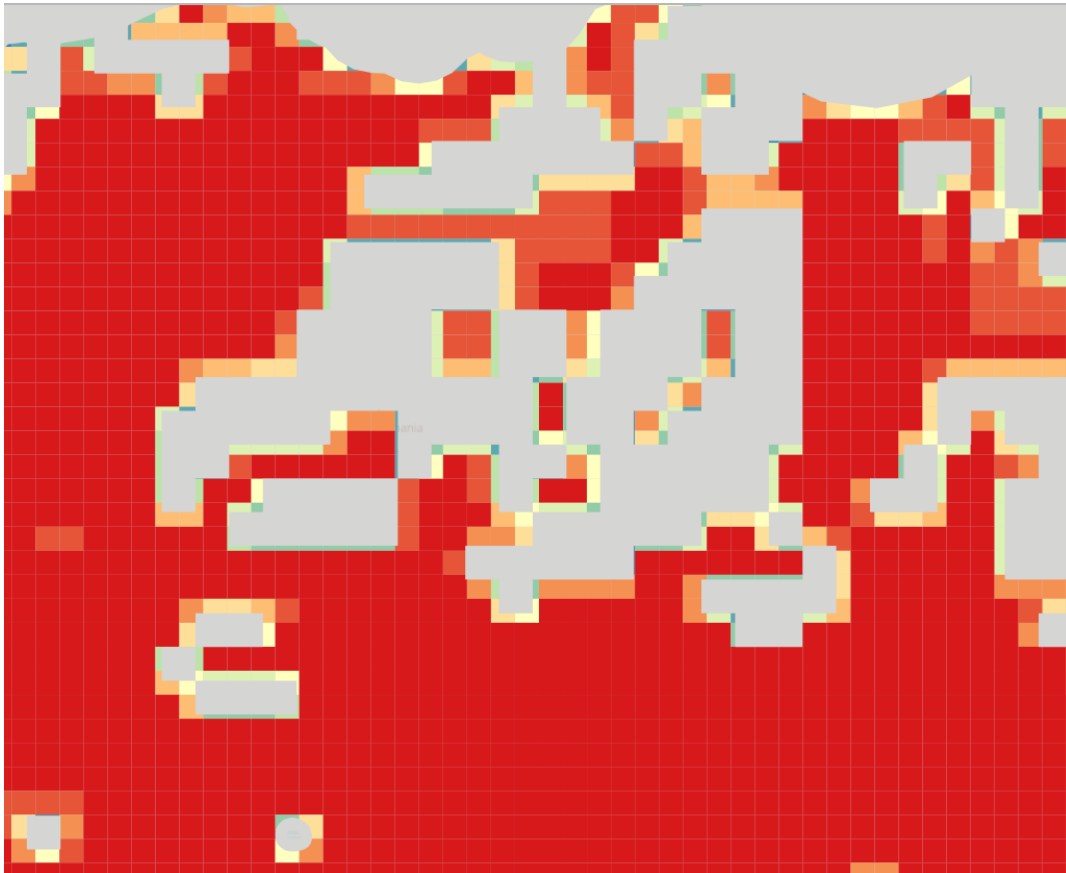


Figure 4.13. Pixel level close-up in the PV Annual Electricity Production vector grid.

Finally, a summarizing table for onshore wind was made. Here are displayed the most important information to better understand the results, for example the final available area, final total installed capacity, and annual electricity production. This can be seen in Table 4.4.

Total Available Area [km ²]	Installed Capacity [GW]	Total Annual Energy Production [GWh/year]	Estimated number of panels
10'499	790.97	1'738'640	1'216'883'451

Table 4.4. Summarizing table for results of technical estimation for solar photovoltaic

5. Discussion

In this section, the results from Section 4 will be brought to comment and discuss, but firstly, before discussing them, it's very important to clarify that these results are halfway into representing the actual feasible potential of a region. The complete methodology needs to include economic aspects and any other missing criteria to arrive at a feasible potential. For example, punctual land use was not considered, as well as religiously important land areas to local indigenous communities. Both are examples that can easily reduce the availability of land, and thus the final potential itself.

Following this line of thought, during the methodology of obtaining the available area for onshore wind and for solar PV the only reference on the Colombian territory was the work done in [8]. The available area from this work can be found in Figure 5.1, and on each side the geographic potentials, being on the left onshore wind, and in the right solar PV. Via a simple visual comparison, the similarity level is very high. Unfortunately, the reference paper did not have any statistics on the available area, so without contacting the authors it's impossible to compare other than by observation. The available area for OW and SPV were 11,252.9km² and 11,014.6km², being 52.1% and 51% of the total department area, respectively. The main difference was the slope and elevation restricted area that changed for both technologies.



Figure 5.1. Comparison between available area from [8] and the results from section 4.

Furthermore, with respect to the resource grids resulting from WasP some observations can be made. The first one being that these files, are not very easy to manipulate, especially if you don't use a GIS software like QGIS. Aside from that, they are a

great source of information. For example, regarding the Mean Speed raster at a given height and comparing it to other downloadable information from databases, the one coming from WasP has considered terrain analysis done with IBZ model or with Computational Fluid-dynamics model, user's choice. Even so, when vectorized, any type of calculations are possible, specially using the P&QGIS interface, where vectorized rasters with hundreds of thousands of resolution cells can be duplicated, removed, modified or used as input for creating more information.

This is the case of the technical potential of both OW and SPV. The information was processed until reaching the tables found in Section 4.3 and Section 4.6. From these results can be observed that even if the total available area from onshore wind is roughly a 10% smaller than solar PV, the values for installed capacity and AEP differ greatly.

One Wind turbine occupies for security reasons a certain area, and in this case, produces at best, at rated power, 4.5 MW. In this same area, that is around 0.56 km², and as seen in Section 3.4.3, it possible to fit the 36% with panel surface. If that surface is divided by the single panel individual area, and multiplied by the nominal power of each panel, the difference in installed capacity, AEP and number of generators/panels is explained.

The electric system of the whole region, and some challenges that appear with it. Can the region, with the current state of distribution and transmission network, include all the planned onshore wind and solar PV into the national grid? The answer is no. The only high tension, 500kV transmission line goes from the marine port *Puerto Bolivar* to the open sky coal mine *El Cerrejón*. The solution is a, still in the planning phase, new transmission line and substation system, also with 500kV, consisting of more than 450 km of work to be done [65]. This transmission line is planned to be able to connect more than 1,000 MW of installed capacity in the north of the country to the rest of it.

Regarding other aspect of the network state, it is not clear, and no studies have been found on how robust and secure the Guajira electricity network currently is. As seen in previous sections, the installed capacity for electricity generation is around 18GW and is planning to grow in only 4 years until 32GW, thanks to the inclusion of renewables. It would be very interesting for future studies to deepen into the self-sufficiency and self-

consumption of the whole region throughout the following years as the installed capacity increases at the accelerated rates that the government has proposed.

Additionally, aspects as network smartness, network flexibility, load management or the levels of customer participation have not been mentioned in the literature review for this region. The term prosumers is not legalized, but legislation around the incoming new sources of energy is something that urges, as the installed capacity and energy transition happens.

6. Conclusion

The main objective of this thesis is to estimate the technical potential for onshore wind and solar PV in a case study region in the north of Colombia using QGIS software together with wind energy modeling software WasP. In Section 1, the introduction, the context is completely explained, including the basics to understand how wind and solar energy are useful to actual society.

The application of GIS-based methodologies enables a more informed and data-driven approach to identifying suitable sites for wind and solar energy projects, aiding in the sustainable and efficient utilization of the region's renewable resources. One of the reasons that wind and solar energy projects are being built is to minimize greenhouse gas emissions and thereby battle climate change. Renewable energy projects, on the other hand, can have environmental consequences, and mitigating them begins with the placement of the project.

During this investigation, it has been evidenced that onshore wind and solar photovoltaic have the biggest potential in the study region and in the whole country. Likewise, it has also been evidenced that extremely slow progress has been made in the past 17 years in Colombia, since the date when the only working wind plant came to be. The second wind farm has recently been finished; however, it is not done with the testing necessary to connect it to the national grid. The solar PV situation is similar; despite having one of the highest mean solar radiations per square meter values in the country, not a single utility scale plant has been built in the region.

This behavior results from various causes: firstly, although La Guajira is rich in clean energy, it is also rich in the “dirtiest” energy source, coal. Around four decades ago, the open-sky carbon extraction plant *Cerrejón* started operation, and since then, has fed an important part of Colombia’s total energy supply and export matrix. The only railroad in La Guajira goes from the carbon mine until a seaport in the north of the region called “Puerto Bolivar”, followed of course by roads, light posts, and an electric distribution system, which is not the average situation in the department, characterized by a lack of infrastructure and government presence.

One of the most essential conclusions is that without political will and the active and honest engagement of all parties involved, no change or development will occur soon, even with the best investigations and discoveries. Recently, the biggest wind farm under construction came to a halt [], because the government and communities do not follow effective, integral communication. This situation has prompted the president to declare a social and economic emergency in the region, a situation might affect the perception of foreign companies and investors who have already planned to construct onshore wind and photovoltaic solar power plants in the region over the next few years. This capital and knowledge from the international community are crucial for Colombia's renewable energy sector at its current stage of development.

Aside from the previous situation, Colombia being able to extract the vast renewable potential in its territory is a huge step towards the goal the country pledged to the international community in 2020 [61] to reduce emissions of greenhouse gases by 51% by 2030. All these pledges and plans must be accompanied by a more robust regulatory framework to, firstly, encourage investment and knowledge to stay in the region and, secondly, strengthen the energy matrix and the network's smartness.

From the onshore wind potential estimation methodology can be concluded that the turbine selection has an immense impact in the final output. If for example, a bigger 10MW rated power turbine was chosen instead of the actual, with a higher hub height and following the same exact same steps, the output technical potential would be much higher. So, it’s crucial to remember that the results found with the Nordex N149 serve as

a reference for similar configurations and that might not be optimal. The resolution of the WAsP resource grid greatly determines the result.

7. Recommendations

By addressing the barriers and leveraging the opportunities, Guajira can unlock its significant renewable energy potential. This requires the continued support of favorable legislation, comprehensive environmental assessments, and strategic infrastructure planning to foster sustainable development, protect the environment, and benefit local communities.

One of the most important recommendations for this project is that, if interested in continuing with the potential's top-down approach, the economic and feasibility criteria must be included to reach the most realistic potential and thus, useful to interested parties. This methodology can also be replicated and modified for other regions of the world. And as long as parts of the methodology are converted into scripts or QGIS models, whole projects that take months can start to take only weeks, thanks to the automation of many processing and geoprocessing steps.

Lastly, the inclusion of other sources of renewable energy is also encouraged. Offshore wind, Tidal, wave energy, geothermal energy, can all be seen through the GIS eyes, and modelled to estimate potential or directly site select the best places to harvest this energy.

References

- [1] NOAA National Centers for Environmental Information (2023). State of the Climate: Global Climate Report for 2022. Accessed January, 2023, from <https://www.ncei.noaa.gov/access/monitoring/monthly-report/global/202213>
- [2] Global Warming of 1.5 °C – Intergovernmental Panel on Climate Change (IPCC). Accessed February 3, 2023, from <https://www.ipcc.ch/sr15/>
- [3] Causes and Effects of Climate Change – United Nations. Accessed January 2023, from <https://www.un.org/en/climatechange/science/causes-effects-climate-change>
- [4] Wuebbles, D., Kunkel, K., Wehner, M., & Zobel, Z. (2014) – Severe Weather in the United States Under a Changing Climate. Eos, Transactions American Geophysical Union.
- [5] Thomas, Vinod and López, Ramón, Global Increase in Climate-Related Disasters (November 2015). Asian Development Bank Economics Working Paper Series No. 466, Available at SSRN: <https://ssrn.com/abstract=2709331>
- [6] The Paris Agreement – United Nations Framework Convention on Climate Change (UNFCCC). Available at: <https://unfccc.int/process-and-meetings/the-paris-agreement>
- [7] United Nations Conference on Sustainable Development – Rio+20. Accessed March 2023. Available at: <https://sustainabledevelopment.un.org/rio20>
- [8] Guerrero Hoyos, Benito & Vélez Macías, Fabio & Quintero, Diana. (2020). Energía eólica y territorio: sistemas de información geográfica y métodos de decisión multicriterio en La Guajira (Colombia). Ambiente y Desarrollo. Available at: https://www.researchgate.net/publication/339220622_Energia_eolica_y_territorio_sistemas_de_informacion_geografica_y_metodos_de_decision_multicriterio_en_La_Guajira_Colombia.
- [9] Jäger, Tobias & Mckenna, Russell & Fichtner, Wolf. (2016). The feasible onshore wind energy potential in Baden-Württemberg: A bottom-up methodology considering socio-economic constraints. Renewable Energy. Available at DOI: 10.1016/j.renene.2016.05.013.
- [10] Europe – Countries & Regions - International Energy Agency. Retrieved March 2023, from <https://www.iea.org/regions/europe>
- [11] Colombia – Countries & Regions – International Energy Agency. Retrieved March 2023, from <https://www.iea.org/countries/colombia>
- [12] Statistical Energy Profile Colombia – International Renewable Energy Agency, IRENA. Available at: https://www.irena.org/-/media/Files/IRENA/Agency/Statistics/Statistical_Profiles/South%20America/Colombia_South%20America_RE_SP.pdf
- [13] World Bank Group. (2021, March 18). Turning the tide: Improving water security for recovery and sustainable growth in Colombia. World Bank. Available at: <https://www.worldbank.org/en/news/feature/2020/09/02/colombia-water-security>
- [14] *REPowerEU: Affordable, secure and Sustainable Energy for Europe*. European Commission. (n.d.). https://commission.europa.eu/strategy-and-policy/priorities-2019-2024/european-green-deal/repowerEU-affordable-secure-and-sustainable-energy-europe_en

- [15] Meyer, Ina & Sommer, Mark W.. (2016). Employment effects of renewable energy deployment - a review. *International Journal of Sustainable Development*: 19. 217. Available at DOI: 10.1504/IJSD.2016.078274.
- [16] Trina Solar – Vertex Backsheet Monocrystalline Module – TSM DE-21 670W. Available at: <https://solaranalytica.com/wp-content/uploads/2022/04/Trina-Vertex-645-670W-Datasheet-Solar-Analytica-Verified.pdf>
- [17] Nordex N149/4.0-4.5 - The Wind Power - Wind Energy Market Intelligence - Manufacturers and turbines - The Wind Power. (2023). Retrieved May 2023, from: https://www.thewindpower.net/turbine_en_1505_nordex_n149-4.0-4.5.php
- [18] World Bank Open Data - Population, Total - Latin America & Caribbean. Available at: https://datos.bancomundial.org/indicador/SP.POP.TOTL?locations=ZJ&most_recent_value_desc=true
- [19] A look at the natural world of Colombia. (2023). Retrieved March 2023, from <https://www.worldwildlife.org/magazine/issues/winter-2017/articles/a-look-at-the-natural-world-of-colombia#:~:text=Colombia%20is%20the%20>
- [20] Colombia - Places in the News | Library of Congress. (2023). Retrieved March 2023, from <https://www.loc.gov/today/placesinthenew>
- [21] La Guajira, Colombia - Genealogía. (2022). Retrieved March 2023, from https://www.familysearch.org/es/wiki/La_Guajira,_Colombia_-_Genealog%C3%ADa
- [22] Relief Map. (2023). Retrieved April 2023. Available at <https://maps-for-free.com/>
- [23] ONIC – Wayuú – Pueblos. (2023). Retrieved April 2023, available at: <https://www.onic.org.co/pueblos/1156-wayuu>
- [24] Aspectos demográficos de La Guajira según El Censo 2018. (2020) Guajira 360°. Available at: <https://guajira360.org/informe-economico-que-tanto-hemos-cambiado-aspectos-demograficos-de-la-guajira-segun-el-censo-2018/> (Accessed: 05 July 2023).
- [25] Atlas marino costero de La Guajira (2023). Retrieved April 2023, Available at: https://aquadocs.org/bitstream/handle/1834/5909/Atlas_Guajira.pdf;jsessionid=F8E01054F50C38E91D357B28E8EAE754?sequence=1
- [26] Díaz, Y. (2023). DANE - Pobreza monetaria. Retrieved 27 June 2023, from <https://www.dane.gov.co/index.php/estadisticas-por-tema/pobreza-y-condiciones-de-vida/pobreza-monetaria>
- [27] Heraldo, E. (no date) *Tasa de empleo y de informalidad laboral Riohacha, EL HERALDO*. Available at: <https://www.elheraldo.co/la-guajira/riohacha-la-ciudad-con-mayor-desempleo-825350> (Accessed: April 2023).
- [28] Ministerio de Ambiente y Desarrollo Sostenible. (2023). La Guajira es el departamento con mayor potencial para la generación de energía limpia en Colombia. Retrieved March 2023, Available at: <https://archivo.minambiente.gov.co/index.php/noticias-minambiente/2743-la-guajira-es-el-departamento-con-mayor-potencial-para-la-generacion-de-energia-limpia-en-colombia>

- [29] Vanegas, G. (2023) El Plan Energético de Petro: ¿Puede La Guajira Iluminar Colombia?, El País América Colombia. Available at: <https://elpais.com/america-colombia/2023-07-03/el-plan-energetico-de-petro-puede-la-guajira-iluminar-colombia.html> (Accessed: 06 July 2023).
- [30] Autoridad Nacional de Licencias Ambientales ANLA (2022) Actualización del Reporte de Alertas de Análisis Regional de la Zona Hidrográfica. Retrieved March 2023, Available at: <https://comisiones.anla.gov.co/images/documentos/reportes-alertas/20230116-reporte-alertas-zona-hidrografica-caribe-guajira.pdf>
- [31] Ministerio de Minas y Energía (2021). Transición energética: un legado para el presente y el futuro de Colombia. Retrieved April 2023. Available at: <https://www.minenergia.gov.co/en/micrositios/enlace-legado-transicion-energetica/>
- [32] International Renewable Energy Agency – IRENA (2022). Energy Profile: Colombia. Retrieved March 2023. Available at: https://www.irena.org/-/media/Files/IRENA/Agency/Statistics/Statistical_Profiles/South%20America/Colombia_South%20America_RE_SP.pdf
- [33] IRENA and USAID (2021), Renewable energy auctions in Colombia: Context, design and results, International Renewable Energy Agency, Abu Dhabi. ISBN 978-92-9260-313-7. Available at: https://www.irena.org/-/media/Files/IRENA/Agency/Publication/2021/March/IRENA_auctions_in_Colombia_2021.pdf
- [34] Fath, K., Stengel, J., Sprenger, W., Wilson, H., Schultmann, F., & Kuhn, T. (2015). A method for predicting the economic potential of (building-integrated) photovoltaics in urban areas based on hourly Radiance simulations. *Solar Energy*, 116, 357-370. doi: 10.1016/j.solener.2015.03.023
- [35] Ley 1715 de 2014 - Gestor Normativo. (2023). Retrieved March 2023, available at: <https://www.funcionpublica.gov.co/eva/gestornormativo/norma.php?i=57353>
- [36] Universidad Externado de Colombia (2021). Ley 2099 de 2021 - Derecho del Medio Ambiente. Retrieved May 2023. Available at: <https://medioambiente.uexternado.edu.co/ley-2099-de-2021-por-medio-de-la-cual-se-dictan-disposiciones-para-la-transicion-energetica-la-dinamizacion-del-mercado-energetico-la-reactivacion-econom/>
- [37] Energía Estratégica (2023) Duro Revés Al Sector Eólico Colombiano: Enel Evalúa La venta de Windpeshi luego de suspender su construcción en La Guajira. Available at: <https://www.energiaestrategica.com/duro-reves-al-sector-eolico-colombiano-enel-evalua-la-venta-de-windpeshi-luego-de-suspender-su-construccion-en-la-guajira/> (Accessed: 07 July 2023).
- [38] Estimation of wind potential in Sardinia, quantitative computation and actual constraints analysis. - Webthesis. (2023). Retrieved May 2023, from <https://webthesis.biblio.polito.it/22149/>
- [39] Tutiempo Network, S. (2023). Los anticiclones: el sobrepeso de la atmósfera - David López-Rey. Retrieved 7 July 2023, from <https://www.tutiempo.net/meteorologia/articulos/los-anticiclones.html>
- [40] Katsigiannis, Yiannis & Stavrakakis, G. (2014). Estimation of wind energy production in various sites in Australia for different wind turbine classes: A comparative technical and economic assessment. *Renewable Energy*. 67. 10.1016/j.renene.2013.11.051.

- [41] IEC – (2019a), IEC 61400-1, Ed. 4 – Wind Turbine Generator Systems, Part 1 – Safety Requirements, International Electrotechnical Commission, Geneva
- [42] Cooperman, Aubryn & Martinez, Marcias. (2014). Load monitoring for active control of wind turbines. *Renewable and Sustainable Energy Reviews*. Vol. 41. 189-201. 10.1016/j.rser.2014.08.029.
- [43] Dupont, Elise & Koppelaar, Rembrandt & Jeanmart, Hervé. (2017). Global available wind energy with physical and energy return on investment constraints. *Applied Energy*. 209. 10.1016/j.apenergy.2017.09.085.
- [44] La Republica. (2022). La Guajira tiene 16 proyectos de energía eólico con inversiones de US\$2.525 millones. Retrieved May 2023, from <https://www.larepublica.co/economia/la-guajira-tiene-16-proyectos-de-energia-eolico-con-inversiones-de-us-2-525-millones-3408676>
- [45] Enerfin (2023). Informe anual integrado del 2022 -- Retrieved May 2023, available at: <https://www.enerfin.es/resources/files/1/Enerfin/enerfin-informe-integrado-2022es.pdf>
- [46] WWF (2020) -- Colombia pledges to reduce its GHG emissions by 51% by 2030, WWF. Available at: https://wwf.panda.org/wwf_news/?1152816%2FColombia-2030-target-NDC (Accessed: May 2023).
- [47] Solar Energy | A Student's Guide to Global Climate Change | US EPA. (2023). Retrieved May 2023. Available at: <https://archive.epa.gov/climatechange/kid>
- [48] Santra, Priyabrata. (2016). Scope of Solar Energy in Cold Arid Region of India at Leh Ladakh. *Annals of arid zone*. 54. 109-117.
- [49] A. Richter, M. Hermle and S. W. Glunz, "Reassessment of the Limiting Efficiency for Crystalline Silicon Solar Cells," in *IEEE Journal of Photovoltaics*, vol. 3, no. 4, pp. 1184-1191, Oct. 2013, doi: 10.1109/JPHOTOV.2013.2270351.
- [50] Solar energy | Definition, Uses, Advantages, & Facts. (2023). Retrieved May 2023. Available at: <https://www.britannica.com/science/solar-energy>
- [51] La Republica (2023). Proyectos de energía solar en el territorio nacional. Retrieved May 2023. Available at: <https://www.larepublica.co/economia/ya-hay-38-proyectos-de-energia-solar-en-funcionamiento-en-todo-el-territorio-nacional-3560668>
- [52] Vega Araújo, J., & Muñoz Cabré, M. (2023). Energía solar y eólica en Colombia: panorama y resumen de políticas 2022. SEI Brief. Stockholm Environment Institute. <https://doi.org/10.51414/sei2023.016>
- [53] Unidad de Planeación Minero Energética (UPME), (2019) – Atlas de radiación solar de Colombia. Retrieved May 2023, Available at: <https://repositoriobi.minenergia.gov.co/handle/>
- [54] Decenas de proyectos de energía solar operarían en Colombia en 2023 . (2023). Retrieved April 2023, from <https://oilchannel.tv/noticias/decenas-de-proyectos-de-energia-solar-operarian-en-colombia-en-2023>
- [55] Unidad de Planeación Minero Energética UPME - Ministerio de Minas y Energía (2019) - Plan Energetico Nacional 2020-2050. Retrieved May 2023. Available at: https://www1.upme.gov.co/DemandaEnergetica/PEN_documento_para_consulta.pdf

- [56] OECD (2022), Enabling Conditions for Bioenergy Finance and Investment in Colombia, Green Finance and Investment, OECD Publishing, Paris, <https://doi.org/10.1787/20f760d6-en>.
- [57] Posso., V. (2023). Parques solares en La Guajira y en territorios étnicos wayúu – por Camilo González Posso – Indepaz. Retrieved 8 July 2023, from <https://indepaz.org.co/parques-solares-en-la-guajira-y-en-territorios-etnicos-wayuu-por-camilo-gonzalez-posso/>
- [58] Deveci, M., Cali, U., & Pamucar, D. (2021). Evaluation of criteria for site selection of solar photovoltaic (PV) projects using fuzzy logarithmic additive estimation of weight coefficients. *Energy Reports*, 7, 8805-8824. doi: 10.1016/j.egy.2021.10.104
- [59] Pradotto, M. (2022, March). Estimation of wind potential in Sardinia, quantitative computation and actual constraints analysis. Available at: <https://webthesis.biblio.polito.it/22149/>
- [60] Moscoloni, C., Zarra, F., Novo, R., Giglio, E., Vargiu, A., Mutani, G., Bracco, G., & Mattiazzo, G. (2022, July). Wind turbines and Rooftop Photovoltaic Technical Potential Assessment: Application to Sicilian minor islands. MDPI. <https://www.mdpi.com/1996-1073/15/15/5548>
- [61] WWF - Colombia pledges to reduce its GHG emissions by 51% by 2030 (2020) WWF. Available at: https://wwf.panda.org/wwf_news/?1152816%2FColombia-2030-target-NDC (Accessed: June 2023).
- [62] Ratti and Richens (1999). Shadow casting algorithm.
- [63] Arturo, F.P.C. (2005) *Atlas de Radiación Solar de Colombia*. Bogotá: Ministerio de Minas y Energía. Available at: <https://biblioteca.minminas.gov.co/pdf/Atlas%20de%20radiación%20solar%20Colombia.pdf> (Accessed: June 2023).
- [64] Avals de comunidades de la Sierra Nevada de Santa Marta para la línea de transmisión Colectora. (2023). Retrieved June 2023, available at: <https://www.portafolio.co/economia/infraestructura/linea-colectora-ya-tiene-aval-de-136-comunidades-561127>
- [65] Yang, Y.; Campana, P.E.; Stridh, B.; Yan, J. Potential analysis of roof-mounted solar photovoltaics in Sweden. *Appl. Energy* (2020) - 279, 115786
- [66] Martinez-Gracia, A.; Arauzo, I.; Uche, J. *Solar Energy Availability*; Elsevier: Amsterdam, The Netherlands, 2019; pp. 113–149.
- [67] Idowu, Oloketuyi & Oyewola, Olarenwaju & Isaac, Odesola. (2020). Determination of optimum tilt angles for solar collectors in low-latitude tropical region. *International Journal of Energy and Environmental Engineering*. 4.
- [68] Rosa-Clot, M.; Tina, G.M. *Photovoltaic Electricity*; Elsevier: Amsterdam, The Netherlands, 2018; pp. 13–32.
- [69] F. Spertino, “Assessment of Energy Production from a Photovoltaic System,” (2020).
- [70] Pavan, A.M.; Mellit, A.; Pieri, D.D. The effect of soiling on energy production for large-scale photovoltaic plants. *Solar Energy* 2011, 85, 1128–1136.

[71] Alamoud, A. Performance Evaluation of Various Flat Plate Photovoltaic Modules in Hot and Arid Environment. J. King Saud Univ. Eng. Sci. 2000, 12, 235–242.

[72] Ekici, S.; Kopru, M.A. Investigation of PV System Cable Losses. Int. J. Renew. Energy Res. 2017, 7, 807–815.

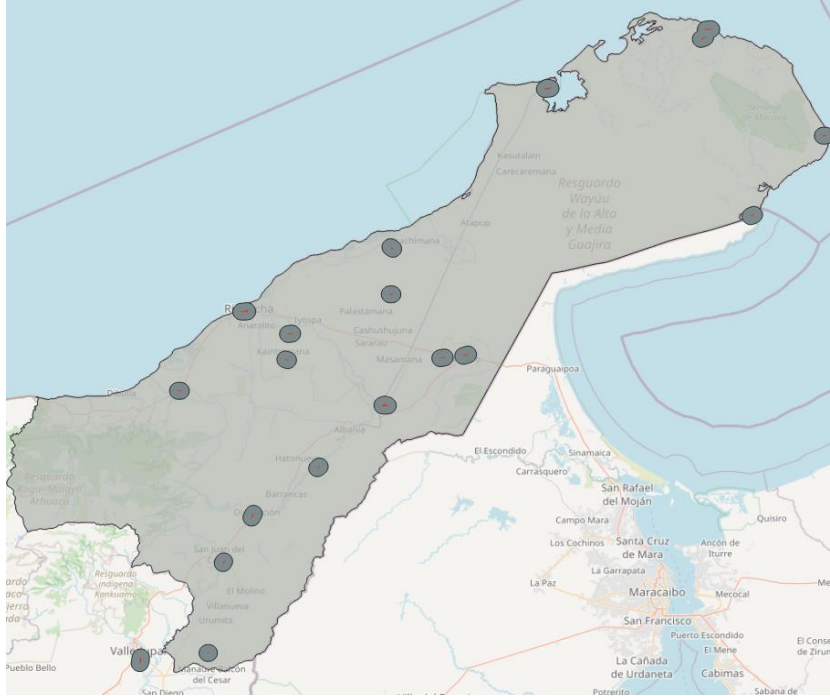
[73] Varga, N.; Mayer, M.J. Model-based analysis of shading losses in ground-mounted photovoltaic power plants. Solar Energy 2021, 216, 428–438.

[74] Huawei. SUN2000-2/3/3.68/4/4.6/5/6KTL-L1 Datasheet. Available online: <https://solar.huawei.com/en-GB/download?p=%2F-%2Fmedia%2FSolar%2Fattachment%2Fpdf%2Feu%2Fdatasheet%2FSUN2000-2-6KTL-L1.pdf>

Appendix

A. Distance-restrictive criteria buffers layers

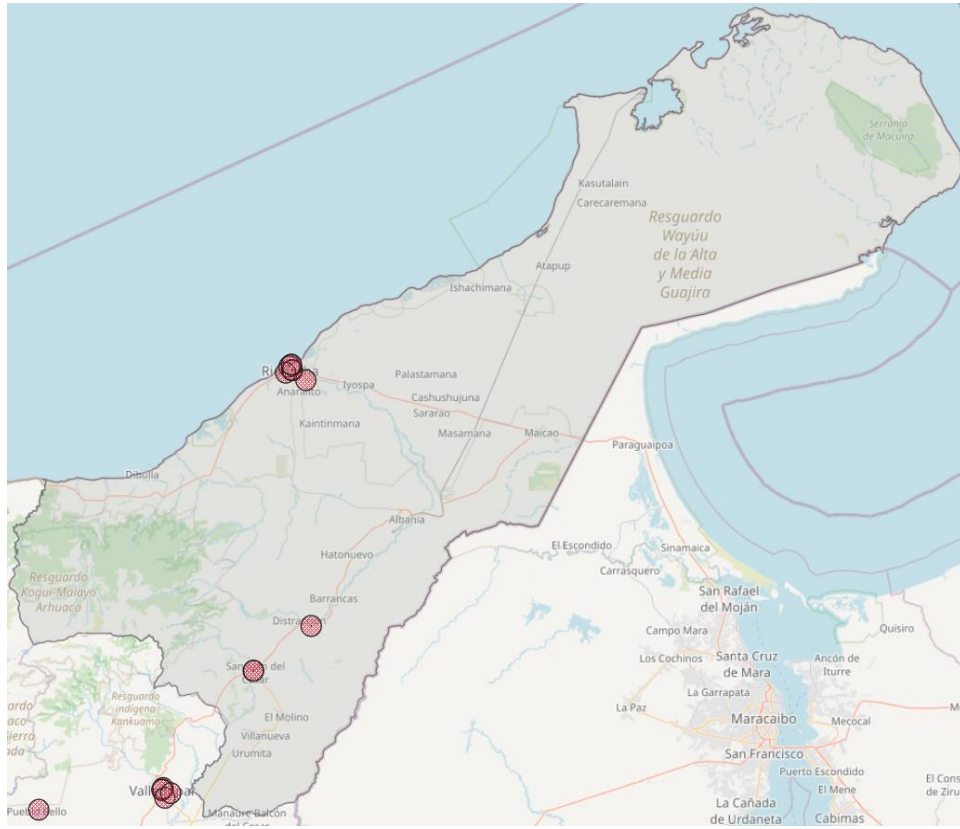
Airports (3000m):



Coastline and boundaries (200m):



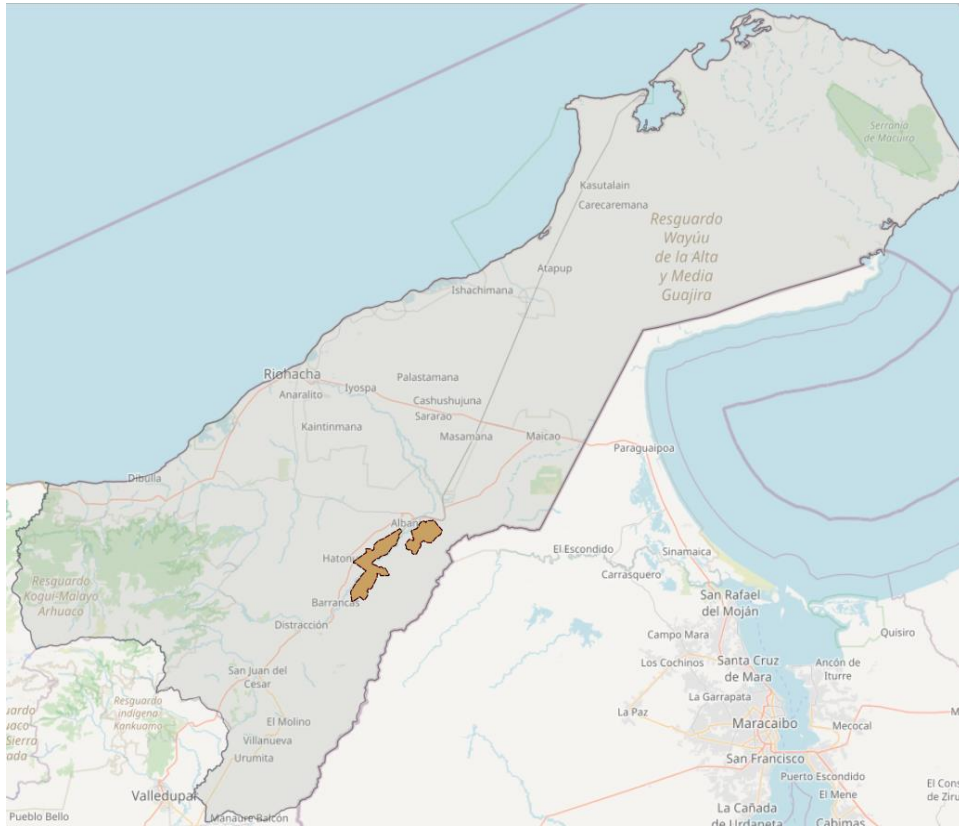
Hospital (3000m):



Military (3000m):



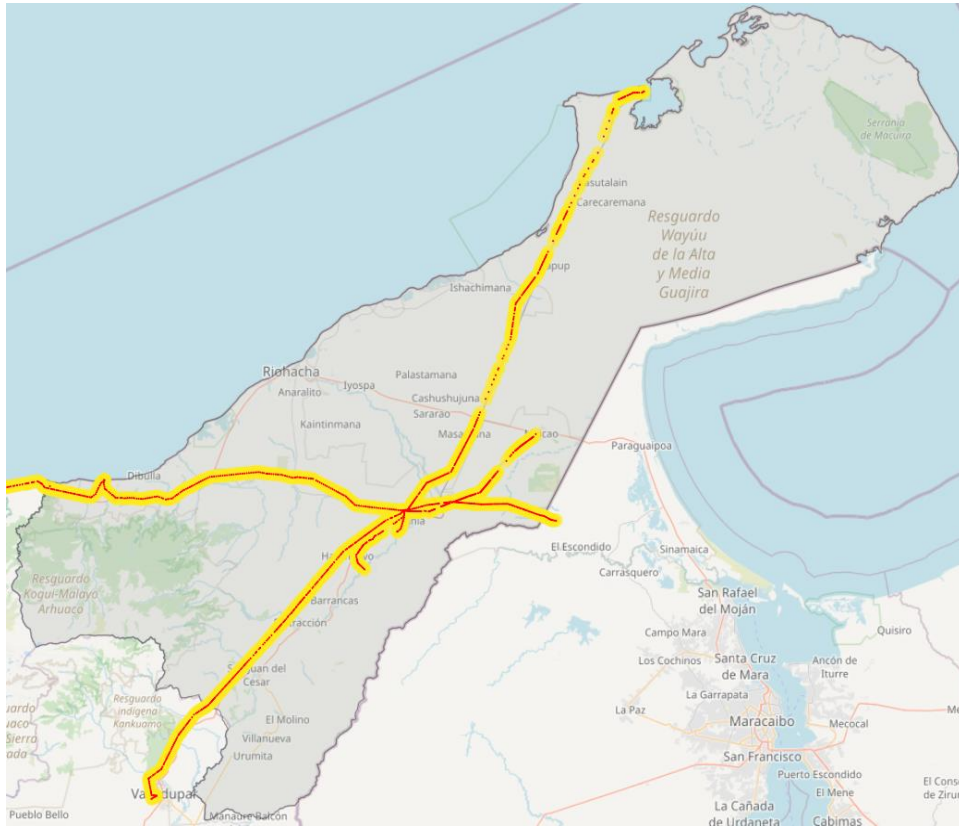
Mines (200m):



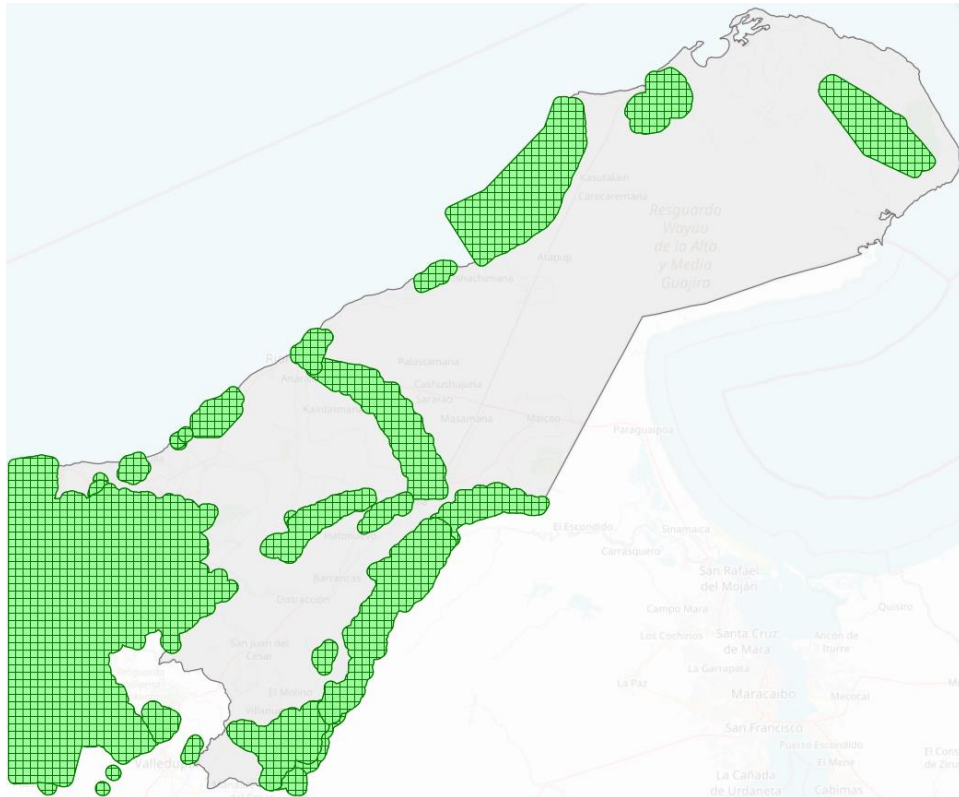
Transmission Power Lines (100m):



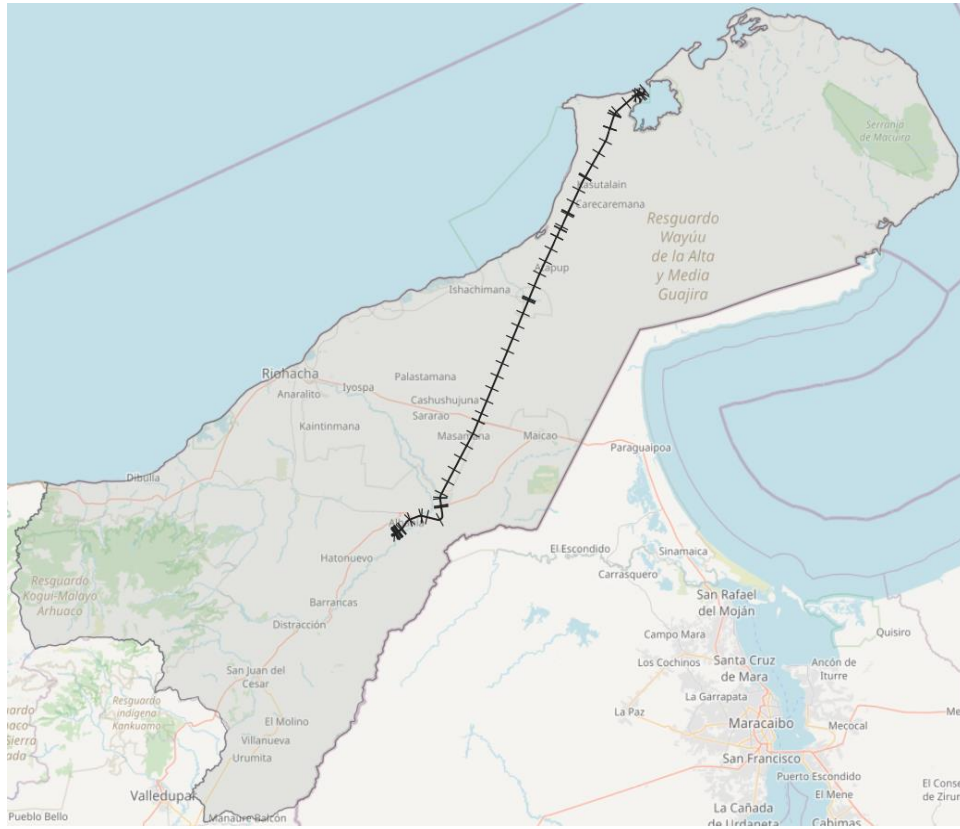
Power Towers (100m):



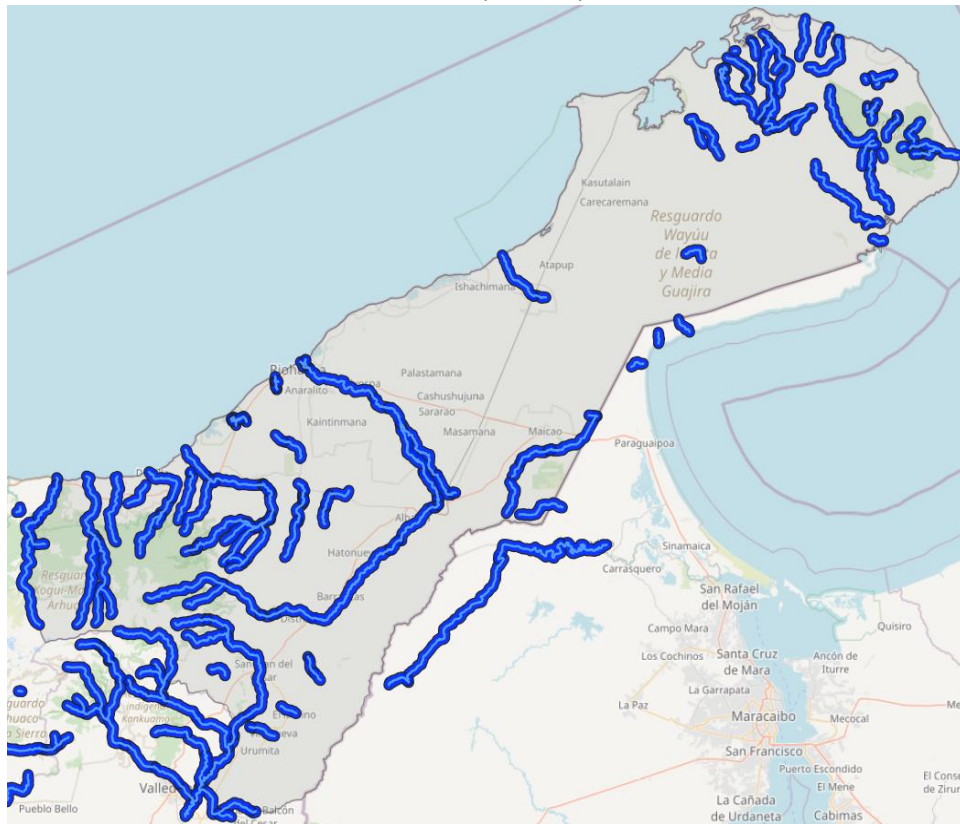
Protected Areas (2000m):



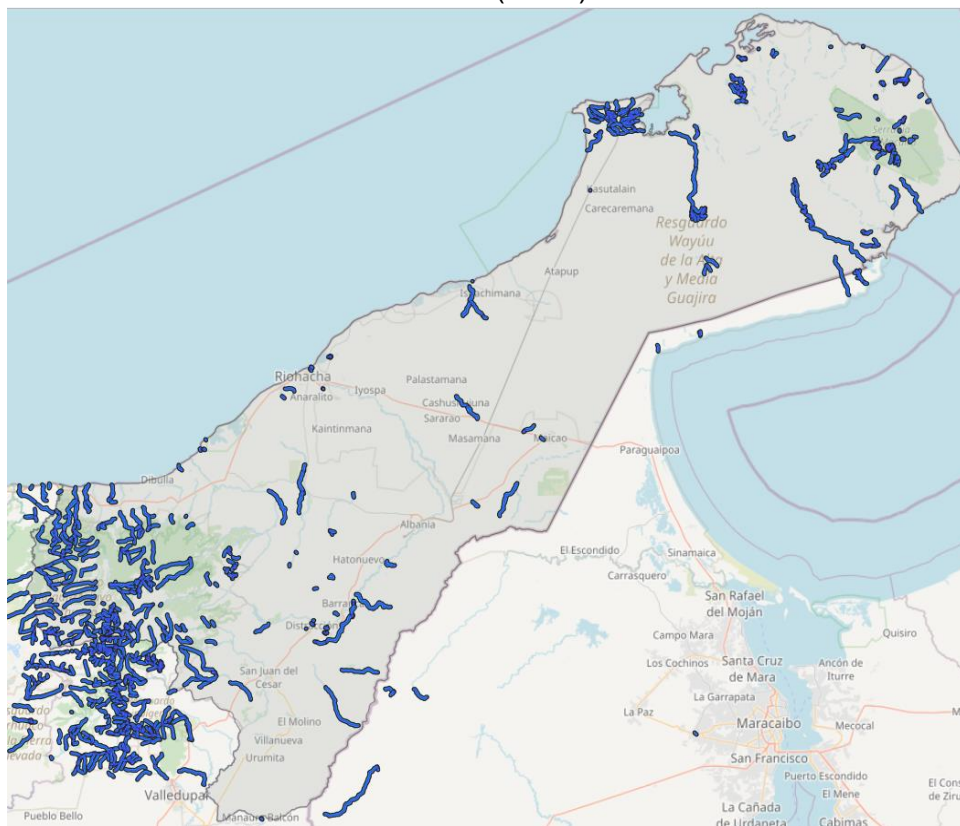
Railways:



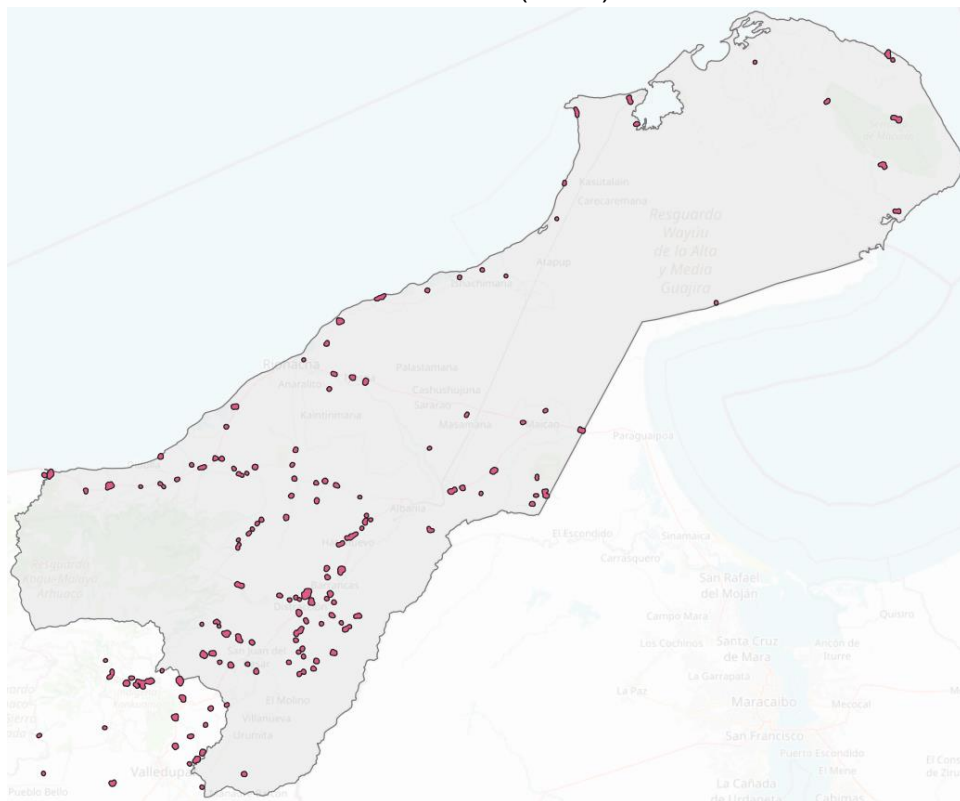
Rivers (1500m)



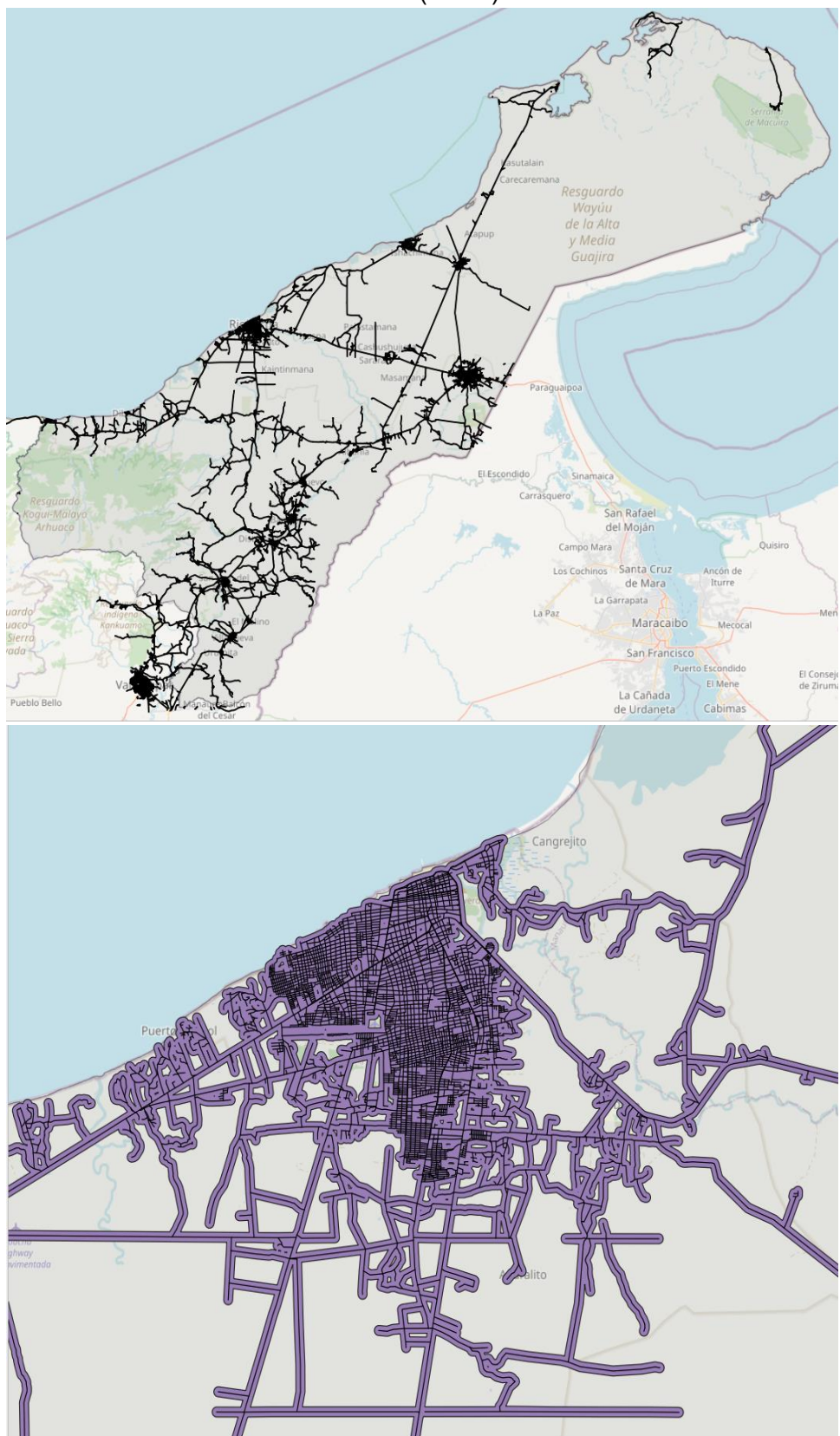
Streams (500m):



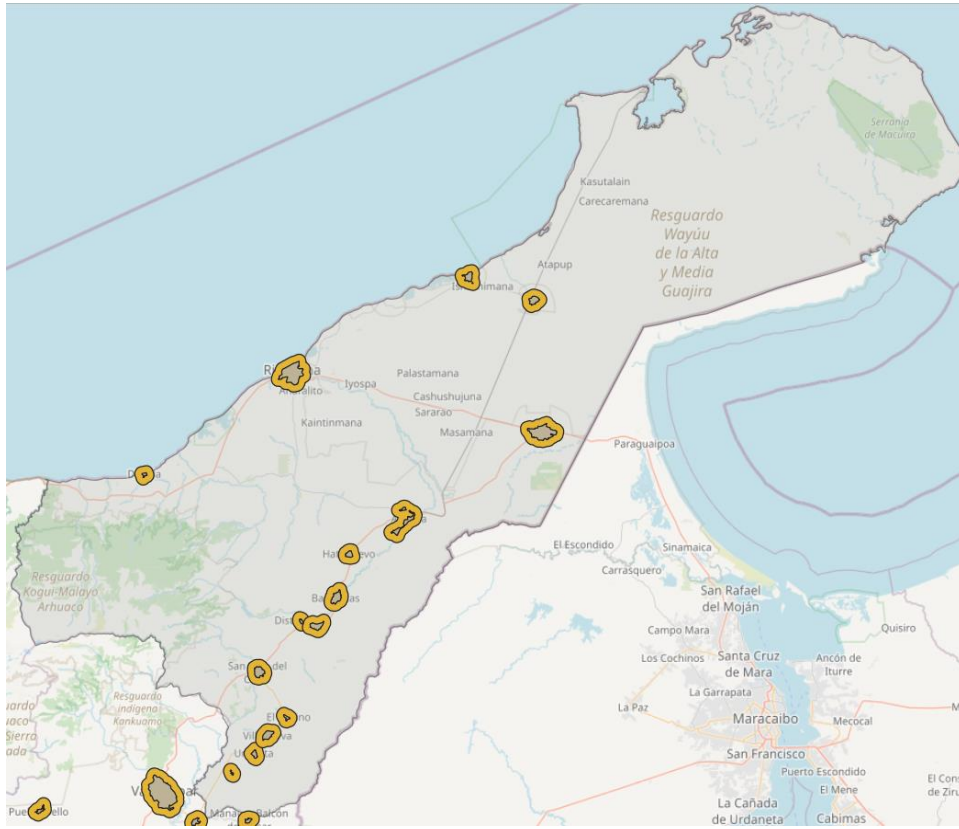
Rural Areas (500m):



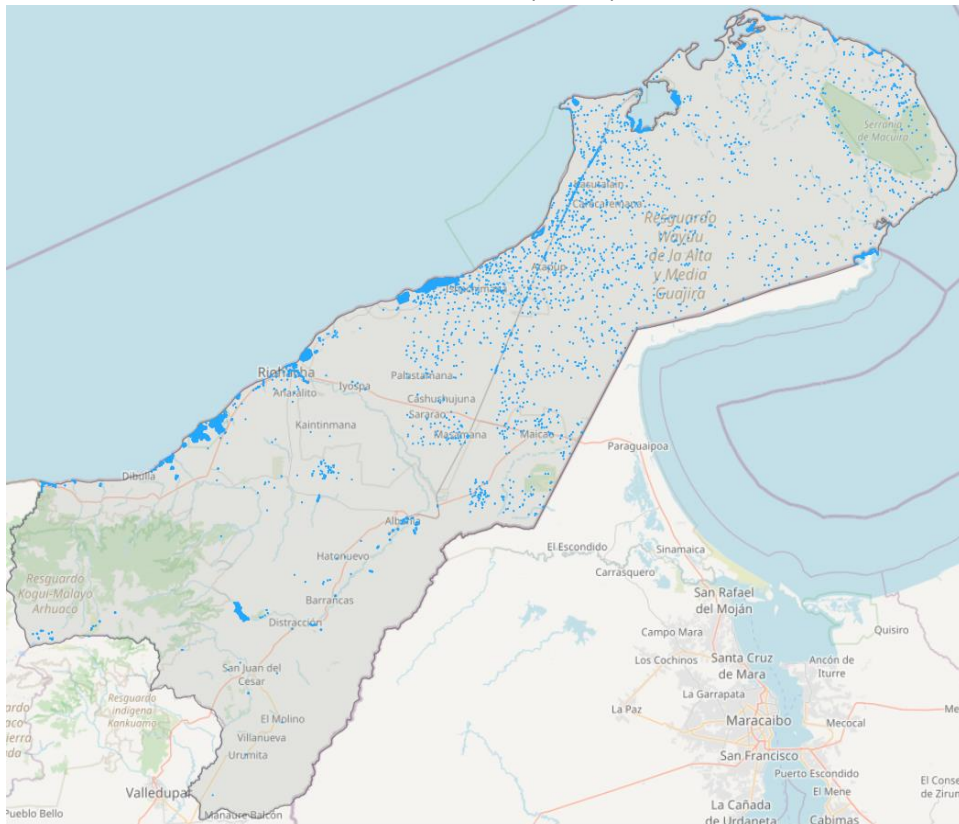
Roads (100m):



Urban Areas (2000m):

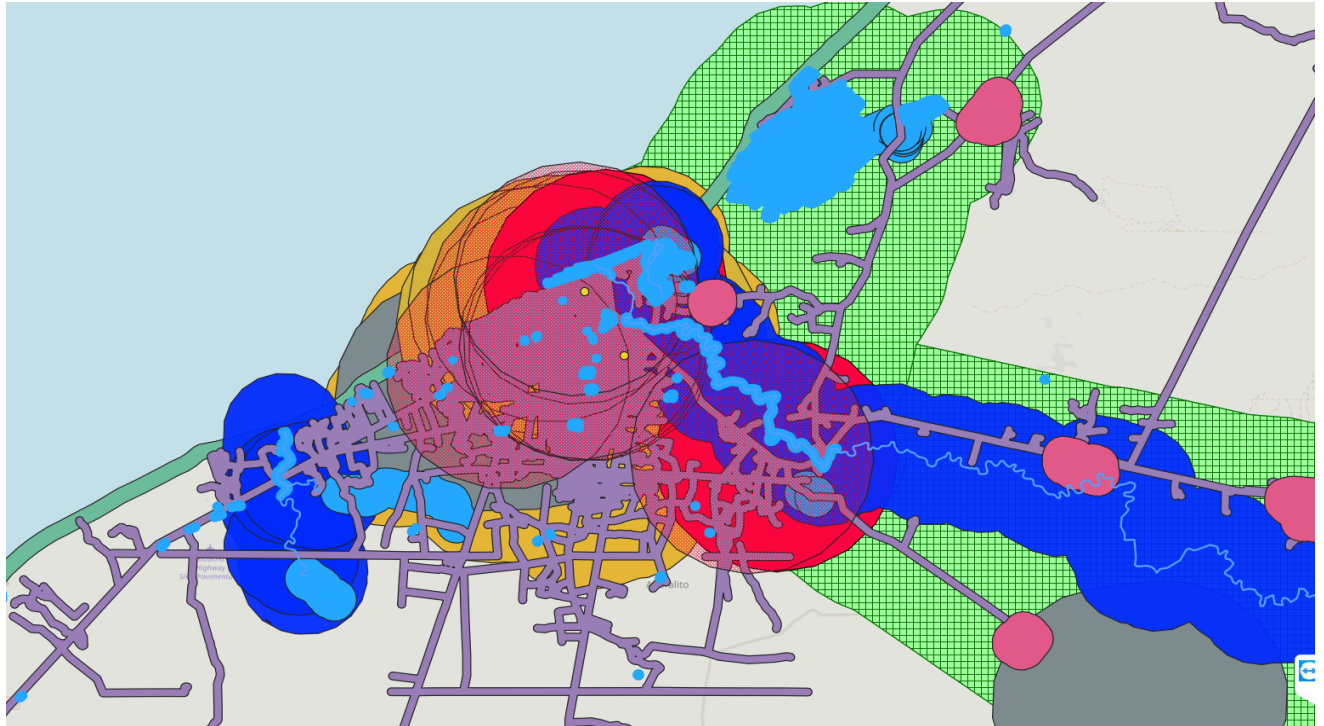


Water bodies (150m):

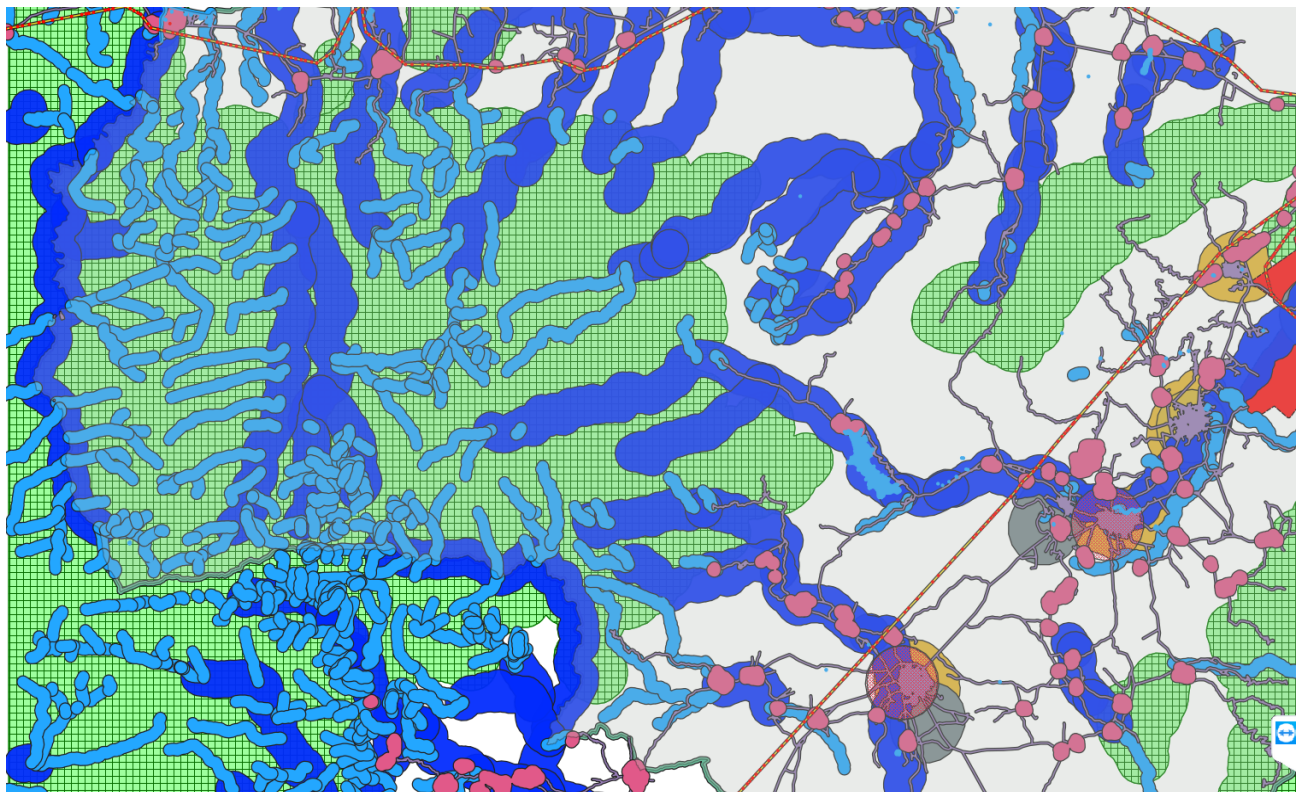


B. Captures from different regions in La Guajira, with all the area-restrictive criteria and their corresponding buffers.

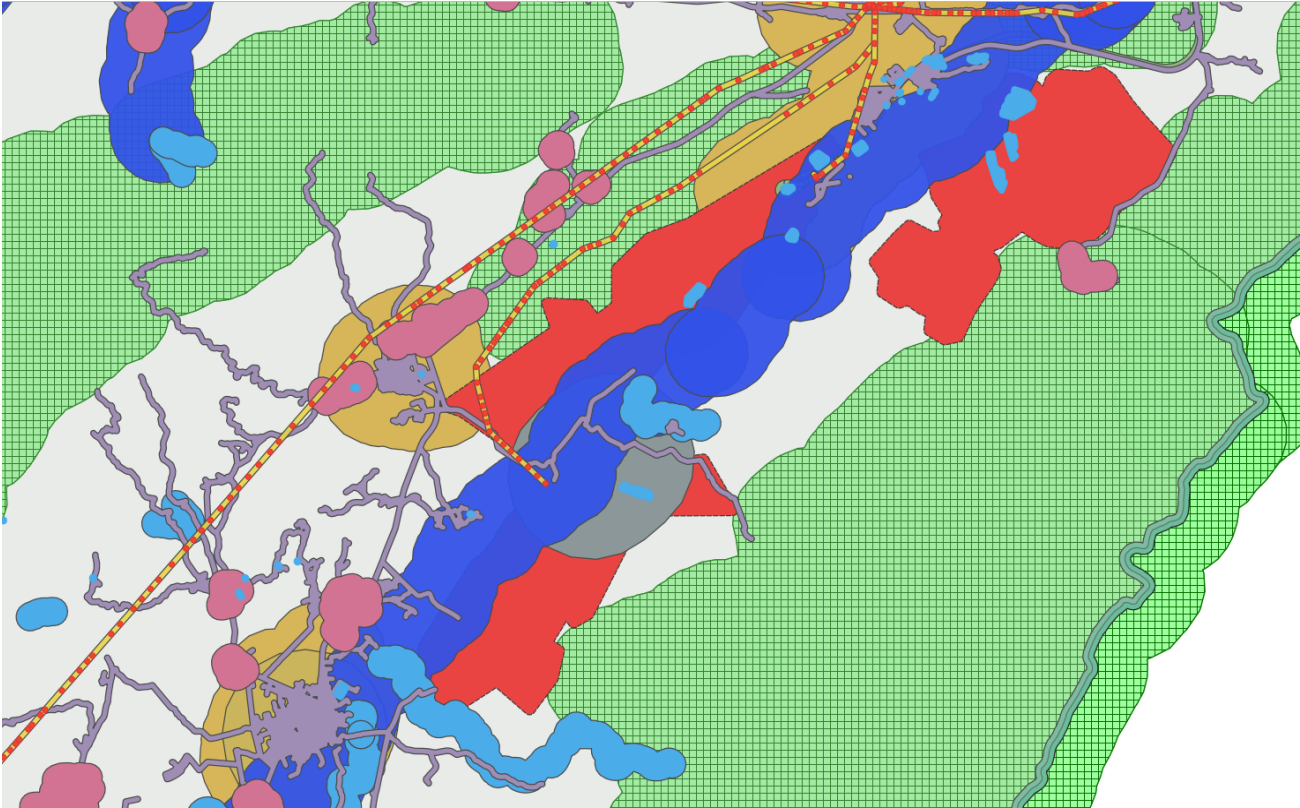
Riohacha:



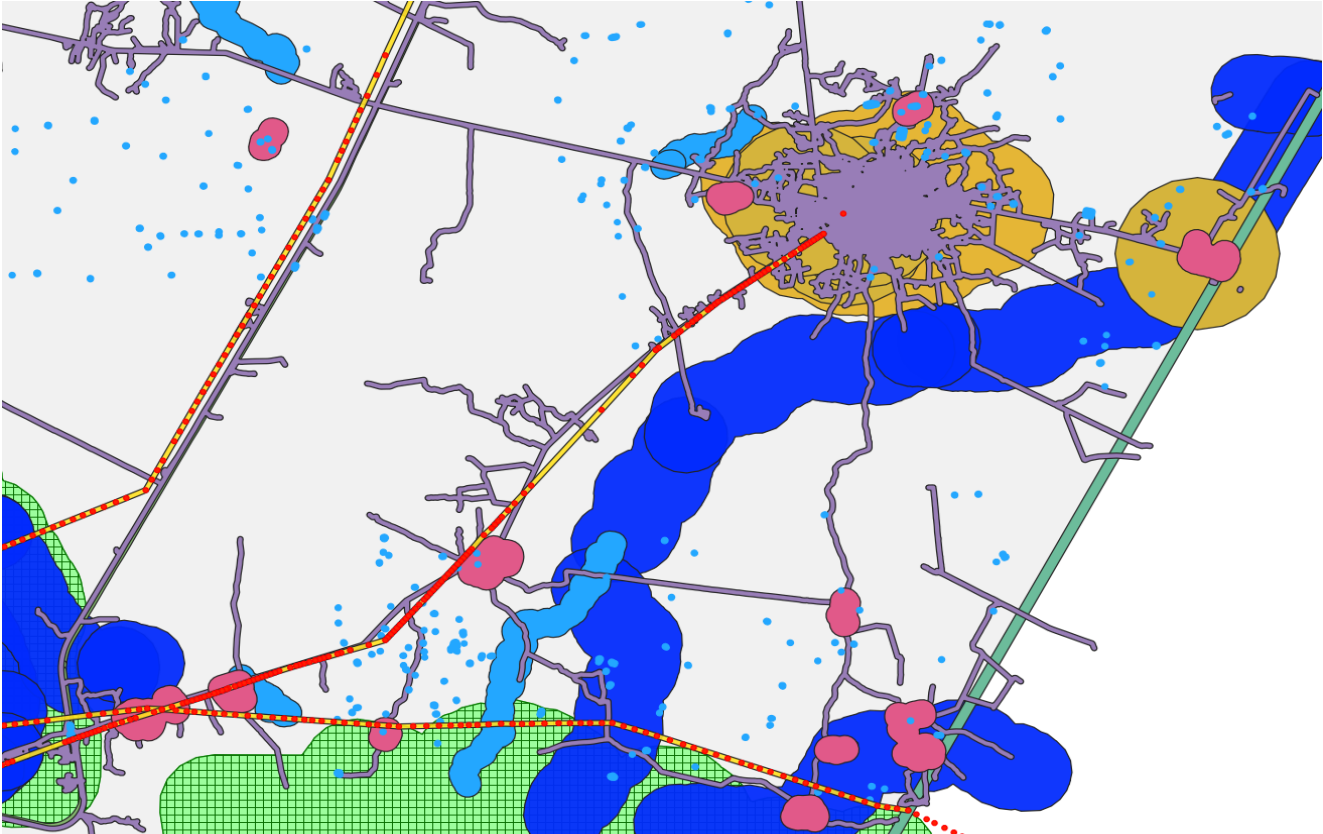
Natural Park Sierra Nevada de Santa Marta:



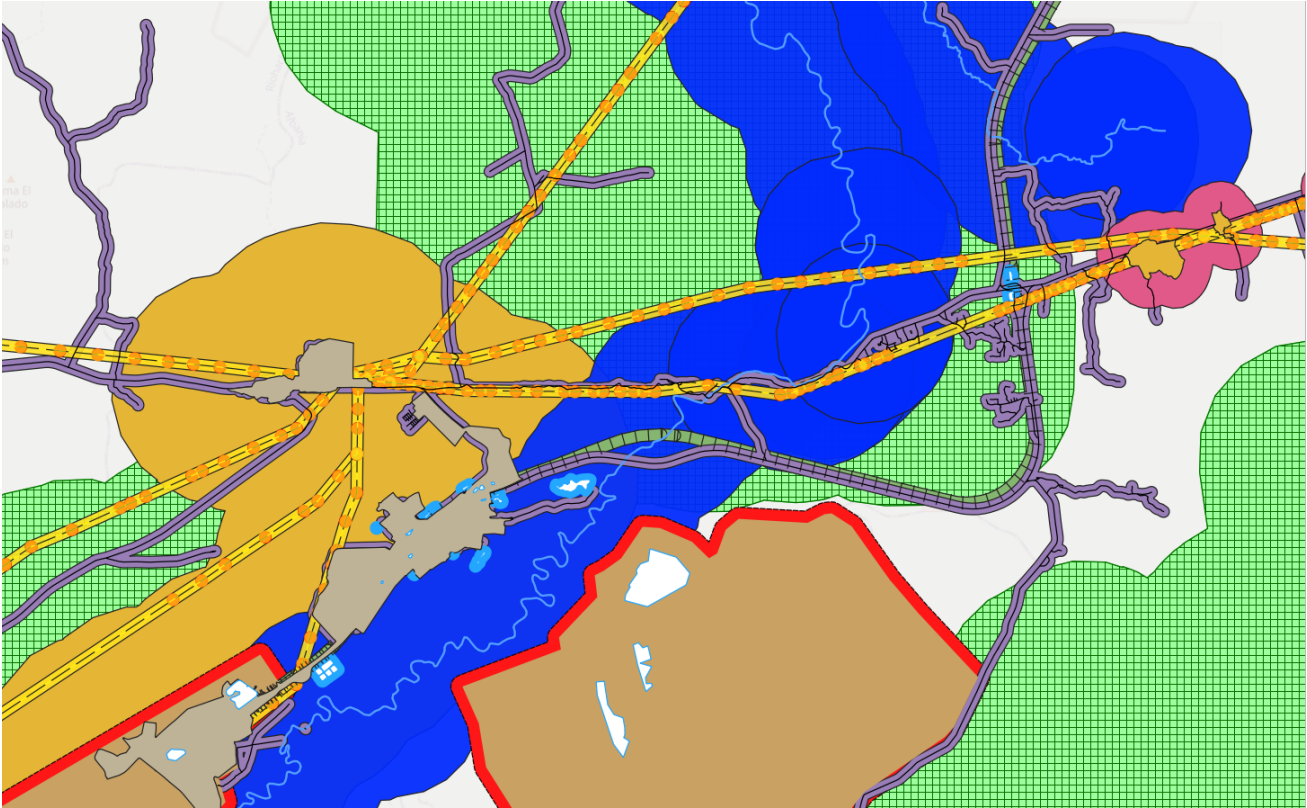
Open-sky Coal Mine Cerrejón:



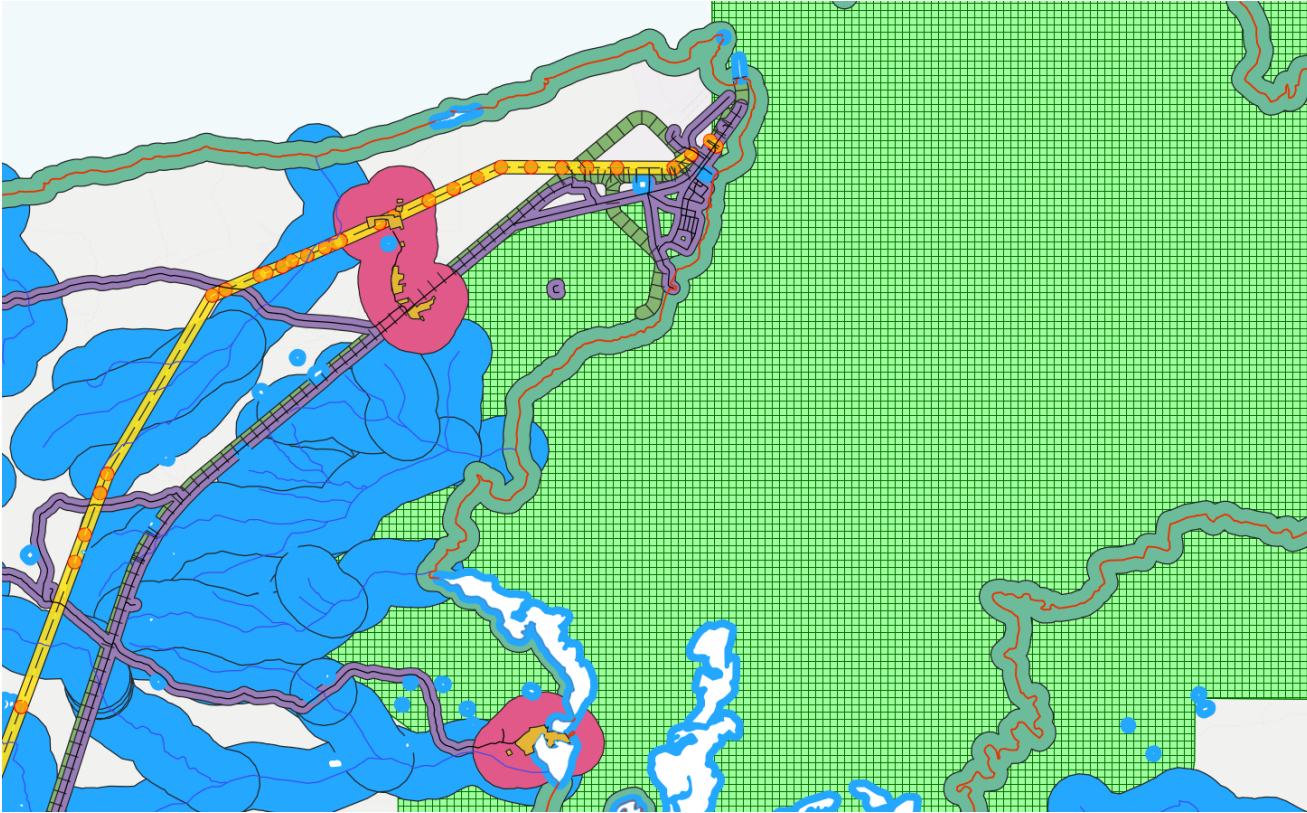
Maicao:



Cuestecita Electric Sub-station:



Puerto Bolivar:



C. P&QGIS Scripts

→ Create Aspect and Slope raster layers with only a Digital Elevation Model raster layer

```
def AspAndSlo():
```

```
    dir='C:/any/location/preferably/where/DEM/is'

    #WE CREATE VARIABLES FOR EACH FILE'S LOCATION
    elevationRaster=dir+'/DEM.tif'
    #elevationRaster=folder+'Elevation.tif'
    #The name we put here will be the name of the file
    aspectRasterOUT=dir+'/AspectDEMM.tif'
    slopeRasterOUT=dir+'/SlopeDEMM.tif'

    #ASPECT:
    processing.run("gdal:aspect",{
        'INPUT':elevationRaster,\
        'BAND':1,\
        'TRIG_ANGLE':False,\
        'ZERO_FLAT':False,\
        'COMPUTE_EDGES':False,\
        'ZEVENBERGEN':False,\
        'OPTIONS':'',\
        'EXTRA':'',\
        'OUTPUT':aspectRasterOUT\
    })

    #SLOPE:
    processing.run("gdal:slope",{
        'INPUT':elevationRaster,\
        'BAND':1, 'SCALE':1,\
        'AS_PERCENT':False,\
        'COMPUTE_EDGES':False,\
        'ZEVENBERGEN':False,\
        'OPTIONS':'',\
        'EXTRA':'',\
        'OUTPUT':slopeRasterOUT\
    })

    #Insert the created files in the QGIS environment
    iface.addRasterLayer(slopeRasterOUT)
    iface.addRasterLayer(aspectRasterOUT)
```

```
AspAndSlo()
```

→ Create global radiation [Wh/m²] and Insolation time [h] raster layers for every day of the year

```

import processing
def insol():
    numdays = 365
    # Iterate over each day and run r.sun.insoltime
    for day in range(1, numdays+1):
        # Set the parameters for r.sun.insoltime
        dir='C:/Users/josep/Desktop/RunInsolationTime'
        elevationRaster = dir+'/DEM.tif'
        aspectt = dir+'/AspectDEM.tif'
        slopee = dir+'/SlopeDEM.tif'
        timeinsolOUT = dir+'/Insol /Insol_' + str(day) + '.tif'
        globradOUT = dir+'/GlobRad/GlobRad_' + str(day) + '.tif'

        dia = day
        print("\n")
        print("It's day number %d" % day)
        parameters = {
            'elevation': elevationRaster,
            'aspect': aspectt, 'aspect_value': 270,
            'slope': slopee, 'slope_value': 0,
            'linke': None,
            'albedo': None, 'albedo_value': 0.35,
            'lat': None, 'long': None,
            'coeff_bh': None, 'coeff_dh': None,
            'horizon_basemap': None,
            'horizon_step': None,
            'day': dia, 'step': 0.5, 'declination': None,
            'distance_step': 1, 'npartitions': 1, 'civil_time': None,
            '-p': False, '-m': False,
            'insol_time': timeinsolOUT,
            'glob_rad': globradOUT,
            'GRASS_REGION_PARAMETER': '-8204085.058200000, -
7895730.068700000,1159811.999800000,1467653.027200000 [EPSG:3857]',
            'GRASS_REGION_CELLSIZE_PARAMETER': 0,
            'GRASS_RASTER_FORMAT_OPT': '',
            'GRASS_RASTER_FORMAT_META': ''
        }
        print("Now running the algorithm")
        # Run the r.sun.insoltime algorithm
        processing.run("grass7:r.sun.insoltime", parameters)
        print("\n End of iteration number %d: " % dia)

insol()

```

→ Add all the values in a specific attribute table column (field):

```

print("\n")
print("Feature List:")
def fields():
    titulos=list(iface.activeLayer().fields())
    x=0
    for i in titulos:
        print((x+1),". "+i.name())
        x=x+1
fields()

NumTuple = QDialog.getInt(None, "Feature Number", "From what feature do you
want the total sum? (Enter the feature number)")
numFeat=NumTuple[0]      #utiliza el primer objeto de la lista, que es el numero

totalSum=0
#I do a list of all the features in the column
features=list(iface.activeLayer().getFeatures())

#The following while is to create a list of all the values in the column
#numFeat. It is done before because it is used in the next if.
y=0
while y < len(features):
    feature=features[y]
    y=y+1
y=0

if type(feature[numFeat-1]) == int or type(feature[numFeat-1]) == float:
    print("\n")
    print("Following are all the numbers in the column, feature # %d:"%(numFeat))
    while y < len(features):
        if feature[numFeat-1] == None:
            print(" %d.%d: Null"%(numFeat,y+1))
        else:
            totalSum=totalSum+float(feature[numFeat-1])
            print(" %d.%d: %.1f" %(numFeat, y+1,feature[numFeat-1]))
            y=y+1
    print("\n")
    print("Total Sum is: %.2f"%(totalSum))
else:
    print("\n")
    print("This is not a number and cannot be added.")

```

D. Other Screenshots:

